NASA/CR—2008-215214

Aerodynamic Design of a Dual-Flow Mach 7 Hypersonic Inlet System for a Turbine-Based Combined-Cycle Hypersonic Propulsion System

Bobby W. Sanders and Lois J. Weir
TechLand Research, Inc., North Olmsted, Ohio

June 2008

NASA STI Program . . . in Profile

Since its founding, NASA has been dedicated to the advancement of aeronautics and space science. The NASA Scientific and Technical Information (STI) program plays a key part in helping NASA maintain this important role.

The NASA STI Program operates under the auspices of the Agency Chief Information Officer. It collects, organizes, provides for archiving, and disseminates NASA's STI. The NASA STI program provides access to the NASA Aeronautics and Space Database and its public interface, the NASA Technical Reports Server, thus providing one of the largest collections of aeronautical and space science STI in the world. Results are published in both non-NASA channels and by NASA in the NASA STI Report Series, which includes the following report types:

- TECHNICAL PUBLICATION. Reports of completed research or a major significant phase of research that present the results of NASA programs and include extensive data or theoretical analysis. Includes compilations of significant scientific and technical data and information deemed to be of continuing reference value. NASA counterpart of peer-reviewed formal professional papers but has less stringent limitations on manuscript length and extent of graphic presentations.

- TECHNICAL MEMORANDUM. Scientific and technical findings that are preliminary or of specialized interest, e.g., quick release reports, working papers, and bibliographies that contain minimal annotation. Does not contain extensive analysis.

- CONTRACTOR REPORT. Scientific and technical findings by NASA-sponsored contractors and grantees.

- CONFERENCE PUBLICATION. Collected papers from scientific and technical conferences, symposia, seminars, or other meetings sponsored or cosponsored by NASA.

- SPECIAL PUBLICATION. Scientific, technical, or historical information from NASA programs, projects, and missions, often concerned with subjects having substantial public interest.

- TECHNICAL TRANSLATION. English-language translations of foreign scientific and technical material pertinent to NASA's mission.

Specialized services also include creating custom thesauri, building customized databases, organizing and publishing research results.

For more information about the NASA STI program, see the following:

- Access the NASA STI program home page at *http://www.sti.nasa.gov*

- E-mail your question via the Internet to *help@sti.nasa.gov*

- Fax your question to the NASA STI Help Desk at 301–621–0134

- Telephone the NASA STI Help Desk at 301–621–0390

- Write to:
  NASA Center for AeroSpace Information (CASI)
  7115 Standard Drive
  Hanover, MD 21076–1320

NASA/CR—2008-215214

Aerodynamic Design of a Dual-Flow Mach 7 Hypersonic Inlet System for a Turbine-Based Combined-Cycle Hypersonic Propulsion System

Bobby W. Sanders and Lois J. Weir
TechLand Research, Inc., North Olmsted, Ohio

Prepared under Contract NAS3–03110

National Aeronautics and
Space Administration

Glenn Research Center
Cleveland, Ohio 44135

June 2008

This work was sponsored by the Fundamental Aeronautics Program
at the NASA Glenn Research Center.

Level of Review: This material has been technically reviewed by NASA technical management OR expert reviewer(s).

Available from

NASA Center for Aerospace Information
7115 Standard Drive
Hanover, MD 21076–1320

National Technical Information Service
5285 Port Royal Road
Springfield, VA 22161

Available electronically at http://gltrs.grc.nasa.gov

Preface

This report documents the inlet aerodynamic design work performed by TechLand Research, Inc. under Task 8 of NASA contract no. NAS3–03110. Under Task 8 of the contract, TechLand Research also provided mechanical design requirements documents for two research test models, a small-scale model for the NASA Glenn 1- by 1-Foot Supersonic Wind Tunnel and a large-scale model to be tested in the NASA Glenn 10- by 10-Foot Supersonic Wind Tunnel. The small-scale model mechanical design was completed by NASA Glenn Research Center and ASRC Aerospace. Fabrication was completed by NASA. ATK was responsible for the mechanical design and fabrication of the large-scale research model. John D. Saunders of NASA served as the contractor technical monitor and provided significant technical input into the design process.

Contents

Aerodynamic Design of a Dual-Flow Mach 7 Hypersonic Inlet System for a Turbine-Based Combined-Cycle Hypersonic Propulsion System

Bobby W. Sanders and Lois J. Weir
TechLand Research, Inc.
North Olmsted, Ohio 44070

Summary

A new hypersonic inlet for a turbine-based combined-cycle (TBCC) engine has been designed. This split-flow inlet is designed to provide flow to an over-under propulsion system with a turbine engine (turbojet or turbofan) and a dual-mode scramjet engine for airbreathing propulsion from takeoff to Mach 7. The two-dimensional inlet system utilizes a variable-geometry ramp, a high-speed cowl with a rotating lip, and a rotating low-speed cowl that serves as a splitter to divide the flow between the low-speed (turbine engine) duct and the high-speed (scramjet) duct and isolate the turbine airflow duct at high Mach number flight conditions. The high-speed inlet was designed for a shock-on-lip Mach number of 7, and incorporates the proper compression to operate at a dynamic pressure of 1760 psf for a hydrocarbon-fueled vehicle, or 880 psf for a hydrogen-fueled vehicle. The low-speed inlet was designed for Mach 4, the maximum transition Mach number. The low-speed inlet is open from takeoff to Mach 4. Above Mach 4, the splitter will be closed such that flow is being supplied only to the scramjet engine. Integration of the low-speed inlet into the high-speed inlet system imposed constraints that significantly impacted the low-speed inlet design, including driving the design to a large amount of internal compression.

The two-dimensional inlet is highly versatile. Alternate design features have been identified that offer options for integration with multiple propulsion system and/or vehicle concepts. These include a translating high-speed cowl concept that will provide more versatility for inlet/engine flow-matching in the high-speed duct. A variable-geometry low-speed cowl concept may allow the elimination of the ramp variable geometry, while providing proper inlet/engine flow matching in the low-speed system.

The inlet design was used to develop mechanical designs for two inlet mode transition experimental research models. A small-scale concept screening Inlet Mode Transition (IMX) model was designed and built for testing in the NASA Glenn Research Center (GRC) 1- by 1-Foot Supersonic Wind Tunnel (1×1 SWT). A Large-scale Inlet Mode Transition (LIMX) model has been designed for testing in the GRC 10- by 10-Foot Supersonic Wind Tunnel (10×10 SWT). This model is designed to facilitate multi-phase testing that includes detailed inlet mode transition testing and inlet performance assessment, controls testing and development, and integrated systems testing with operating turbofan and scramjet engines.

Introduction

Airbreathing propulsion can enable improved efficiencies for quick space access and for global reach. Therefore, NASA and the Department of Defense have an interest in developing design technology for advanced integrated airframe/inlet propulsion concepts (refs. 1 to 7). Of specific interest are hypersonic propulsion flow paths with adequate low-speed performance and operability. Various propulsion modes have been proposed for the range of Mach numbers encountered by an accelerating hypersonic vehicle. One promising propulsion scheme is the Turbine-Based Combined-Cycle (TBCC). The TBCC uses a high Mach number capable engine (turbine-based) to accelerate the vehicle to scramjet take-over speeds. In the remainder of this report the turbine engine will be referred to as a turbofan; however, either a turbojet or a turbofan engine would be compatible with the inlet system described herein. The two propulsion systems

(turbofan and scramjet) that operate over different Mach number ranges dominate the inlet system design. A design could feature two separate inlets feeding the separate propulsion systems. However, this approach would result in a heavy inlet system. Therefore, the two engines of the TBCC are typically placed in an over-and-under arrangement and share a common inlet and a common nozzle to save weight. A representative dual-flow, over/under, inlet/engine system integrated into a hypersonic vehicle is presented in figure 1. In the nacelle, the turbofan engine is placed above the scramjet with the turbofan closed off for high-hypersonic scramjet operation. The last external ramp of the high-speed inlet is hinged to allow the upper inlet to be opened for turbofan operation at lower flight speeds. Switching between the turbine cycle (dual flow) propulsion and dual-mode scramjet operation is termed inlet mode transition. The focus of the inlet design study described herein was to design and verify an inlet concept for the TBCC that is termed IMX for Inlet Mode Transition.

Specific operation procedures for the two engine systems of the TBCC during the acceleration part of the flight envelope have not been determined. Therefore, a general approach for operation of the systems is described herein. From takeoff to the mode transition flight condition, both inlet ducts will be open with thrust being provided by the turbojet. The high-speed inlet duct will be cold-flowed until a flight condition that will allow combustion in the dual-mode isolator/combustor is achieved. After combustion conditions have been achieved, the Mach number at which the high-speed engine will begin operation will depend on required thrust or operation to reduce drag. Even though the high-speed engine may not provide much thrust at lower Mach numbers, combustion to help fill the nozzle and reduce base drag may be required. At the mode transitioning condition, the turbojet will be shut down and the low-speed inlet duct will be closed. The high-speed inlet/engine will provide the required thrust at all flight Mach numbers beyond the mode transitioning condition. Operation and scheduling of the two inlet and engine systems during mode transition requires an experimental program that includes operating engines.

Past NASA high-speed and space access vehicle programs that included research investigations of inlet designs for dual-flow hybrid hypersonic propulsion systems were mainly limited to the high-speed (scramjet or ramjet) part of the inlet system. Very little research was completed on the low-speed inlet of the dual-flow hypersonic inlet system. One example of previous mode transitioning research is presented in reference 8. This study effort was limited to a small, simple model and did not include a complete low-speed inlet design. Therefore, the inlet design effort reported herein was directed toward addressing the crucial technical issues associated with dual-flow hypersonic combined-cycle airbreathing propulsion systems, especially the critical need for experimental performance and operability data on the dual-flow inlet system. The objective of this effort was to provide the aerodynamic design of a dual-flow hypersonic inlet system to be used in the development of experimental research hardware that will allow the development of inlet operating procedures and assessment of inlet performance levels during mode transition.

A hypersonic aircraft propulsion system presents unusual challenges to the propulsion system designer. The inlet/engine system must operate over the entire flight regime, from takeoff to hypersonic speeds. While the propulsion system is not required to perform at optimum efficiency at the lower Mach numbers of the flight envelope, it must propel the vehicle through them safely to cruise conditions. Thus, the inlet designer is faced with a series of design problems. The inlet must operate at the high-speed design Mach number while also providing the required variable geometry that will allow it to operate at lower-speed conditions. In addition, the inlet is integrated into the fuselage of the aircraft such that the forebody serves as the initial compression surface for the inlet. The resulting long compression surface leads to the growth of extremely thick boundary layers that enter the inlet, often resulting in a large percentage of the flow entering the inlet being comprised of low energy boundary layer. The ingestion of large boundary layers can lead to serious performance problems in the inlet. A turbofan engine requires airflow that is sufficiently uniform and low in distortion to be capable of operation, if not particularly efficient. A previous Mach 5 inlet design (refs. 9 to 11) and research study (ref. 12) showed that thick sidewall boundary layers in two-dimensional inlets can lead to shock-boundary layer interactions, which set up large regions of vortical flow that propagate downstream and can result in large regions of separated flow in the subsonic diffuser. Frequently, as much as one half of the flow in the duct at the

diffuser exit (engine face) was completely separated, even in a slowly diffusing subsonic duct. Other CFD and experimental studies have also revealed large separations in the subsonic diffusers of inlets designed for high Mach numbers and tested at lower-speed conditions. Such separations in the subsonic diffuser can result in turbofan engine stall, or in the high-speed engine, may lead to insufficient fuel mixing and poor performance of the propulsion system.

The conceptual design for the IMX was derived from designs conceived by TechLand Research under a NASA Small Business Innovative Research program (ref. 13). The NASA Fundamental Aeronautics/Hypersonics Project adopted the design approach and directed the design effort toward the development of a Mach 7 capable hypersonic propulsion system. Consequently, TechLand provided the aerodynamic design of a dual-mode hypersonic inlet system and provided mechanical design requirements documents for the development of both small-scale (IMX) and large-scale (LIMX) inlet research models. A major challenge of the IMX design was the identification of feasible variable geometry based on sets of cowl and ramp contours. Hydraulic actuation was selected for cowl geometry variation (rotation) to provide smooth transitioning from turbofan to dual-mode ramjet operation. The inlet design balances the objectives of high performance (low total pressure loss), engine demand flow matching and mechanical feasibility. A contoured splitter surface directs flow into the turbofan from takeoff up to the transition Mach number of 4 and then closes to provide added compression to improve the dual-mode ramjet operation and performance. To match turbofan flow demand at lower Mach numbers, a variable geometry ramp was also included in the design. NASA Glenn Research Center (GRC), in collaboration with TechLand, carried the inlet concept through mechanical design and fabrication of a small-scale screening model for testing in the GRC 1- by 1-Foot Supersonic Wind Tunnel (1×1 SWT). The small-scale IMX inlet model included variable cowls with parametrics for fixed ramp positions. NASA Glenn researchers used computational fluid dynamics (CFD) codes to perform three-dimensional, turbulent flow analysis to validate the basic inlet design.

The large-scale dual flow propulsion system (LIMX) was sized for the GRC 10- by 10-Foot Supersonic Wind Tunnel (10×10 SWT). The large-scale inlet design includes the aerodynamic design of an integrated inlet system (both low-speed and high-speed inlets) and a complex variable-geometry system. In addition to the variable-geometry (rotating) cowls, a remotely-controlled variable-geometry ramp was incorporated into the model. The model design includes the inlet subsystems that are necessary to allow inlet aerodynamic performance, operability, and mode transitioning with operating engines to be evaluated. A series of experimental testing efforts on the large-scale research model are planned to accomplish this objective. The test series include: (1) inlet development testing, (2) controls development testing, and (3) fully integrated mode transition testing with a full-up propulsion system including engines. This experimental evaluation will represent a “first-of-its-kind” effort on a fully integrated inlet/engine hypersonic dual-mode propulsion system. The hardware will serve as the test-bed/platform for acquiring research data and characterizing inlet-operability limits and inlet-control strategies to develop and ultimately validate the next generation of inlet design tools. The database to be developed will be applicable to a combined-cycle-engine inlet-compression system comprised of a coupled ramjet/scramjet propulsion duct and a turbine-engine, low-speed propulsion duct. Therefore, the emphasis is on understanding and predicting performance and operability during mode transition from the low speed (turbine engine) to the high speed (ramjet/scramjet engine) propulsion system.

This report documents the aerodynamic inlet design for an over/under dual mode hypersonic airbreathing propulsion system. A design concept and approach for a viable inlet system are included.

Nomenclature

A	Local angle, deg
C1, C2	Cowl bleeds
CFD	Computational fluid dynamics
D	Diameter

H	Cowl lip height
H1A	Inlet configuration with cowl translated to adjust for boundary layer, $H1A/H_c = 1.01173$
H1B	Inlet configuration with cowl translated to adjust for boundary layer, $H1B/H_c = 1.027656$
IMX	Inlet mode transition (also used to refer to small-scale mode transitioning model)
LIMX	Large-scale inlet mode transitioning model
M	Mach number
P	Static pressure
P	Total pressure
psf	Pounds per square foot
q	Dynamic pressure
RX, R1–R4	Ramp bleeds
SW1–SW3	Sidewall bleeds
VGC	Variable geometry cowl
W	Inlet width
x	Axial distance
y	Vertical height
δ	Ramp angle, degrees
θ	Compressive turning angle, degrees

Subscripts:

0	Free stream
1	Upstream of shock
2	Downstream of shock, also entrance station to turbine
c	Cowl
c1A	Cowl lip for configuration H1A
cowl	Cowl
i	Inlet
hs	High speed
l	Local
ls	Low speed
ramp	Ramp
te	Throat exit

Inlet Design (Inviscid Throat Mach Number of 1.5)

Inlet Design Challenges

A sketch that illustrates a hypersonic aircraft with a dual-flow, over/under, propulsion system (configured for high Mach operation) is presented in figure 1. The inlet will require a complex variable geometry system. The dual-flow inlet includes a variable geometry ramp and rotatable cowl lips for both the low-speed and high-speed inlets. The low-speed cowl serves as the splitter that divides the flow between the upper (turbofan) and lower (scramjet) ducts. Hypersonic cruise aircraft propulsion system design presents some unusual design challenges. A bulleted list of some of these design challenges is presented in figure 1.

The high-speed flow path has the greatest length due to the low compression shock angles. As a consequence, the low-speed inlet design can be built into the existing high-speed inlet aerodynamic contours. The aerodynamic lines of the high-speed inlet impose significant design constraints on this low-speed inlet. When integration of the low-speed inlet into the compression field of the high-speed inlet is considered, the amount of compression external to the cowl lip is limited to a less than desirable amount for the low-speed inlet. At Mach 7, the high-speed inlet only requires about 24° to 32° of compressive airflow turning (ref. 13), with about one-half to one-third of that amount accomplished external to the cowl lip. Theoretical total compressive turning curves for scramjet inlets designed for one-half atmosphere (for hydrogen-fueled systems) or 1 atm (for hydrocarbon-fueled systems) static pressure within the inlet are presented in figures 2 and 3. A total turning angle of 30.5° was selected for this inlet design effort. This compressive turning would define an inlet that would be representative of a design for either fuel type. The 30.5° compressive inlet will provide 1/2-atm combustor pressure at a dynamic pressure of about 880 psf and 1 atm at a dynamic pressure of 1760 psf. If the over-under inlet arrangement is similar to the conceptual sketch presented in figure 1, only the first two ramp surfaces of the high-speed inlet provide compression for the low-speed inlet. These two ramps provide a total compression of 12.5°. In comparison, a traditionally designed, isolated, Mach 3 low-speed inlet needs a total of about 42° of compressive turning (for $M_{throat} = 1.3$), and an isolated Mach 4 inlet requires total compressive turning of about 58°. When the low-speed inlet is integrated into the high-speed inlet, the additional compressive turning that is required beyond the turning provided by the first two compression surfaces of the high-speed inlet must be provided by a large amount of turning internally on the cowl and ramp surfaces. Typically, supersonic inlets with high amounts of internal compression provide less natural operability and tolerance to external disturbances than do inlets with more balanced external-to-internal compression splits. Highly internal contraction inlets are also subject to more violent unstart transients. Rotation of the low-speed inlet lip to the closed position further complicates the internal design of the low-speed inlet. The impact on inlet design resulting from lip closure is discussed in the report section on the Mach 4 inlet design.

Two propulsion systems operating over different Mach ranges with very different airflow requirements drive the inlet system design. The integrated inlet system must operate at high-speed cruise while also providing the variable geometry required to operate at lower-speed conditions. Not only must the inlet system perform effectively at the high Mach conditions in scramjet mode, but it also must perform sufficiently well to accelerate the vehicle through the low-speed flight speeds. The dual-flow inlet must function over the entire flight regime. This imposes inlet requirements on the turbomachinery-based low-speed system that accelerates the vehicle from takeoff through low supersonic Mach numbers and on the high-speed system from dual-mode ramjet operation at Mach 4.0 to scramjet operation at Mach 7. In addition, the inlet is generally integrated into the forebody of the aircraft, such that the forebody serves as the initial compression surface for the inlet. This long compression surface leads to the growth of thick boundary layers that can make up a large percentage of the flow entering the high-speed inlet at high Mach numbers, or can lead to serious problems at lower flight speeds if ingested by the low-speed inlet. For the high-speed inlet, separations resulting from inlet shock interactions with large boundary layers may lead to insufficient fuel mixing in the dual-mode scramjet, causing poor performance of the propulsion system or inlet unstart. For the low-speed inlet, the subsonic diffuser duct must transition from rectangular to round and also provide airflow with distortion levels that are sufficiently low enough to allow operation of the turbojet engine. Such a design is not easily accomplished, considering the thickness of the boundary layer that will likely be ingested by the turbofan inlet. The subsonic diffuser can be a major contributor to inlet total pressure losses. Secondary flows and separations can cause large unsteady distortions that can induce engine stalls. The Mach 5 inlet research effort of reference 12 and other experimental studies have revealed large separations in the subsonic diffusers of inlets designed for high Mach numbers.

Integration of hybrid propulsion subsystems, mode transition, low-speed operation, and subsonic diffuser performance of hypersonic inlets pose significant challenges to the design of a hypersonic

airbreathing propulsion system. The inlet design presented herein represents one approach to identifying and validating a workable solution.

Mach 7 Inlet Design

Basic Inviscid Inlet Design

The high-speed inlet for the TBCC hypersonic propulsion system was designed for operation to Mach 7. As presented in figure 4, the design was optimized at Mach 7 with all of the external shock systems focused on the inlet cowl lip. The external compression system for the high-speed inlet is shown in the figure. The three ramps provide compression wedges of 6.5°, 6°, and 7° for a total of 19.5° of external compression. The internal cowl angle is 8.5° with a resulting compression angle of 11° (19.5° to 8.5°) for the cowl shock. As indicated in figure 4, the cowl shock was cancelled at the inlet shoulder. A variable geometry (rotating) cowl provides the variation in mass-flow capture from Mach 4 to Mach 7. The position schedule for the high-speed cowl lip at lower Mach numbers when the low speed inlet is open will be determined in an experimental test program. Dimensions for the cowl lip reflect an adjustment to the inviscid inlet design as a result of boundary layer influence on the captured airflow. After the basic inviscid inlet design was completed, the entire cowl was translated vertically by $0.011791*H_c$ to account for boundary layer. As indicated on the inlet sketch and in the table on figure 4, the axial distance to the cowl lip is $4.29544*H_c$. Basic aerodynamic characteristics (inviscid) for the high-speed inlet at the design Mach number of 7.0 are presented in figure 5. A sketch showing the inlet surface dimensions is presented in figure 5(a), and the aerodynamic characteristics are presented in figure 5(b). Local Mach number, local static pressure recovery, and local surface angle are shown. The inlet compression reduces the inviscid Mach number from Mach 7 to Mach 3.4 at the entrance to the isolator of the high-speed engine system. Notice that the Mach number downstream of the cowl shock, both near the ramp and the cowl surfaces, is nearly constant (about Mach 3.4) within the high-speed inlet duct. The duct angle at the throat of the inlet is 4°. The amount of compression to the inlet throat was selected to provide approximately 1/2-atm combustion pressure for a hydrogen-fueled system or about 1 atm pressure for a hydrocarbon-fueled system. A table that reflects the aerodynamic characteristics of the Mach 7 inlet design is presented in figure 6. Non-dimensional ramp and cowl coordinates for the original inviscid design are presented in figure 7. The inlet designs identified and described herein were developed by using a combination of design capabilities. These design tools include the code of reference 15 and TechLand Research, Inc. in-house design codes and tools.

Design Adjustment for Boundary Layer

Two-dimensional viscous computational fluid dynamics analysis of the original inviscid high-speed inlet design at Mach 7 indicated that the inlet external shock system was passing ahead of the cowl lip with resulting spillage. Therefore, CFD solutions for two additional inlet configurations with the cowl translated were performed. These configurations H1A and H1B are compared to the original design in figure 8. For each of these configurations, the entire cowl surface was moved vertically (equal distance along the cowl) from the inviscid location to adjust for boundary layer growth in the duct. An increased cowl lip height of slightly more than 1 percent (height at cowl lip increased from an original H/H_c of 1.0 to 1.01173) was provided for configuration H1A. The cowl lip height was increased by almost 3 percent for configuration H1B (height at the cowl lip increased from H/H_c of 1.0 to 1.027656). The results of the CFD analysis for H1A and H1B are presented in figures 9 to 12. Mach number contours derived from the CFD analysis of H1A are shown in figure 9. As indicated in the figure, the initial shock system from the upstream compression wedges intersects the cowl lip. Boundary layer on these upstream wedges resulted in a slight increase in shock angle and would cause spillage if the cowl remained in the original design position. Therefore, adjusting the cowl position for boundary layer influence on the internal flow provides a positive influence on the capture flow of the inlet. The CFD of figure 9 also indicates that the cowl

shock is pointed toward the shoulder with some slight interaction of the shock with the boundary layer in the shoulder region. A similar plot of CFD results for configuration H1B is presented in figure 10. The increased vertical translation of the cowl surface from configuration H1A to H1B results in the initial shock system being inside the cowl lip in an overspeed position, and the cowl shock interaction with the ramp is at a location downstream of the shoulder. A comparison of the CFD results for H1A and H1B is presented in figure 11. Mach contours are labeled in the figures. A comparison of the two results indicates that the configuration H1A is clearly better than H1B, with the flow field being more uniform within the inlet duct. Notice that the Mach number at the throat of the inlet of about 3.35 is very near the inviscid design value of 3.4 (fig. 5). Figure 12 presents total pressure recovery and Mach number profiles at the throat station for configurations H1A and H1B. Based on the CFD results, H1A cowl contours were selected for the high-speed Mach 7 inlet. H1A cowl coordinates and coordinates for the ramp are presented in figure 13. These coordinates were used for the mechanical design and fabrication of the small-scale IMX inlet model.

Design Adjustment for Large-Scale Inlet Model

The large-scale inlet test model (LIMX) was sized for a 12 in. turbofan engine. This engine dimension sets all other model dimensions. A report section containing a discussion of inlet sizing is presented following the low-speed inlet design section. The inlet sidewalls are parallel from leading edge to engine face and are spaced 1 engine diameter apart. One of the objectives of the large-scale test is to mate the inlet system with a turbofan engine and dual-mode scramjet hardware that will be made available from other research efforts. Because the sizing of the scramjet hardware required a smaller high-speed inlet duct (smaller than the size obtained if the system were sized for the 12-in. turbofan), the contours of the high-speed inlet were altered from the design used for the small-scale IMX to accommodate the integration of the available high-speed engine. Otherwise, the aerodynamic designs of the large- and small-scale inlets are substantially the same. To accommodate the smaller existing isolator, the duct for the high-speed inlet was reduced in size. This size reduction was accomplished by moving the cowl vertically until the inlet exit/isolator entrance height was the desired dimension. The relationship of the resulting cowl geometry to the original design and to configuration H1A is presented in figure 14. As shown in figure 14, the cowl for configuration H1A was translated vertically from the original inviscid contour. To obtain the LIMX cowl, the cowl was translated downward and the initial part of the cowl was removed (cut back). The portion of the cowl that was removed is more clearly shown in figure 15. Figure 15 presents the CFD for configuration H1A that was previously shown in figure 9, and includes the position of the LIMX inlet model cowl. The initial portion of the cowl was cut back along the CFD predicted cowl shock. By placing the LIMX cowl in this position, the resulting flow field and the cowl shock/ramp shoulder interaction should be similar to the interaction as shown for configuration H1A. The entrance to the isolator (dashed line) as shown in figure 14 appears to be axially distorted. This is the result of the expanded vertical scale of the figure. The isolator entrance (inlet throat) is more correctly presented in figure 11. Coordinates for the large-scale inlet LIMX cowl configuration are presented in figure 16.

Mach 4 Low-Speed Inlet Design and Integration

Mach 4 Inlet Design

A sketch of the dual-mode hypersonic propulsion system with the inlet system configured for Mach 4 operation is presented in figure 17. For Mach 4 operation, the third ramp of the high-speed inlet is rotated about a hinge line that coincides with the shoulder of the high-speed inlet. This rotating part of the high-speed inlet becomes the variable geometry cowl lip for the low-speed inlet system. Rotation of the lip opens up the entrance to the low-speed inlet duct. Isometric sketches that provide a comparison of the high-speed Mach 7 and the lower speed Mach 4 inlet configurations are presented in figure 18. For

Mach 7 conditions (fig. 18(a)), all of the captured flow is processed by the high-speed propulsion engine. For Mach 4 and below freestream conditions (fig. 18(b)), the low-speed inlet cowl is open with part of captured airflow being split between the low-speed and high-speed inlets. At these conditions, the low-speed inlet is supplying airflow to the turbofan, which provides a significant part of the thrust.

The design of the low-speed inlet and its integration into the high-speed inlet are presented in figures 19 to 27. Figure 19 shows the third ramp of the high-speed inlet rotated to several positions. Since the inlet design described in this design report was not based on a particular aircraft or mission, specific sizing requirements for the low and high-speed systems were unavailable. However, the approach was to integrate the low-speed inlet while maximizing low-speed capture airflow and providing a reasonable design with respect to variable geometry and mechanical feasibility. This approach required the rotation of the intended cowl surface (3rd ramp of the high-speed inlet) to a location where the leading edge (low-speed cowl lip) would be just downstream of the oblique shock from the second ramp of the high-speed inlet at Mach 4 as shown in figure 19. This provides maximum capture airflow without ingestion of oblique shocks from the upstream compression system (inlet overspeed). The next part of the inlet design effort was to develop an inlet with contours that would allow the cowl lip to be rotated about a hinge located at (near) the high-speed inlet shoulder, provide the capability of closing for flight conditions greater than Mach 4, and prevent interference of the internal contour of the cowl surface with the inlet shoulder of the low-speed inlet when the cowl was fully closed. This problem is illustrated in figures 20 and 21. In figure 20, the low-speed inlet internal cowl contour is shown at several angles of rotation. A cowl rotation from the Mach 4 design position of 0° to a closed rotation position of 11° results in the internal cowl surface of the low-speed inlet nearly touching the inlet ramp shoulder. This near-interference can be seen more clearly in figure 21. The internal cowl surface presented in figures 20 and 21 was developed using an iterative design process in which several inlet design contours were evaluated to assess their suitability for a rotation to cowl closure and avoidance of interference with the ramp surface at a location other than at the cowl lip. For a model sized as the NASA large-scale inlet, the clearance distance between the cowl internal surface and ramp shoulder when the cowl lip is touching the ramp surface would be approximately 1/8 in. This dimension is based on an assumption that a hinge diameter of about 3/8 in. would be used in the mechanical design of the model. A smaller hinge dimension could place the surface even closer. Although the influence is minor, the selected hinge diameter affects the clearance dimension and also the rotation angle that is required to close the cowl from the design Mach 4 position to closed.

The aerodynamic design of the inlet that was selected as meeting the criteria (closeable with no surface contact other than at the cowl lip) is presented in figures 22 and 23. Surface contours and aerodynamic characteristics of the supersonic diffuser are presented in figure 22 in a fashion analogous to that of figure 5. Numerical details of the Mach 4 inlet design are presented in figure 23. The initial ramp wedge angles (6.5° and 12.5°) are set by the angles used for the high-speed inlet design. An internal low-speed inlet cowl angle of 3.5° was selected. This angle results in 9° of compression (12.5° to 3.5°) through the cowl shock. With possible minor variations from the theoretical hinge center at the shoulder point as a result of the influence of the hinge diameter on rotated positions, the 3.5° internal angle provides a cowl lip with an included angle of 5°. Correct positioning of a hinge at the shoulder is presented in figure 24. Rotation about hinges of different diameters will result in minor changes in the final contours of the inlet surfaces; however, these changes are not large enough to significantly alter the aerodynamics of the inlet. The design constraints dictated by the closing of the low-speed inlet and the integration of the low-speed inlet into the high-speed hypersonic inlet greatly influence (compromise) the design of the low-speed inlet. Evaluation of the static pressure distribution in figure 22 indicates a small amount of compression (low pressure rise) from the cowl surface until a station near x/H_c of 4.5. Downstream of this station the pressure increases rather quickly to the inlet throat (x/H_c of about 5.5). In a typical inlet design, the design would be adjusted to provide a smoother, nearly parabolic pressure rise to the throat. This compromise in the inlet design was necessary to prevent interference with the ramp shoulder during closing of the cowl. If the cowl surface turning was more aggressive than the turning shown in figure 22, and also shown in figures 20 and 21, the cowl surface would hit the ramp shoulder

before reaching the close-off position (cowl lip touching the ramp). The aerodynamic characteristic curves of figure 22 show a throat angle of 0° and a throat Mach number of 1.5. An inviscid throat Mach number of 1.5 was selected for the baseline inlet configuration instead of a more nominal value of 1.3 because of the predicted influence of large boundary layer (see fig. 25). About one-half of the estimated 22 percent throat blockage due to boundary layer was offset by designing for the increased inviscid throat Mach number. It was assumed that the remainder of the blockage would be managed by inlet bleed. For comparison purposes, an additional Mach 4 inlet design with an inviscid throat Mach number of 1.3 was developed as part of the design study. Description of this design is presented in a later section of the report.

Integration of the low-speed inlet into the high-speed inlet is illustrated in figures 26 and 27. Two inlets, a low-speed inlet and a high-speed inlet, as shown in figure 26(a) were defined. The two inlets were to be integrated into a single dual-flow propulsion system resembling the sketch in figure 1. The low-speed inlet was integrated into the high-speed inlet as shown in figure 26 (b). The low-speed inlet was scaled to fit into the high-speed inlet with: (1) the ramp surfaces of the low-speed inlet matching the ramp surfaces of the high speed inlet, and (2) the scaling defined such that the low-speed cowl lip was on or very near the oblique shock from the intersection of the two inlet ramps. For the design/scaling of the low speed inlet, the cowl lip was positioned a very small distance downstream of the oblique shock. The method of characteristics net for each of the two inlets is presented in figure 27. The individual inlets are shown in figures 27(a) and 27 (b), and the combined integrated configuration is presented in figure 27 (c). The supersonic diffusers of the dual inlet system were defined. The next step in the design process is to define a subsonic diffuser for the low-speed inlet.

Inlet Sizing and Subsonic Diffuser

Sizing of the inlet requires an airflow demand for the engine and estimated inlet performance and bleed requirements. A generic turbofan engine airflow demand schedule (defined in terms of engine face Mach number) was supplied by NASA (fig. 28). At the low-speed inlet design condition of Mach 4.0, inlet performance levels of 0.647 total pressure recovery and 0.1023 bleed mass-flow ratio were selected to use for inlet sizing. These values for inlet performance and an engine face Mach number of 0.15 define the relationship between the inlet capture and the engine face diameter. If the engine size is known, this capture size with the previously designed supersonic diffuser can be used to define/size all other inlet components. This exercise provides a low-speed inlet capture area to engine face area (A_i/A_2) of 1.97562. As a result of the integration of the low-speed inlet into the Mach 7 inlet, the low-speed inlet captures a mass-flow ratio of 0.5719 (based on the inviscid Mach 7 theoretical capture area). Therefore, the theoretical inviscid capture area of the Mach 7 inlet is 3.4563 times the size of the turbofan engine area.

The subsonic diffuser design for the low-speed Mach 4 inlet is presented in figures 29 to 31. Vertical coordinates along the axial centerline of the duct are shown in figure 29, and diffuser aerodynamic characteristics are presented in figure 30. The equivalent conical diffusion half-angle is about 4°. This diffusion occurs from the throat station (x/H_c of 6.1039) to station x/H_c of 6.1039. The large area ratio in figure 30 is the result of the required diffusion to an engine face Mach number of 0.15 for the Mach 4 freestream condition. The local Mach number curve is based on an assumed effective throat Mach number of 1.3 (after adjustments for the 22 percent estimated throat blockage). The Mach number downstream of a normal shock at the nominal throat Mach number of 1.3 would be 0.786 at the entrance to the subsonic diffuser, as shown in the figure. Downstream of station 6.1039, the diffuser area is altered by filleting in the corners with elliptical arcs as presented in figure 31. Typically, the corner fairing from a rectangular cross-section to a round cross-section begins at a location just downstream of the last ramp hinge (x/H_c = 5.6553). This transitioning was moved downstream in the Mach 4 inlet to a station where all of the diffusion was complete. This downstream location (x/H_c = 6.1039) was chosen because of the desire to minimize model cost. Upstream extension of the contouring would result in increased hardware cost. In some inlets, long rectangular subsonic diffusers without the benefit of corner transitioning have resulted

in large regions of separation. The last section of the ramp is a part of the variable geometry ramp as indicated in figure 31. Inlet variable geometry is defined in the next section of this report.

Ramp and cowl coordinates for the Mach 4 inlet (including the centerline of the subsonic diffuser) are presented in figure 32. The coordinates are non-dimensionalized by the theoretical (inviscid) capture cowl lip height of the Mach 7 high-speed inlet ($y/H_c = 1.0$).

Variable Geometry

Variable geometry components of the hypersonic inlet design are identified in figure 33. The dual flow inlet has a variable ramp and rotating cowl lip segments (both low-speed and high-speed inlet ducts). Variable geometry requirements are presented in figure 34. Figure 34 shows the 3-segment variable geometry ramp that is used from takeoff to Mach 4. Required control of the ramp movement is indicated in the figure. The ramp system is anchored at the first hinge, which is located at the intersection of the first and second ramp sections of the high-speed inlet. The second ramp section is controlled by an actuation system that would have a similar function to the simplified actuation system that is shown in figure 34. This actuation system works as a parallelogram to keep the surface of the 3rd ramp parallel to the original design surface as the ramp section is collapsed to effect an increase the inlet throat area. The 4th ramp section then rotates about the 3rd hinge, with the downstream end controlled such that the 4th segment provides a smooth duct to the engine face. This generally requires that the section be directed into the overboard bypass cavity because the ramp motion (flattening) results in an increased overall axial length. Control of the aft end of the segment can be provided by a roller in a guide slot (fig. 35). This aft (4th ramp section) segment is the moveable ramp section that is shown in figure 31. A sketch of the downstream end of the inlet with an overboard-bypass is shown in figure 35. The variable ramp, bypass entrance with cascades, bypass plenum, and engine face are shown.

Surface contours for the inlet when configured for operation at Mach 7, 4, 3 and 2 are presented in figure 36. A nominal schedule for the 2nd ramp angle is presented in figure 37. This schedule is based on inviscid calculations and positions the ramp such that the cowl shock is on the ramp shoulder from Mach 3 to Mach 4. During low-speed inlet operation, the intent is to position the cowl in the Mach 4 position for operation from Mach 3 to 4. Below Mach 3 the most optimum inlet performance will probably require both ramp and cowl lip rotation. Optimum positioning will be determined during an experimental test program. Obviously, the scheduling of the inlet variable geometry will ultimately depend on the engine airflow demand schedule. Positioning the inlet to allow proper inlet operation and to also meet engine airflow requirements requires adjustment of several inlet parameters, including the ramp, the rotatable lip (spillage), bleed, and overboard-bypass airflow.

While the inlet system design reported herein is designed for mode transitioning at Mach 4, there is also an interest in investigating mode transitioning at Mach 3. Therefore, coordinates for Mach 3 operation are presented in figure 38. These coordinates are for the Mach 3 position of the second ramp per the schedule shown in figure 37. Mode transitioning at a selected Mach number maybe difficult to achieve because of changes in effective thrust and drag. Most likely the transition from one propulsion system to another will occur with some variation in flight Mach number, either while accelerating or decelerating.

Bleed is necessary if a high level of performance is expected for the low-speed inlet. Sketches that illustrate the bleed regions that were specified for the large-scale inlet model are presented in figures 39 to 43. All of the various bleed regions are shown in figure 39. The ramp has 5 bleed regions (RX, and R1 to R5). Bleed R1 is just upstream of the ramp shoulder. R2 is just downstream of the shoulder with R3 being located between R2 and the throat bleed (R4). The cowl has 2 bleed regions: C1 located at a similar station to R3 and a throat bleed C2. There are 3 bleed regions on the sidewall. SW1 is positioned to control the cowl sidewall glancing shock and the shock interaction in the ramp-sidewall corner. An additional bleed region (RX) was placed on the ramp at a station opposite the cowl lip. This bleed capability was located such that the interaction of a normal shock (caused by inlet unstart) with the ramp could be controlled with bleed. During mode transitioning, in which the low-speed inlet cowl lip is

rotated from the Mach 4 position to closed, the inlet will unstart. The effectiveness of the RX bleed in controlling the shock interaction and reducing transients in engine airflow will be determined. This bleed would normally be closed until activated as needed.

Details of the inlet bleed regions are presented in figures 40 to 43. The dimensions provided in these figures represent initial requirements. It was anticipated that small changes in location would occur during mechanical design of the model hardware. Bleed regions are composed of porous bleed plates with normal holes at 40 percent porosity that extend from bulkhead to bulkhead. Bleed sizing is based on information from reference 16 and bleed information in TechLand Research files. Each ramp and cowl bleed region extends from sidewall to sidewall, and sidewall bleed is extended in the vertical direction so that bleed can be removed from the sidewall for design and off-design (collapsed) ramp positions.

Sketches that illustrate some of the inlet configuration changes that are required during flight are shown in figures 44 to 46. Figure 44 presents the inlet configurations for takeoff, Mach 2 and Mach 3 conditions. At takeoff (fig. 44(a)) the second ramp is collapsed until the delta angle between ramp sections 1 and 2 is 0°. For Mach 2 (fig. 44(b)), both the ramp and low-speed cowl are moved to an appropriate position to provide the necessary capture flow and to provide acceptable performance. For Mach 3 (fig. 44(c)) the intent is to operate with the low-speed cowl lip in the Mach 4 design position with the ramp set such that the cowl shock intersects the ramp shoulder. This arrangement would require a second ramp angle of 9.96°. For Mach 3, other combinations of cowl lip and ramp positions may also provide acceptable performance levels. Figure 45 presents inlet configurations for operation during mode transition. Figure 45(a) shows the inlet as just prior to the start of mode transition, with the low-speed system operating at Mach 4. During mode transition, the inlet changes from the configuration of figure 45(a) to the inlet configuration of figure 45(b). The ramp position remains unchanged, the low-speed cowl lip closes, and the high-speed cowl lip rotates toward closed until acceptable high-speed inlet aerodynamics are achieved. Initial aerodynamic analysis indicates that a lip rotation of at least 7° will be required. A rotation of about 11° would align the internal cowl surface of the high-speed inlet with the external surface of the closed low-speed inlet. The inlet design is intended to also allow evaluation of mode transition at Mach 3. Therefore, a sketch of the inlet configured for transitioning at Mach 3 is presented in figure 45(c). During mode transition at Mach 3, the inlet configuration would change from the configuration that is shown in figure 44(c) to the configuration of figure 45(c). The dual-mode inlet was designed for transitioning at Mach 4. When this configuration is used for transitioning at Mach 3, the cowl lip must rotate through a greater angle than at Mach 4 because the ramp surface is positioned further away from the design cowl lip position (2nd ramp angle of 9.96° instead of 12.5°). Inlet configurations for operation from Mach 4 to 7 are presented in figure 46. The low-speed inlet is closed and the high-speed inlet cowl lip is positioned for the appropriate Mach number. The configuration shown in figure 46(b) represents the Mach 7 inlet design configuration.

Design Versatility

While the high-speed inlet design described herein utilizes a fixed cowl with a rotating lip, two-dimensional (2–D) inlet designs offer a significant amount of versatility. An inlet configuration that offers ease of modification is very important when attempting to develop a new and complex design. Two-dimensional type designs offer the capability of easily changing contours, compression, capture, cowl lip location, etc. They offer a variety of approaches to provide variable geometry, and have reasonably well-understood aerodynamic characteristics. While 2–D type designs can readily be changed and offer a variety of desirable options, three-dimensional (3–D) type configurations are not as easily changed or modified. If a change in compression or contouring is required for a 3–D configuration, a complete redesign is probably required. More importantly, if research hardware already exists for a 3–D configuration, a large portion of it may have to be almost completely replaced if significant changes are required. If a 2–D configuration modification is required, often a small part can be altered with less cost and a greater chance of success. Two possible variations on the basic design (of many that may be considered) that may offer advantages for some vehicles and/or integration schemes are described below.

Translating/Rotating Cowl

One example of an alternate variable geometry that is available for a 2–D inlet configuration is shown in figure 47. This option is a translating (rather than rotating) cowl. The sketch of figure 47(a) illustrates the translating cowl concept. Typically, the cowl would be translated along a track that would include opening up the high-speed inlet and moving the cowl lip to a more downstream station. Possible movement of the lip is illustrated in figure 47(b). One desired cowl position (translation A) might capture more airflow and position the cowl shock on the inlet shoulder. Translation B might be along a capture streamline, providing the same capture but better positioning the cowl shock on the shoulder. Cowl translation also provides the capability of adjusting the internal flow passage for blockage due to large incoming boundary layers. The optimum cowl design would include cowl translation and a rotatable cowl lip. Required cowl translation, amount and direction, would be based on the requirements for the high-speed propulsion system. A high-speed inlet translatable cowl also offers the option of reducing drag at low speeds (below the transition Mach number) by positioning the cowl near/against the ramp surface and significantly reducing the frontal blockage area.

Variable Geometry Low-Speed Cowl

Typically, throat area variation for a 2–D inlet is provided by a variable ramp. However, for a highly integrated inlet system in which the low-speed inlet is integrated into the high-speed inlet, the variable geometry ramp occupies valuable fuselage volume that could be used for fuel or payload. An alternate to the variable-geometry ramp is presented in figure 48. The variable geometry concept depicted in the figure does not impact the volume of the vehicle fuselage, because the ramp is fixed and the area underneath is not needed for the ramp actuation system. This design option could offer significant improvements to the design of the flight vehicle. The inlet sketch in this figure includes a rotatable lip and a cowl variable geometry system that provides a similar function to a variable geometry ramp. This variable-geometry cowl surface moves in such a way that the inlet throat area is opened up for off-design operation. Figure 48(a) presents a sketch of the concept when the inlet is configured for Mach 4 operation. The inlet duct is the same as shown in previous figures for the Mach 4 condition. However, in addition to the rotating cowl lip that has been identified for the basic inlet concept, the configuration of figure 48(a) includes an additional hinge on the cowl lip and an additional hinge just downstream of the inlet throat. The operation of this additional variable geometry capability is illustrated in figure 48(b). The first cowl segment rotates about the upstream hinge. The second cowl segment would rotate about the second hinge and the increased length (due to flattening of the cowl) would be accommodated by a sliding joint at the downstream end. The variable-geometry cowl would be used between Mach 3 and 4. For operation below Mach 3, the variable geometry cowl and the cowl lip rotation would be used. Coordinates for the Mach 3.0 off-design configuration are presented in figure 49. Hinge locations are at an x/H_c of 4.05557 and 5.17936. This configuration was not the major focus of the design defined herein; therefore, a more detailed design process would be required to optimize the location of the hinges. A comparison of the cowl coordinates at the design condition of Mach 4 and the collapsed (Mach 3) cowl position is presented in figure 50.

Inlet Test Models

Small Scale Inlet Model

Photographs and sketches of the small-scale model are presented in figures 51 to 56. Mechanical design and fabrication of the small-scale research model was performed at NASA Glenn Research Center. The small-scale model has a high-speed inlet capture height of 5.001 in. (inviscid 4.943 in.) and a width of 1.821 in. The two cowl lip lips are actuated by arms extending from an actuation system mounted outside the tunnel as shown in figure 51(b). Pictures of the wall mounted model that show the low-speed

cowl in open and closed positions are presented in figures 52 and 53, respectively. Details of the internal surfaces and bleed systems can be seen in figure 54. External views are shown in figures 55 and 56, and sketches that provide additional model details are presented in figures 57 and 58.

Large Scale Inlet Model

Pictures and sketches of the large-scale model are presented in figures 59 to 62. Mechanical design and fabrication of this research model are being performed under a NASA contract by a large aerospace research hardware vendor. The large-scale model has a high-speed inlet capture height of 32.957 in., a width of 12.0 in., and will be approximately 30 ft long. This model will have rotatable cowl lips, both low-speed and high-speed, a variable geometry ramp, and variable geometry exit controls for all bleed regions. It will also include all of the subsystems (such as an overboard bypass) that are necessary to develop inlet controls and to allow mode transitioning testing with operating engines. The model will be strut mounted in the 10×10 SWT and will be installed with a large trapezoidal plate that was used during testing of a large-scale Mach 5 inlet (ref. 12). A series of research tests are planned. These include: (1) aerodynamic test to assess inlet performance and mode transitioning procedures, (2) controls development, and (3) mode transition testing with operating engines. One of the objectives of the test is to mate the inlet system with a turbofan engine and dual-mode scramjet hardware that will be made available from other hypersonic propulsion research efforts. An example of developing an inlet with high performance and operability and testing with an operating engine is presented in references 17 to 19. Because the size of the existing scramjet hardware required a smaller high-speed inlet duct, the contours of the high-speed inlet were altered from the design presented herein to accommodate the integration of the high-speed engine (see the "design adjustment for large-scale inlet model" section of this report**.** Otherwise, the aerodynamic designs of the large- and small-scale inlets are substantially the same.

Inlet Design (Inviscid Throat Mach Number of 1.3)

For comparison purposes a Mach 4 inlet with an inviscid throat Mach number of 1.3 was also developed during the design study. This design took into consideration all of the integration issues that impacted the design of the basic configuration (Mach 4 inlet with an inviscid throat Mach number of 1.5). In particular, the compression inside the low-speed inlet was delayed to a location downstream of the shoulder point. This design consideration was necessary to prevent the internal cowl surface from hitting the ramp shoulder when the cowl was rotated to a closed position. Contours and aerodynamic characteristics for this alternate inlet design are presented in figure 63. These contours are in non-dimensional coordinates with the divisor being the cowl height of the basic low-speed inlet (H_{cls}), before it is scaled to fit within the high-speed inlet as shown in figure 26. This height is different than the H_c (inviscid cowl height for the high speed inlet) that is used for most of the report. The difference between the inlets designed for throat Mach numbers of 1.5 and 1.3 can be evaluated by comparing figures 22 and 63, respectively. Plots that provide a comparison of several inlet parameters are presented in figures 64, 65, and 66. A plot of cowl contours is presented in figure 64. In this plot the dimensioning of the contours has been changed to the integration of the low-speed inlet into the Mach 7 high-speed inlet. As a result the non-dimensioning constant is H_c. A comparison of the cowl contours for the two configurations (M_{throat} = 1.5 and 1.3) is presented in figure 65. The contours of figure 65 show that the configuration with a throat designed for Mach 1.3 deviates from the contour of the Mach 1.5 throat design configuration at an x/H_c of about 4.4. Downstream of the Mach 1.3 configuration throat station (x/H_c of 4.83), the new inlet cowl surface is faired into the cowl surface of the original basic cowl configuration. The relative location of the ramp shoulder to the cowl surface variation for the two configurations is shown in figure 65. As shown in this figure, the re-contouring of the cowl is delayed to a location downstream of the shoulder. This design approach will allow the cowl to rotate to the closed position (like the Mach 1.5 throat configuration) without the cowl internal surface hitting the ramp shoulder. In fact, redesigning the low-speed inlet to provide an inviscid throat Mach number of 1.3 only involved

changing the cowl contour as presented in figure 64. The ramp contours for the two low-speed inlet configurations were the same. Again, this redesign shows the versatility of a 2–D inlet design. The compression was easily changed by re-contouring a small portion of the cowl surface. Local inviscid Mach numbers near the cowl surface for the two configurations are presented in figure 66. This plot shows the change in Mach number distribution beginning at the x/H_c of 4.4. Cowl coordinates for the inlet configuration that was designed for an inviscid throat Mach number of 1.3 are presented in figure 67.

If an inlet is designed without adjustment of the surfaces for boundary layer, the required adjustment of the internal geometry can be achieved by a slight re-positioning of the ramp position. The optimum ramp position can then determined during an experimental test program.

Summary of Results

An aerodynamic design of a 2–D inlet system for an airbreathing, dual-mode, hypersonic propulsion system has been completed. This inlet design includes a low-speed Mach 4 inlet that is integrated into the flow path of a Mach 7 high-speed inlet. The low-speed inlet was designed to provide high performance from takeoff to Mach 4 flight conditions. At Mach 4, the low-speed inlet is closed to allow operation of the high-speed propulsion system from Mach 4 to Mach 7. Integration of a low-speed inlet in the flow field of a high-speed inlet with multiple flow streams, large boundary layers, extensive variable geometry, and engine mode transitioning presented multiple challenges. The design includes consideration of all of the normal subsystems required by traditional supersonic mixed-compression inlets. These systems include a subsonic diffuser, multiple bleed regions, overboard-bypass, controls, stability system(s), and vortex generators. The design effort resulted in the identification of an aerodynamic design that offers high performance and operability and is compatible with a realistic and practical variable geometry system. The inlet configuration developed in the design effort has been incorporated into the mechanical design and fabrication of two mode-transitioning research models—small-scale and large-scale. Testing of these inlets will provide both inlet performance assessments and mode transitioning data.

Specific results from the inlet design study are:

Inlet design study results indicate that a viable dual-mode inlet can be designed for a hypersonic airbreathing vehicle that operates from takeoff to Mach 7.

An aerodynamic design of a 2–D, dual-flow, Mach 7 capable inlet system with an integrated low-speed inlet/propulsion system for mode transitioning research has been completed. The design includes a low-speed inlet designed for operation to Mach 4 and a high-speed Mach 7 inlet. Both low-speed and high-speed inlets have variable geometry (rotating) cowl lip sections, and the low-speed inlet has a variable geometry ramp.

The Mach 7 inlet was designed to accept airflow from takeoff to Mach 7. This inlet ingests part of the dual-flow inlet airflow until the low-speed inlet is closed off at the end of mode transitioning (Mach 4). After mode transitioning occurs, the proper amount of airflow capture for flight from Mach 4 to 7 is provided to the high-speed propulsion system by positioning of the variable geometry cowl lip.

The aerodynamic design of a high-performance, low-speed, Mach 4 inlet was completed. This inlet operates from take-off to Mach 4, where the low-speed accelerator engine (turbofan) is shut down and the low-speed inlet is closed. A variable geometry cowl lip is used during engine mode transitioning, when airflow to the low-speed engine is shut off. Variable geometry and bleed requirements have been identified. A variable geometry ramp and rotatable cowl lip provides the inlet variability that is necessary to capture the required airflow at off-design flight conditions.

Design considerations for all of the inlet subsystems that are necessary for proper propulsion system operation during normal flight and for mode transitioning, in both directions—accelerating to higher Mach numbers or decelerating to lower Mach numbers—were included.

Although the low-speed inlet was designed for mode transitioning at Mach 4, the design configuration can also be utilized to investigate mode transitioning at Mach 3.

A bleed system necessary for high low-speed inlet performance has been identified.

Additional versatility that can be incorporated in a 2–D hypersonic inlet has been identified. A 2–D type inlet geometry can be easily changed to include other variable geometry concepts such as a translating cowl for the high-speed inlet or a collapsible cowl for the low-speed inlet.

An alternate Mach 4 inlet with an inviscid throat Mach number of 1.3 has been designed to provide the same integration characteristics as the basic inlet that had an inviscid design throat Mach number of 1.5. This design was accomplished by a simple re-contouring of the cowl surface with the ramp geometry for the two inlets remaining the same. This redesign also provides an indication of the versatility of a 2–D-type inlet.

References

1. Pittman, James L.: Hypersonic Project Overview. NASA Fundamental Aeronautics Program 2007 Annual Meeting. New Orleans Riverside Hotel. October 30–November 1, 2007.
2. Auslender, Aaron H. and Walker, James F.: An Overview of Hypersonic Airbreathing Propulsion Technical Discipline. NASA Fundamental Aeronautics Program 2007 Annual Meeting. New Orleans Riverside Hotel. October 30–November 1, 2007.
3. Suder, Kennneth L.: TBCC Fan Stage Operability and Performance. NASA Fundamental Aeronautics Program 2007 Annual Meeting. New Orleans Riverside Hotel. October 30–November 1, 2007.
4. Canan, James W.: Breathing New Hope into Hypersonics. Aerospace America, pp. 26–31. November 2007.
5. Wilson, J.R.: High Hopes for HiFire Scramjet. Aerospace America, pp. 32–37. November 2007.
6. Saunders, John D.; Frate, Franco C.; and Wendt, Bruce J.: Inlet Design Methods for an X43B Demonstrator Vehicle. Presented at the 27th JANNAF Airbreathing Subcommittee Meeting. December 2003.
7. Saunders, John D. et al.: Initial Screening Results of a Small-Scale Inlet Mode Transition Experiment and progress toward a Large-scale IMX Testbed. NASA Fundamental Aeronautics Program 2007 Annual Meeting. New Orleans Riverside Hotel. October 30–November 1, 2007.
8. Albertson, Cindy W.; Emami, Saied; and Trexler, Carl A.: Mach 4 Test Results of a Dual-Flowpath, Turbine Based Combined Cycle Inlet. AIAA–2006–8138.
9. Perkins, E.W.; Rose, W.C.; and Horie, G.: Design of a Mach 5 Inlet System Model. NASA CR–3830, August, 1984.
10. Watts, J.D. et al.: Mach 5 Cruise Aircraft Research. NASA CP–2398, Volume II, 1985.
11. Cassidy, M.D.: Performance Sensitivities of a High Altitude Mach 5 Penetrator Aircraft Concept. NASA CR–3932.
12. Weir, L.J. and Sanders, B.W.: Investigation of a Two-Dimensional, Mixed-Compression Mach 5.0 Inlet. NASA/CR—2004-213122; July 2004.
13. TechLand Research, Inc.: Mode Transition Variable Geometry for High Speed Inlets for Hypersonic Aircraft. SBIR Phase I. July 2005.
14. Van Wie, David M.: Scramjet Propulsion. AIAA Volume 189, Chapter 7.
15. Anderson, B.H.: Design of Supersonic Inlets by a Computer Program Incorporating the Method of Characteristics. NASA TN D–4960. January 1969.
16. McLafferty, G.: Pressure Losses and Flow Coefficients of Slanted Perforations Discharging from within a Simulated Supersonic Inlet. UTRC R–0920–1, Dec. 1958.
17. Sanders, Bobby W. and Mitchell, Glenn A.: “Throat-bypass Bleed Systems for Increasing the Stable Airflow Range of a Mach 2.50 Axisymmetric Inlet with 40-Percent Internal Contraction.” NASA TM X–2779.
18. Sanders, Bobby W: Dynamic Response of a Mach 2.5 Axisymmetric Inlet and Turbojet Engine with a Poppet-Valve Controlled Inlet Stability Bypass System when Subjected to Internal and External Airflow Transients. NASA TP–1531.

19. Sanders, Bobby W: “Turbojet -Exhaust-Nozzle Secondary-Airflow Pumping as an Exit Control of an Inlet-Stability Bypass System for a Mach 2.5 Axisymmetric Mixed-Compression Inlet.” NASA TP–1532.
20. Witte, David W. et al.: Propulsion Airframe Integration Test Techniques for Hypersonic Airbreathing Configurations at NASA Langley Research Center. 39th AIAA/ASME/SAE/ASEE Joint Propulsion Conference, July 2003.
21. Simmons, J.M. and Weidner, E.H.: Design of Scramjet Inlets with Rectangular Capture Cross-section and Circular Throat. NASA TM–87752, June 1986.
22. Sanders, B.W. and Weir, L.J.: 2–D Inlet Test in NASA Lewis Research Center 1xl SWT. Presented at Third National Aero-Space Plane Technology Symposium: Moffett Field, CA; June 2–4, 1987; Paper Number 12.
23. Fernandez, R.; Sanders, B.W.; and Weir, L.J.: Small Scale Multi-Module Inlet Test Results, $M_o = 3.5$. Presented at Fifth National Aero-Space Plane Technology Symposium; Hampton, VA: October 17–21, 1988: Paper Number 46.
24. Sanders, B.W. and Weir, L.J.: “DRACO Flowpath Hypersonic Inlet Design,” Final report for NASA MSFC Purchase Order H–31407D, December 1999.

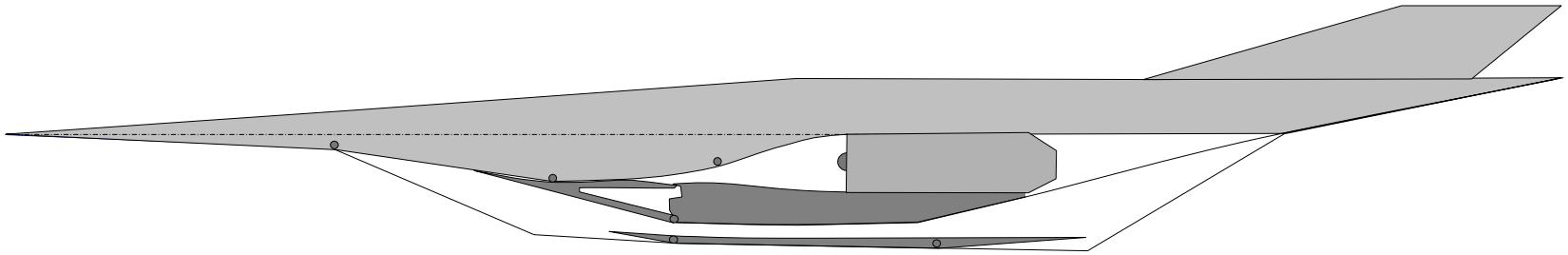

Low-speed inlet Design Challenges

- The high-speed aerodynamic lines become a constraint on the design of the low-speed inlet.
- Two propulsion systems operating over different Mach number ranges with very different airflow requirements dominate the inlet system design.
- The low-speed inlet must include variable geometry as a means of matching airflow variations of the turbine engine (variable cowl and probable variable ramp).
- Acceptable inlet performance and operability must be provided.
- One characteristic that represents an extreme challenge to the low-speed design is ingestion of the forebody boundary layer.

Figure 1. – Mach 7 dual-mode propulsion system.

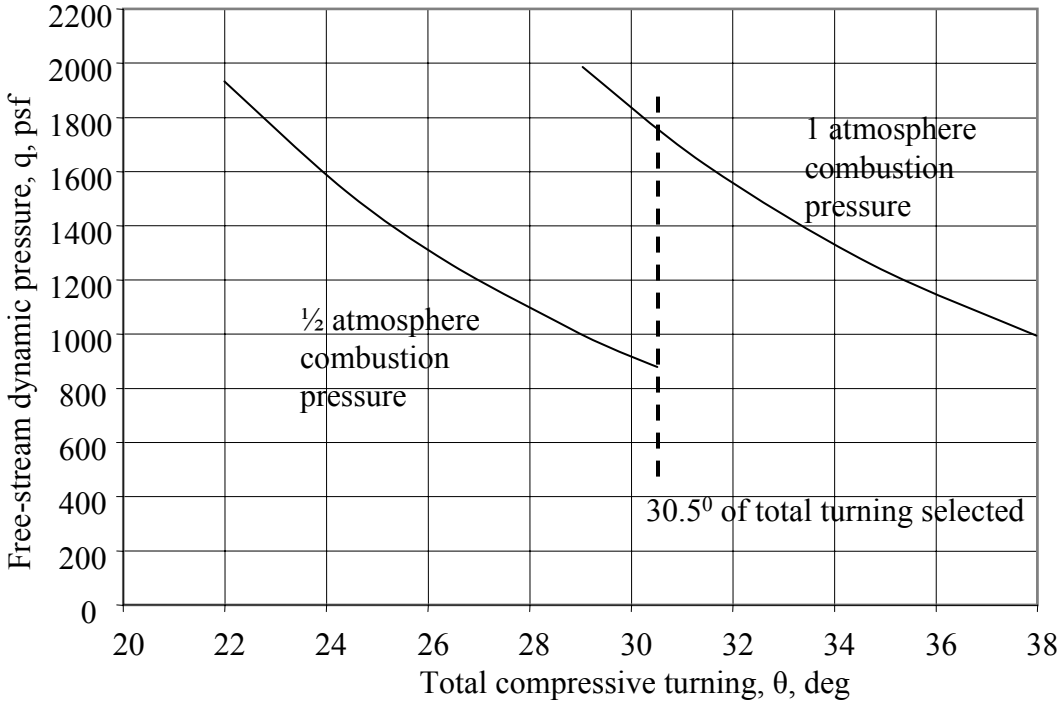

Figure 2. - Total compressive turning and dynamic pressure required for 1/2 atmosphere combustor pressure (left curve) or 1.0 atmosphere (right curve).

Reference: Scramjet Propulsion AIAA Volume 189, Chapter 7, David M. Van Wie

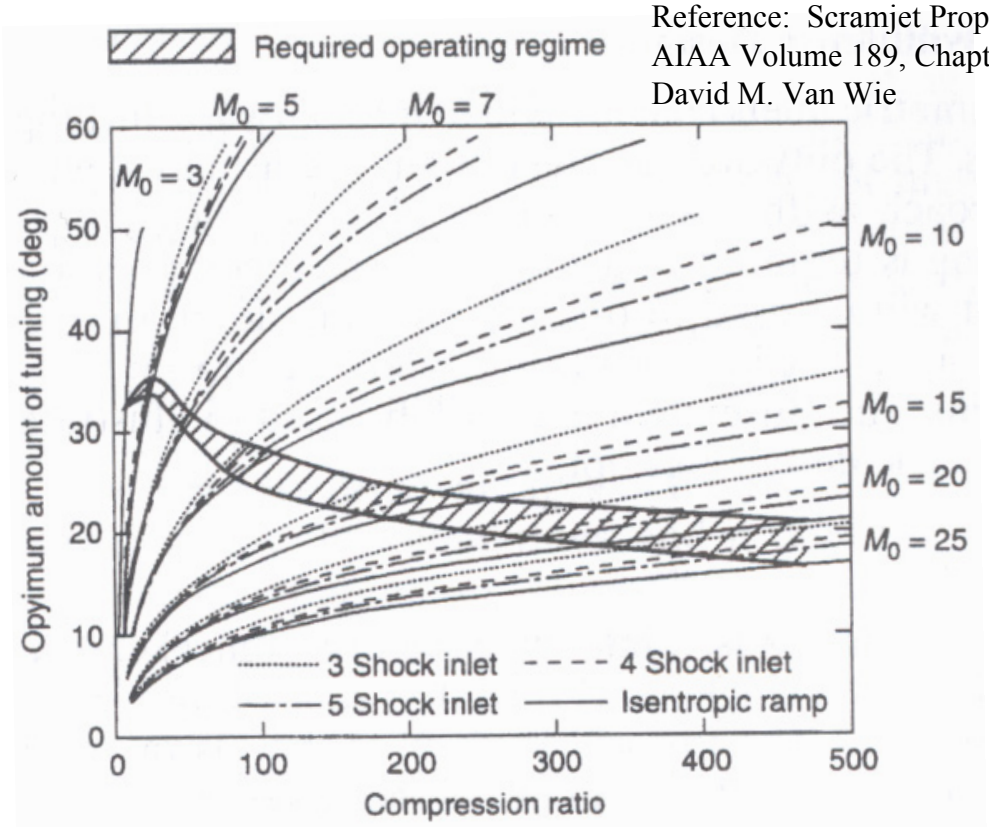

Figure 3. - Optimum inviscid compressive turning for scramjet inlets to provide one-half atmosphere static pressure in inlet.

Hypersonic Inlet Design

- Design Mach number of 7.0
- Compressive turning (including cowl shock) of 30.5^0
  - 3 compression wedges: 6.5^0, 12.5^0, 19.5^0 (deltas of 6.5^0, 6^0, and 7^0)
    - includes 4^0 vehicle angle-of-attack
- Cowl shock cancelled on the shoulder
  - Actual shoulder can be rounded
- Rotating cowl lip for Mach 4 to 7 operation
- Designed for mode transition at Mach 4

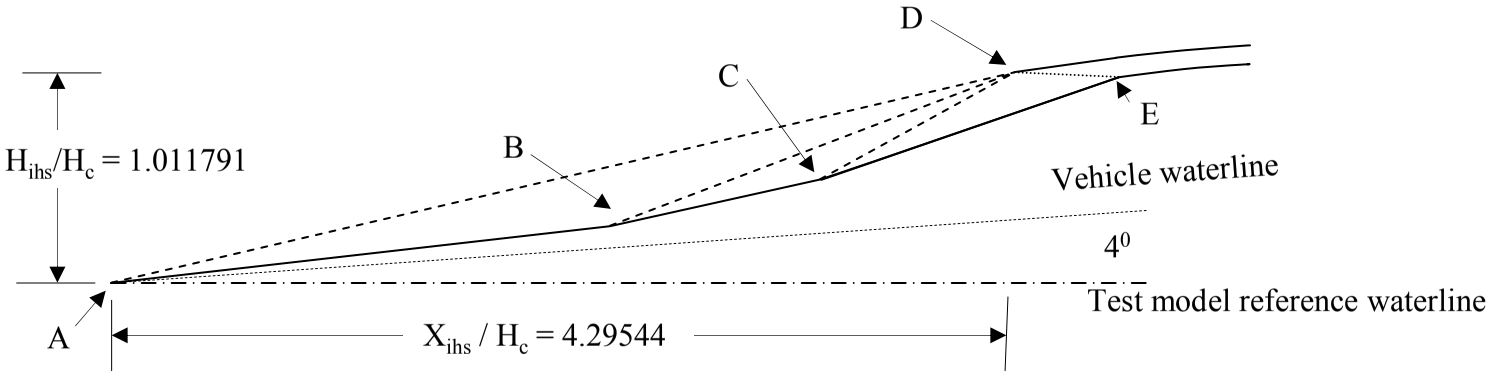

Points	x/H_c	y/H_c
A	0	0
B	2.36514	0.2695
C	3.38978	0.49661
D	4.29544	1.0
E	4.75471	0.980045

1.011791 ← Cowl height after adjustment for boundary layer influence

Figure 4. – Compression system for hypersonic Mach 7 inlet.

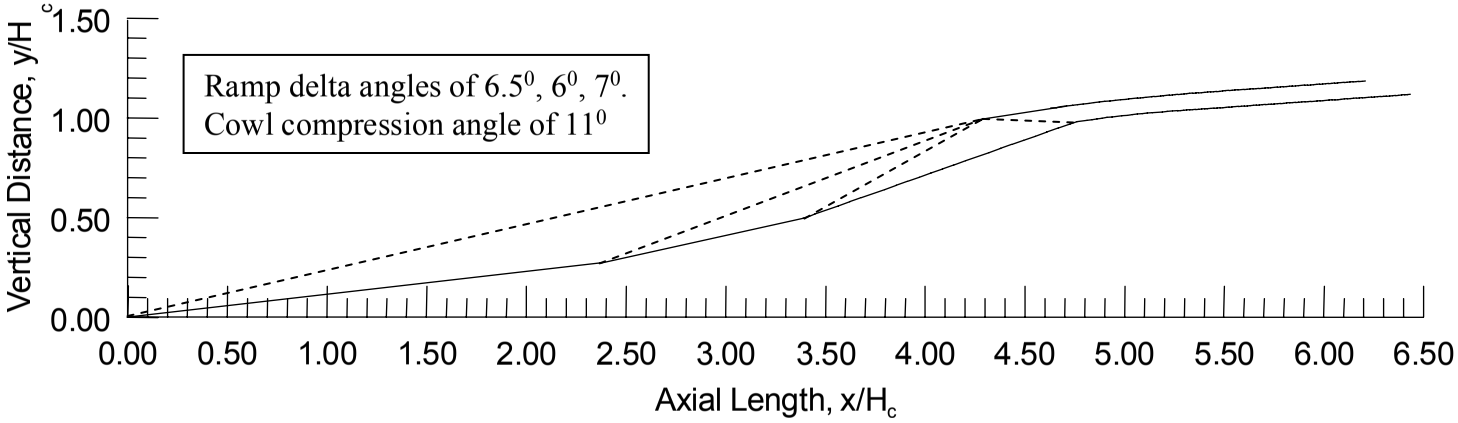

(a). Inlet surface contours and shock system.

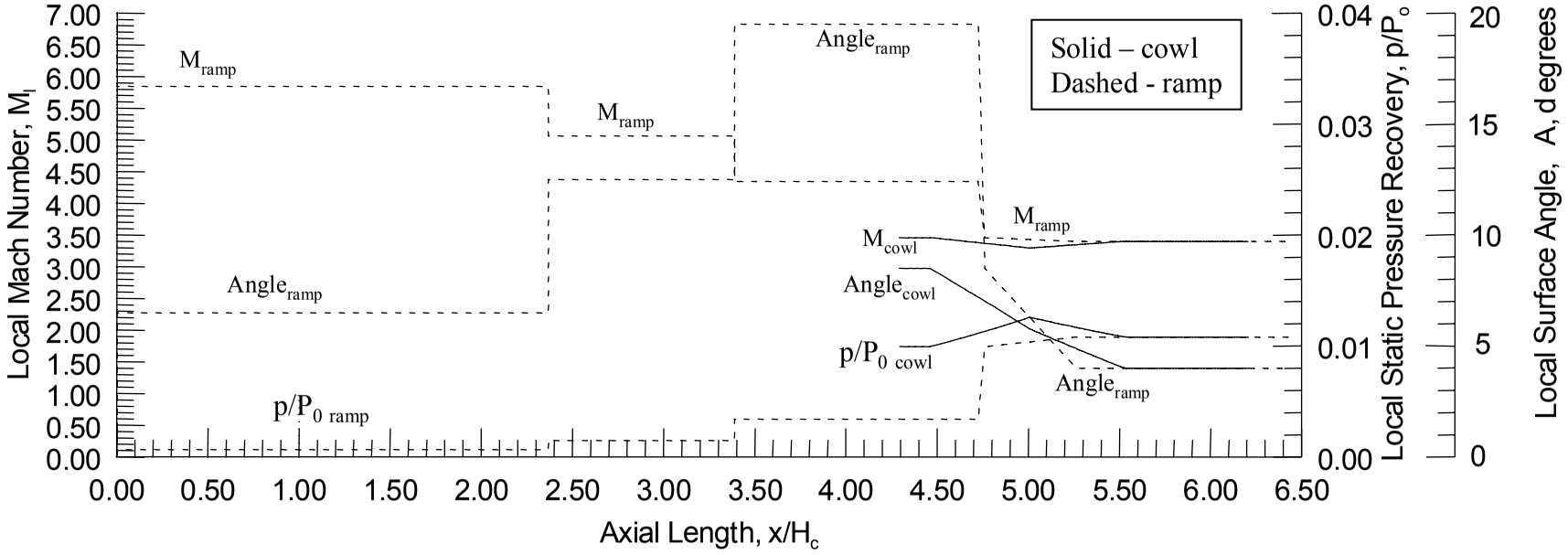

(b). Inlet aerodynamics at design (Mach 7) conditions.

Figure 5. – Compression system for Mach 7 inlet including design of internal duct and inlet aerodynamic characteristics.

Two-dimensional Mach 7 Inlet					
		Ramp 1	Ramp 2	Ramp 3	Cowl
Incoming Mach number		7.0	5.84405	5.06198	4.34394
Deflecting surface angle (degrees)		6.5	12.50000	19.50	8.5
Compression angle (degrees)		6.5	6.0	7.0	11.0
Surface leading edge (axial), x/H_c		0.0	2.36514	3.38958	4.29520
Surface leading edge (vertical), y/H_c		0.0	0.26947	0.49659	1.0
Surface trailing edge (axial), x/H_c		2.36514	3.38958	4.75443	
Surface trailing edge (vertical), y/H_c		0.26947	0.49659	0.97991	
Local Mach number		5.84405	5.06198	4.34394	3.45879
Shock recovery		0.89990	0.94856	0.94667	0.88472
Local recovery, P_l/P_0		0.89990	0.85361	0.80809	0.71493
Capture, m_i/m_0					1.0

Figure 6. – Theoretical aerodynamics of high-speed Mach 7 inlet.

Ramp Coordinates for Mach 7 Inlet

x/Hc	y/Hc		x/Hc	y/Hc
0	0		5.215732	1.032545
2.365363	0.2695		5.241046	1.034464
2.365363	0.2695		5.266371	1.036287
3.389777	0.496614		5.281569	1.03735
3.389777	0.496614		5.296767	1.038413
4.75471	0.980045		5.311966	1.039475
4.762012	0.981054		5.327165	1.040538
4.787123	0.984758		5.342363	1.0416
4.812244	0.98836		5.357561	1.042663
4.837378	0.991862		5.37276	1.043726
4.862523	0.995269		5.387958	1.044788
4.887679	0.998574		5.403157	1.045851
4.912846	1.001784		5.418356	1.046915
4.938024	1.004892		5.433554	1.047977
4.963214	1.0079		5.448753	1.04904
4.988415	1.010812		5.46395	1.050102
5.013627	1.013624		5.479149	1.051165
5.038851	1.016334		5.494348	1.052228
5.064085	1.018949		5.509546	1.05329
5.089331	1.021463		5.524745	1.054353
5.11459	1.023875		5.539944	1.055416
5.139857	1.026193		5.555141	1.056478
5.165138	1.028409		5.56395	1.057094
5.190429	1.030525			

Cowl Coordinates for Mach 7 Inlet (original inviscid contours)

x/Hc	y/Hc		x/Hc	y/Hc		x/Hc	y/Hc
4.295445	1		4.901907	1.082176		5.269031	1.117713
4.344043	1.007263		4.928634	1.085098		5.283759	1.118962
4.383253	1.013125		4.955271	1.087954		5.298534	1.120196
4.422457	1.01898		4.981825	1.090729		5.313311	1.121425
4.46166	1.024841		5.008301	1.093439		5.328144	1.12264
4.46166	1.024841		5.022557	1.094875		5.342995	1.123847
4.489943	1.029034		5.036847	1.096298		5.357861	1.12504
4.518118	1.033143		5.051152	1.097714		5.37277	1.126223
4.546179	1.037167		5.065499	1.099125		5.387685	1.127397
4.574138	1.041103		5.079853	1.10052		5.402653	1.12856
4.601987	1.044966		5.094254	1.101905		5.417622	1.129709
4.629736	1.04874		5.108657	1.103276		5.432644	1.130849
4.657379	1.052436		5.123115	1.104642		5.447686	1.131975
4.684927	1.056049		5.137591	1.106		5.462741	1.133093
4.712379	1.059585		5.152079	1.107339		5.477837	1.134201
4.739729	1.063044		5.166614	1.108673		5.492946	1.135295
4.754648	1.064884		5.181149	1.109997		5.5081	1.136383
4.766985	1.066426		5.195736	1.111312		5.523263	1.137451
4.794154	1.069725		5.210326	1.112612		5.53847	1.13852
4.821223	1.072952		5.224972	1.113903		5.553668	1.139583
4.848205	1.076103		5.239635	1.115185		5.56395	1.140302
4.875103	1.079177		5.254309	1.116455			

Figure 7. – Inviscid surface coordinates for the high-speed Mach 7 inlet, original inlet design before adjustment for boundary layer or matching to existing hardware.

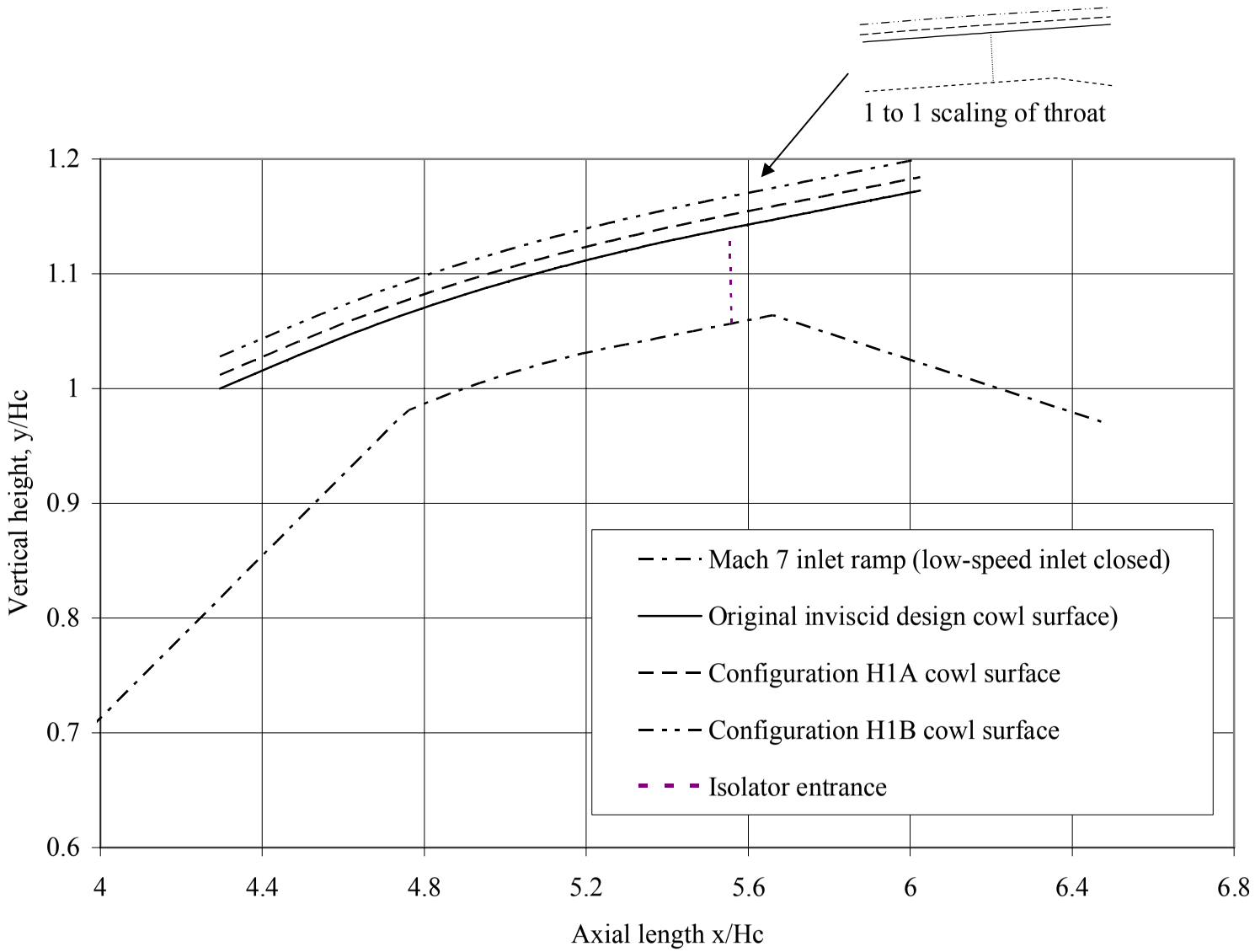

Figure 8. – Comparison of resized cowl for the H1A and H1B configurations to the original inviscid cowl contours.

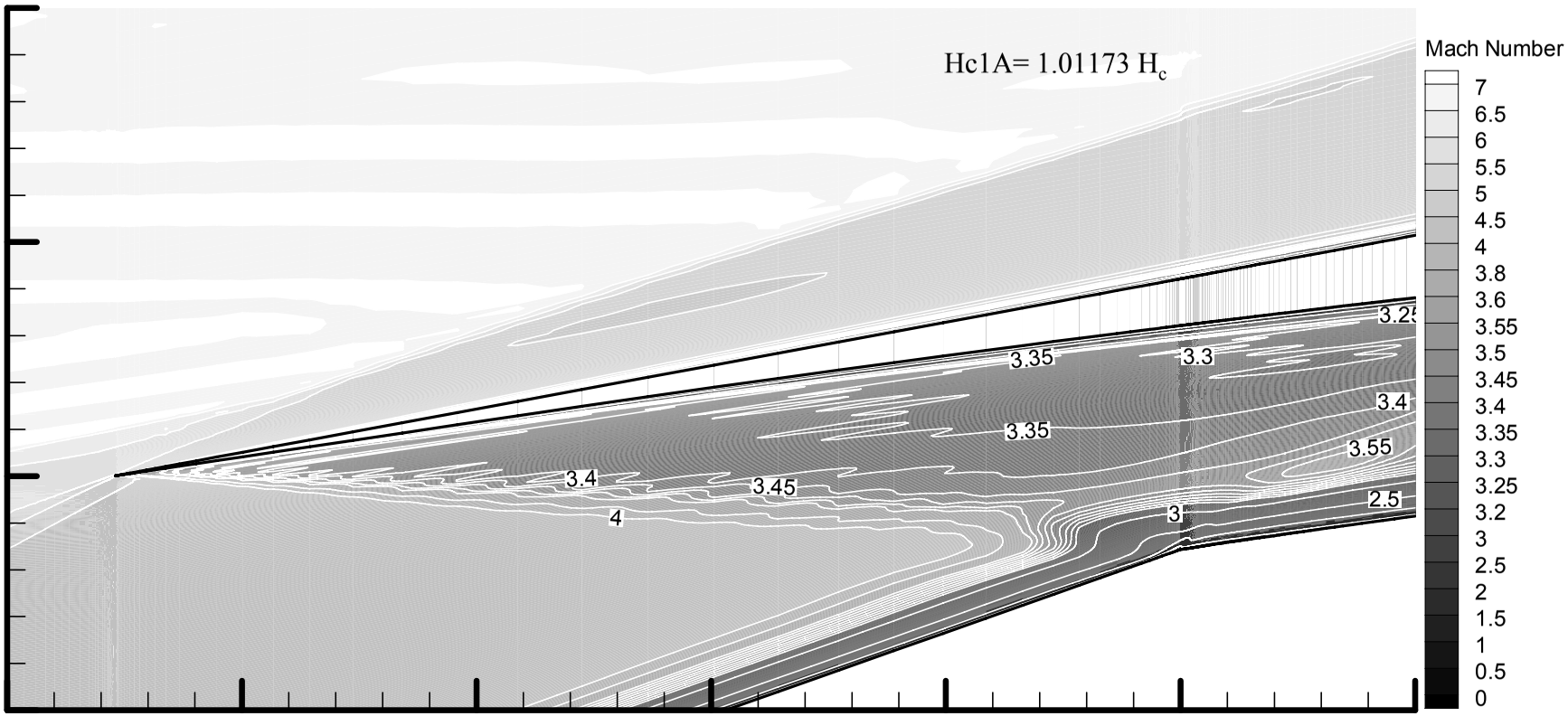

Figure 9. – Mach number contours in the vicinity of the cowl shock for nominal cowl configuration H1A.

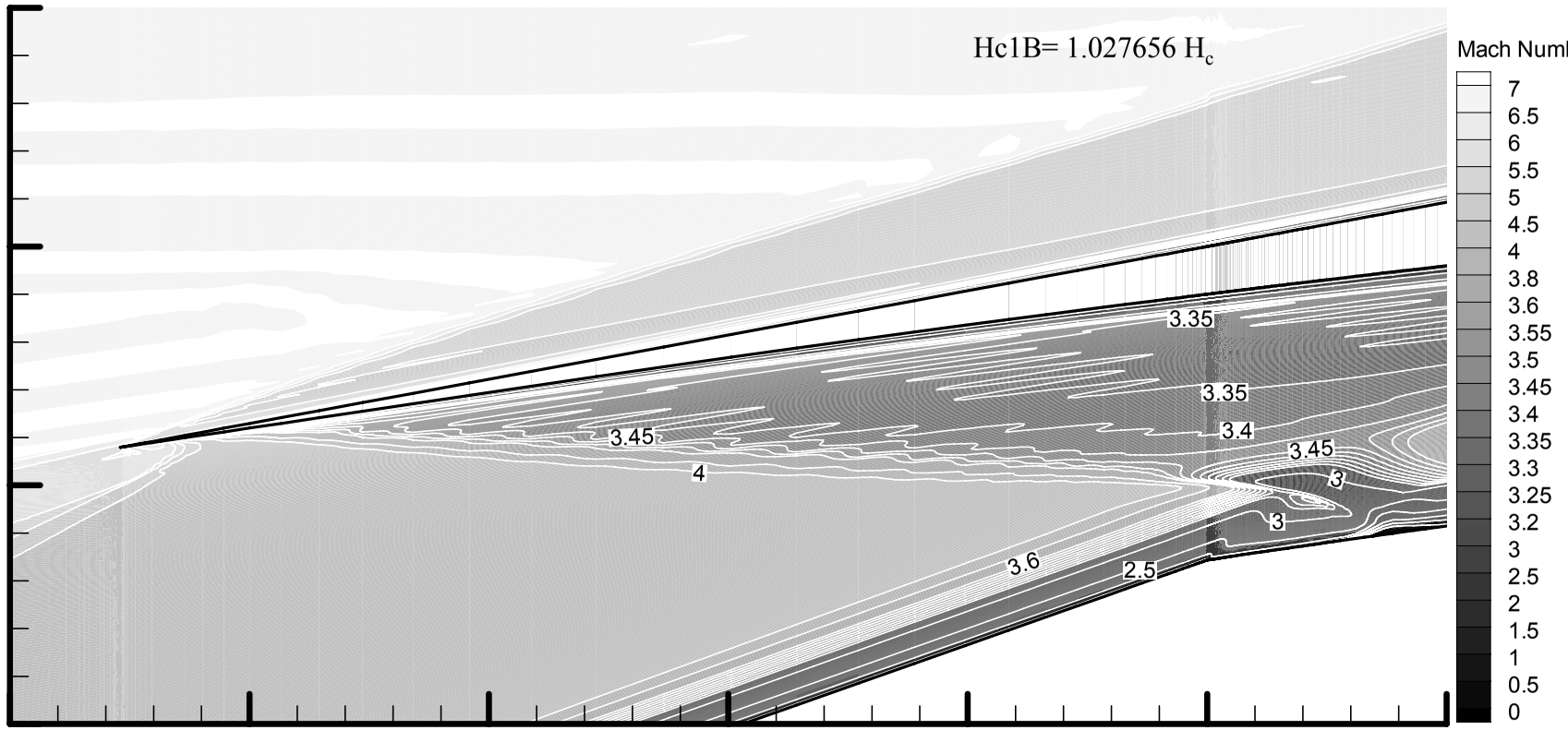

Figure 10. – Mach number contours in the vicinity of the cowl shock for nominal cowl configuration H1B.

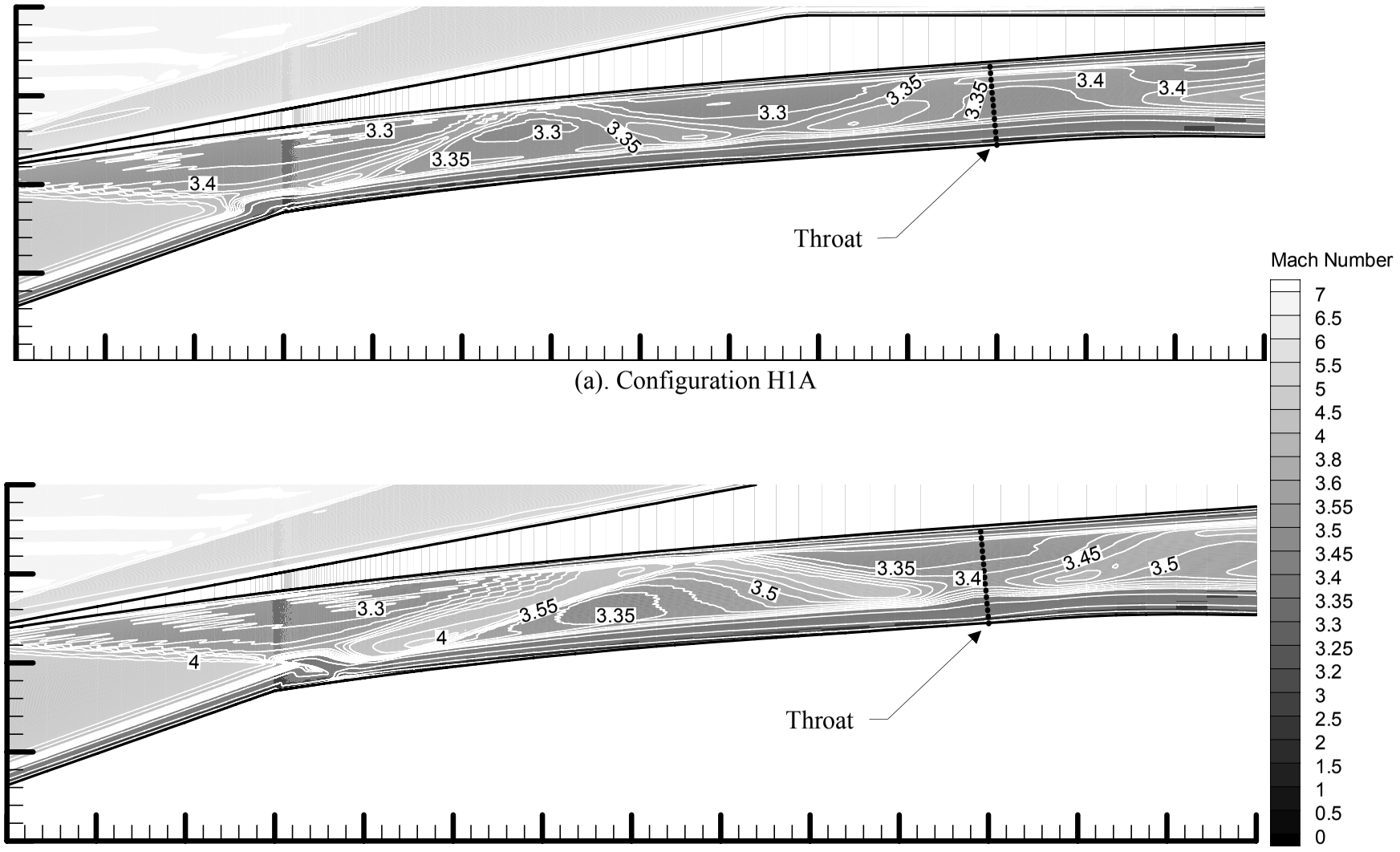

(a). Configuration H1A

(b). Configuration H1B

Figure 11. – Comparison of CFD Mach contour predictions of for configurations H1A and H1B.

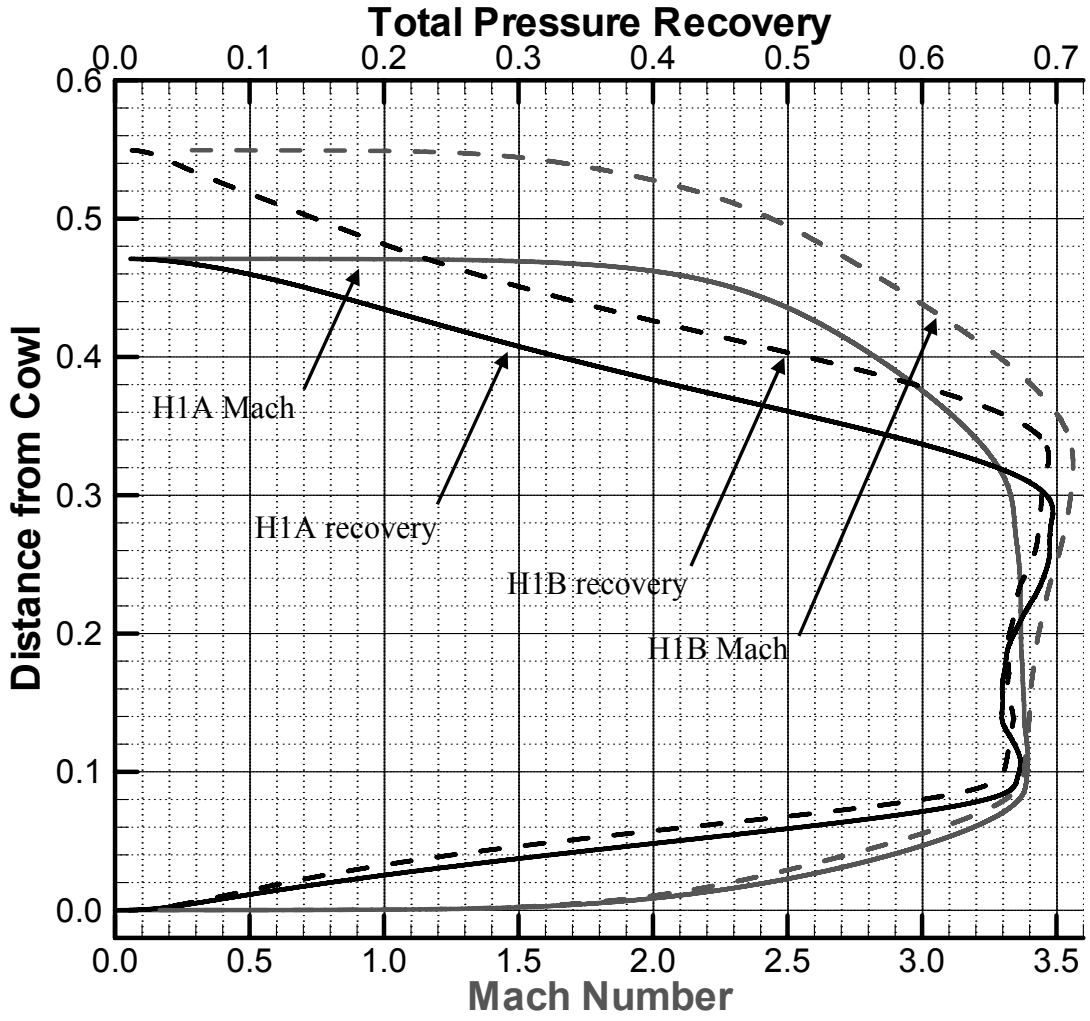

Figure 12. – Throat Mach number and total pressure recovery profiles extracted from Mach 7 CFD analyses of inlet configurations H1A and H1B.

Ramp Coordinates for Mach 7 Inlet				
x/Hc	y/Hc		x/Hc	y/Hc
0	0		5.215732	1.032545
2.365363	0.2695		5.241046	1.034464
2.365363	0.2695		5.266371	1.036287
3.389777	0.496614		5.281569	1.03735
3.389777	0.496614		5.296767	1.038413
4.75471	0.980045		5.311966	1.039475
4.762012	0.981054		5.327165	1.040538
4.787123	0.984758		5.342363	1.0416
4.812244	0.98836		5.357561	1.042663
4.837378	0.991862		5.37276	1.043726
4.862523	0.995269		5.387958	1.044788
4.887679	0.998574		5.403157	1.045851
4.912846	1.001784		5.418356	1.046915
4.938024	1.004892		5.433554	1.047977
4.963214	1.0079		5.448753	1.04904
4.988415	1.010812		5.46395	1.050102
5.013627	1.013624		5.479149	1.051165
5.038851	1.016334		5.494348	1.052228
5.064085	1.018949		5.509546	1.05329
5.089331	1.021463		5.524745	1.054353
5.11459	1.023875		5.539944	1.055416
5.139857	1.026193		5.555141	1.056478
5.165138	1.028409		5.56395	1.057094
5.190429	1.030525			

Cowl Coordinates for Mach 7 Inlet							
x/Hc	y/Hc		x/Hc	y/Hc		x/Hc	y/Hc
4.295445	1.011791		4.901907	1.093966		5.269031	1.129503
4.344043	1.019054		4.928634	1.096889		5.283759	1.130752
4.383253	1.024916		4.955271	1.099745		5.298534	1.131986
4.422457	1.030771		4.981825	1.10252		5.313311	1.133216
4.46166	1.036632		5.008301	1.10523		5.328144	1.134431
4.46166	1.036632		5.022557	1.106666		5.342995	1.135638
4.489943	1.040824		5.036847	1.108089		5.357861	1.136831
4.518118	1.044934		5.051152	1.109505		5.37277	1.138014
4.546179	1.048958		5.065499	1.110915		5.387685	1.139188
4.574138	1.052894		5.079853	1.11231		5.402653	1.140351
4.601987	1.056756		5.094254	1.113695		5.417622	1.1415
4.629736	1.06053		5.108657	1.115067		5.432644	1.14264
4.657379	1.064227		5.123115	1.116433		5.447686	1.143766
4.684927	1.06784		5.137591	1.117791		5.462741	1.144884
4.712379	1.071376		5.152079	1.11913		5.477837	1.145991
4.739729	1.074834		5.166614	1.120464		5.492946	1.147085
4.754648	1.076675		5.181149	1.121788		5.5081	1.148173
4.766985	1.078216		5.195736	1.123103		5.523263	1.149241
4.794154	1.081516		5.210326	1.124403		5.53847	1.150311
4.821223	1.084743		5.224972	1.125694		5.553668	1.151374
4.848205	1.087894		5.239635	1.126976		5.56395	1.152093
4.875103	1.090968		5.254309	1.128245			

Figure 13. – Surface coordinates for the high-speed Mach 7 inlet HIA configuration (after cowl surface adjustment based on CFD flow field predictions).

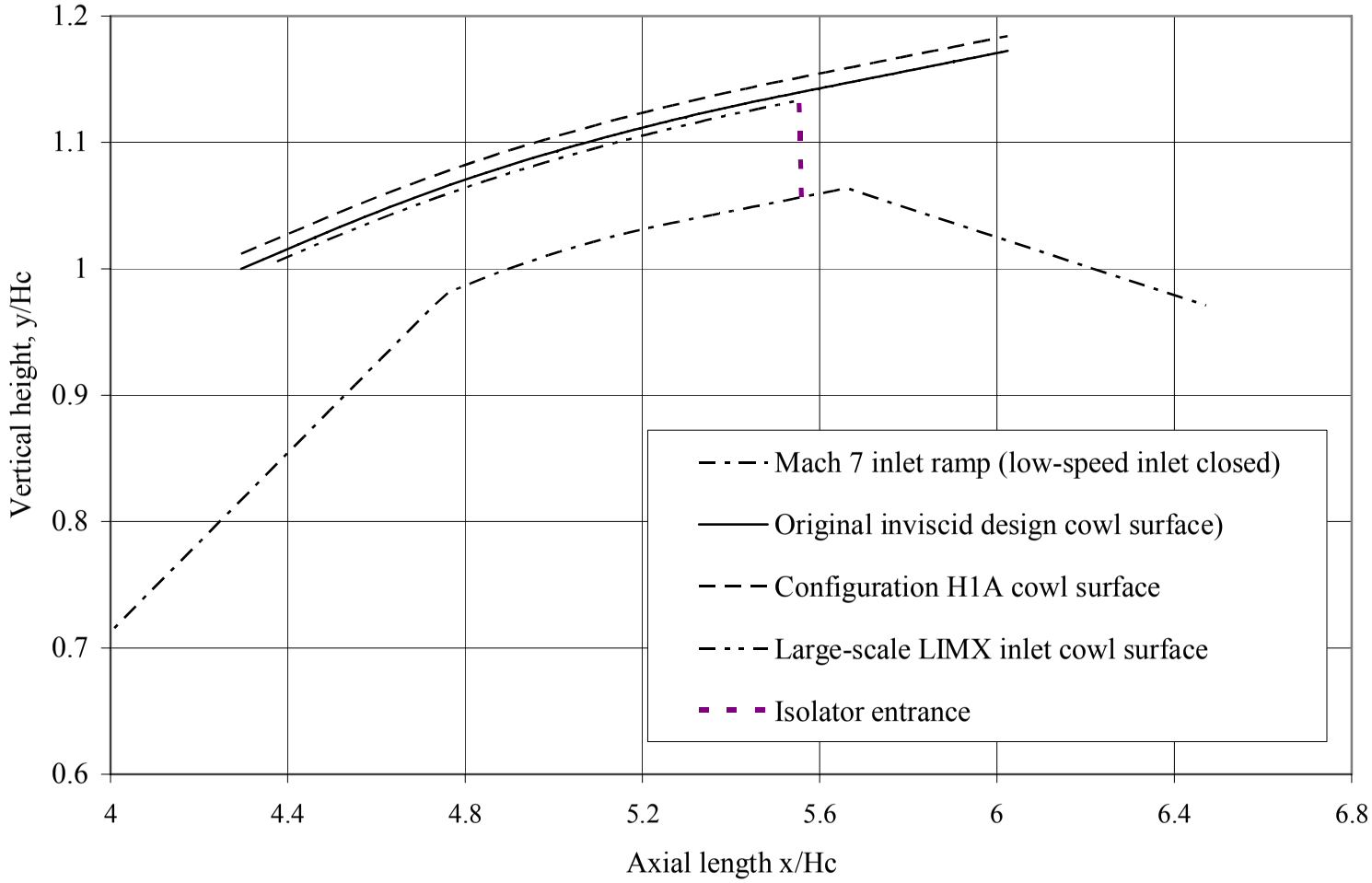

Figure 14. – Comparison of resized cowl for the large-scale LIMX configuration to the original inviscid and H1A cowl contours.

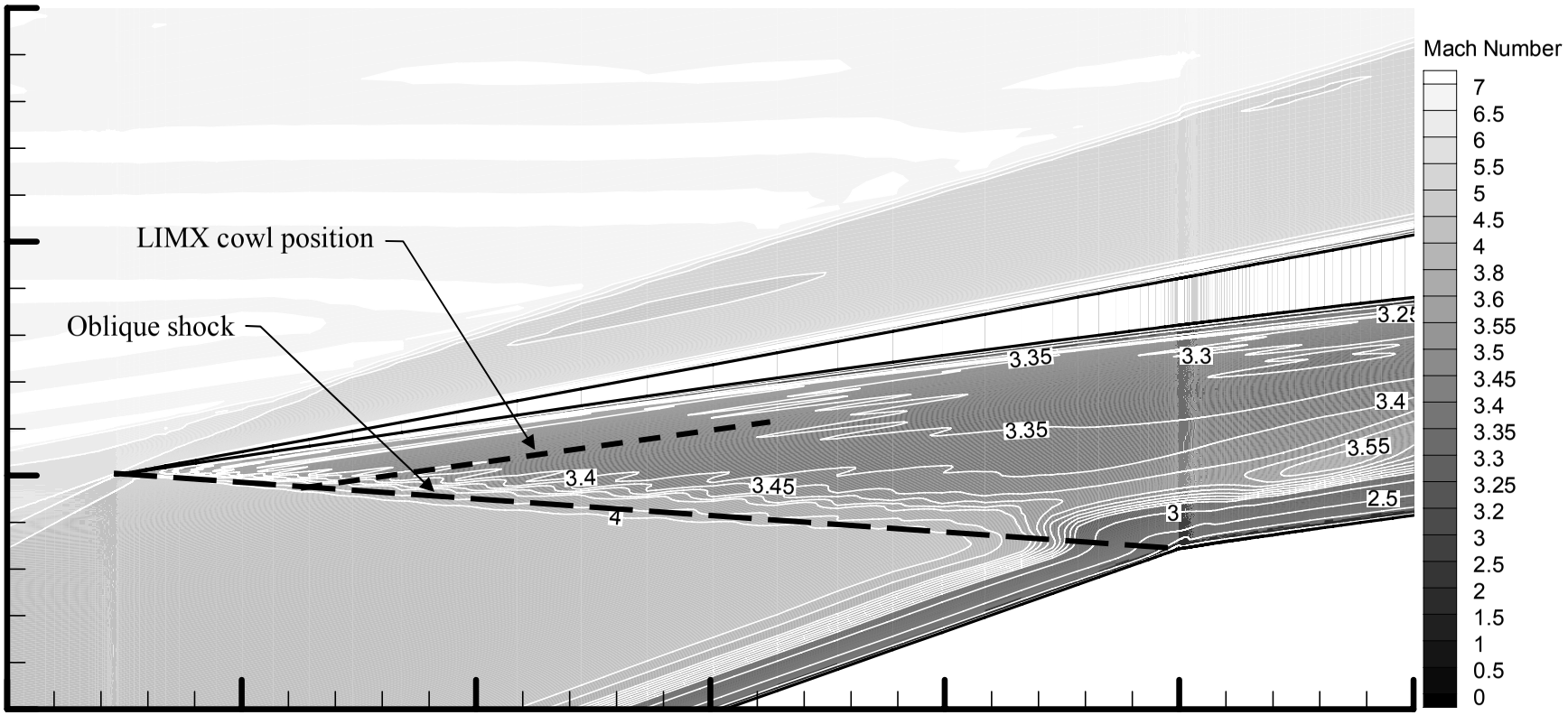

Figure 15. – Large –scale inlet (LIMX) cowl position shown on CFD solution for configuration H1A.

Ramp Coordinates for Mach 7 Inlet

x/Hc	y/Hc		x/Hc	y/Hc
0	0		5.215732	1.032545
2.365363	0.2695		5.241046	1.034464
2.365363	0.2695		5.266371	1.036287
3.389777	0.496614		5.281569	1.03735
3.389777	0.496614		5.296767	1.038413
4.75471	0.980045		5.311966	1.039475
4.762012	0.981054		5.327165	1.040538
4.787123	0.984758		5.342363	1.0416
4.812244	0.98836		5.357561	1.042663
4.837378	0.991862		5.37276	1.043726
4.862523	0.995269		5.387958	1.044788
4.887679	0.998574		5.403157	1.045851
4.912846	1.001784		5.418356	1.046915
4.938024	1.004892		5.433554	1.047977
4.963214	1.0079		5.448753	1.04904
4.988415	1.010812		5.46395	1.050102
5.013627	1.013624		5.479149	1.051165
5.038851	1.016334		5.494348	1.052228
5.064085	1.018949		5.509546	1.05329
5.089331	1.021463		5.524745	1.054353
5.11459	1.023875		5.539944	1.055416
5.139857	1.026193		5.555141	1.056478
5.165138	1.028409		5.56395	1.057094
5.190429	1.030525			

Cowl Coordinates for large-scale LIMX Mach 7 Inlet

x/Hc	y/Hc		x/Hc	y/Hc		x/Hc	y/Hc
4.375642	1.005701		4.981077	1.084333		5.297738	1.113795
4.421793	1.012595		5.007549	1.087043		5.312513	1.115024
4.46099	1.018455		5.021802	1.088479		5.327343	1.116239
4.489268	1.022647		5.03609	1.089902		5.342192	1.117446
4.517439	1.026756		5.050394	1.091317		5.357057	1.118639
4.545496	1.030779		5.064738	1.092727		5.371963	1.119822
4.573451	1.034715		5.07909	1.094122		5.386876	1.120996
4.601296	1.038576		5.093488	1.095507		5.401841	1.122159
4.62904	1.04235		5.107889	1.096878		5.416808	1.123307
4.65668	1.046046		5.122346	1.098244		5.431828	1.124447
4.684223	1.049658		5.136819	1.099602		5.446868	1.125573
4.711672	1.053194		5.151305	1.100941		5.461921	1.126691
4.739017	1.056652		5.165838	1.102274		5.477014	1.127798
4.766269	1.060033		5.18037	1.103598		5.492121	1.128892
4.793434	1.063332		5.194956	1.104913		5.507272	1.12998
4.820499	1.066559		5.209544	1.106213		5.522433	1.131048
4.847477	1.06971		5.224187	1.107504		5.537638	1.132117
4.874371	1.072783		5.238848	1.108786		5.552834	1.13318
4.901171	1.075781		5.253519	1.110055		5.553707	1.133241
4.927894	1.078703		5.26824	1.111313			
4.954527	1.081558		5.282966	1.112561			

Figure 16. – Surface coordinates for the high-speed Mach 7 inlet for the large-scale LIMX configuration.

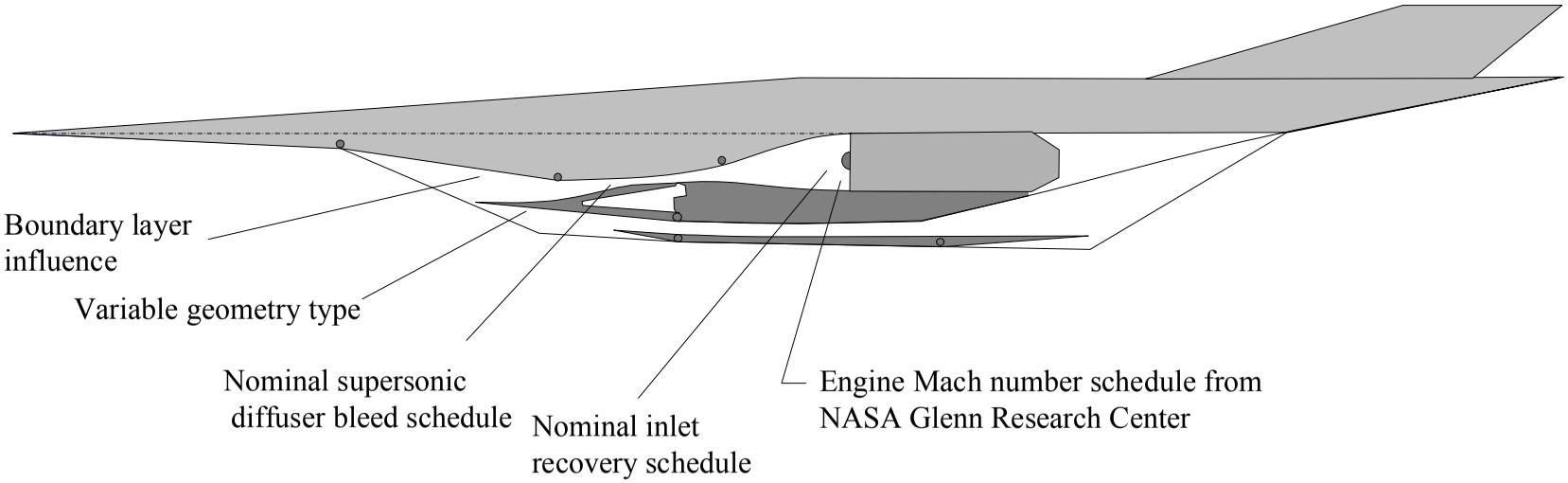

Figure 17. – Dual mode propulsion system with inlet system positioned for Mach 4 operation.

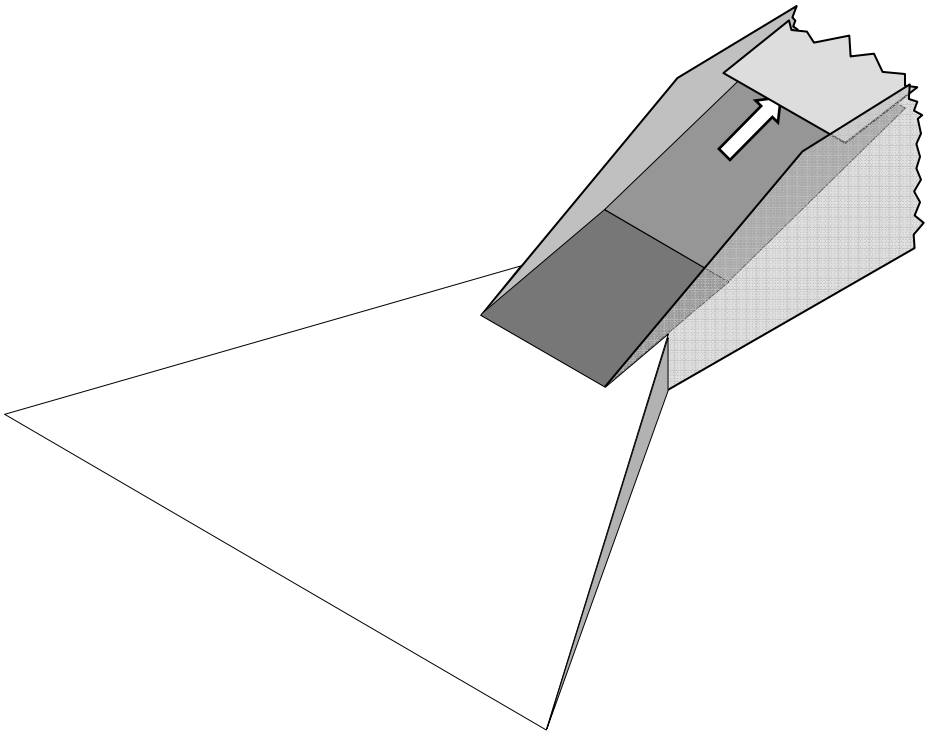

(a). Mach 7 inlet configuration (low-speed inlet closed)

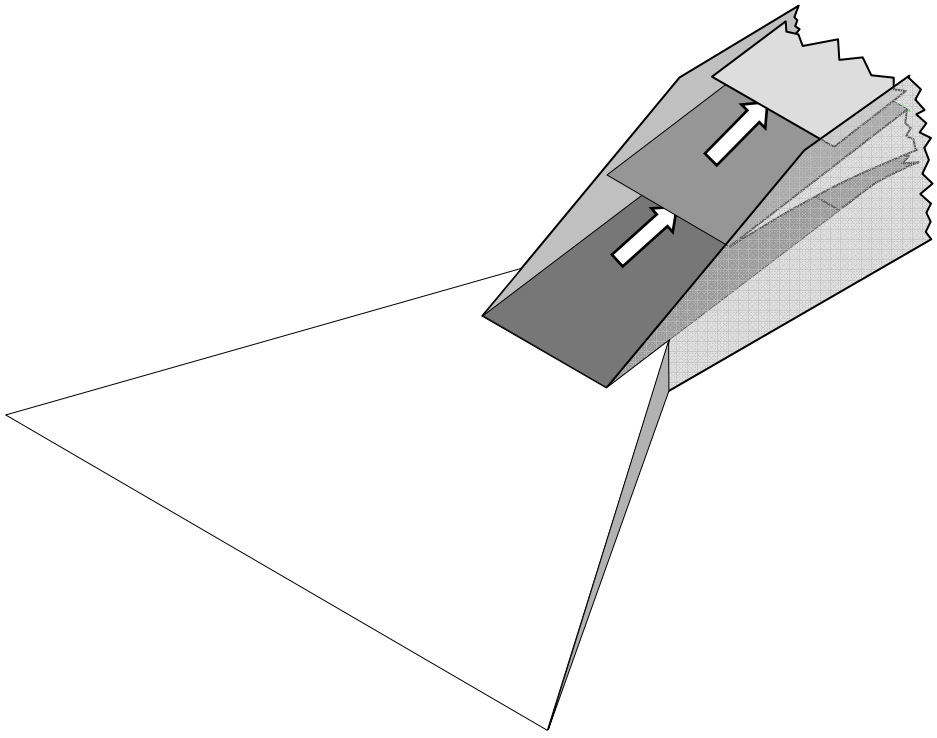

(b). Mach 4 inlet configuration (low-speed inlet open)

Figure 18. – Sketches showing inlet operation at Mach 4 and 7.

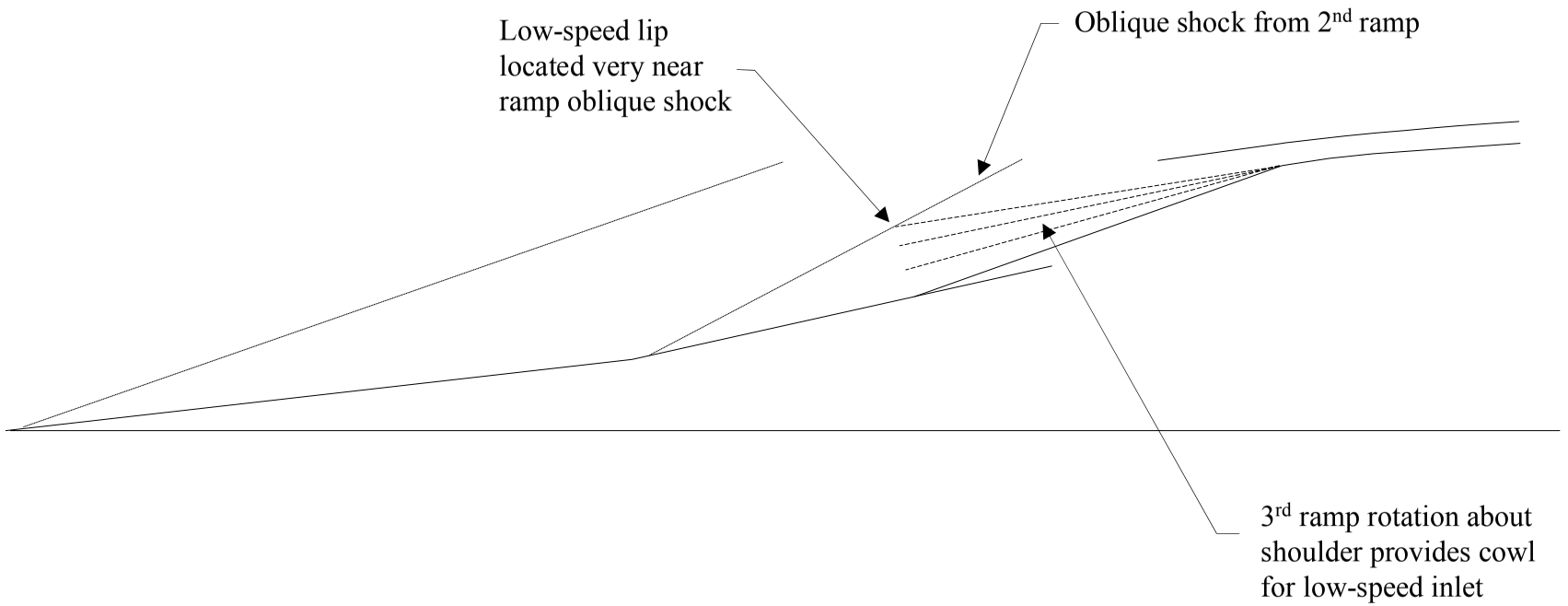

Figure 19. – Development of an integrated Mach 4 inlet into the Mach 7 high-speed inlet. Last ramp of the Mach 7 inlet is rotated about the shoulder to open a duct for the Mach 4 inlet.

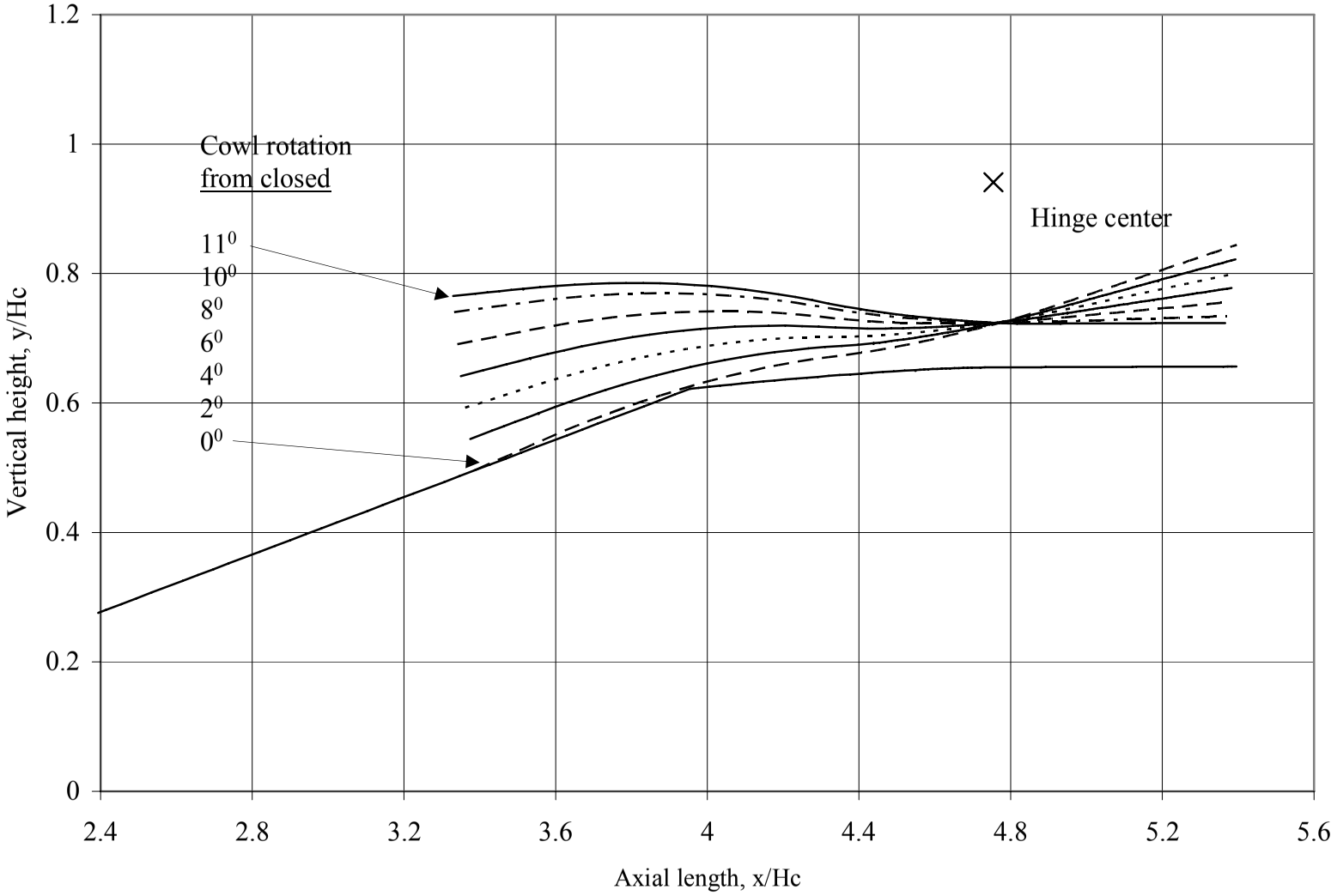

Figure 20. – Internal low-speed inlet cowl surface for several angles of rotation. The inlet is closed for a rotation of 0^0. Internal cowl surface must not contract ramp surface other than at the lip. Vertical scale is enlarged.

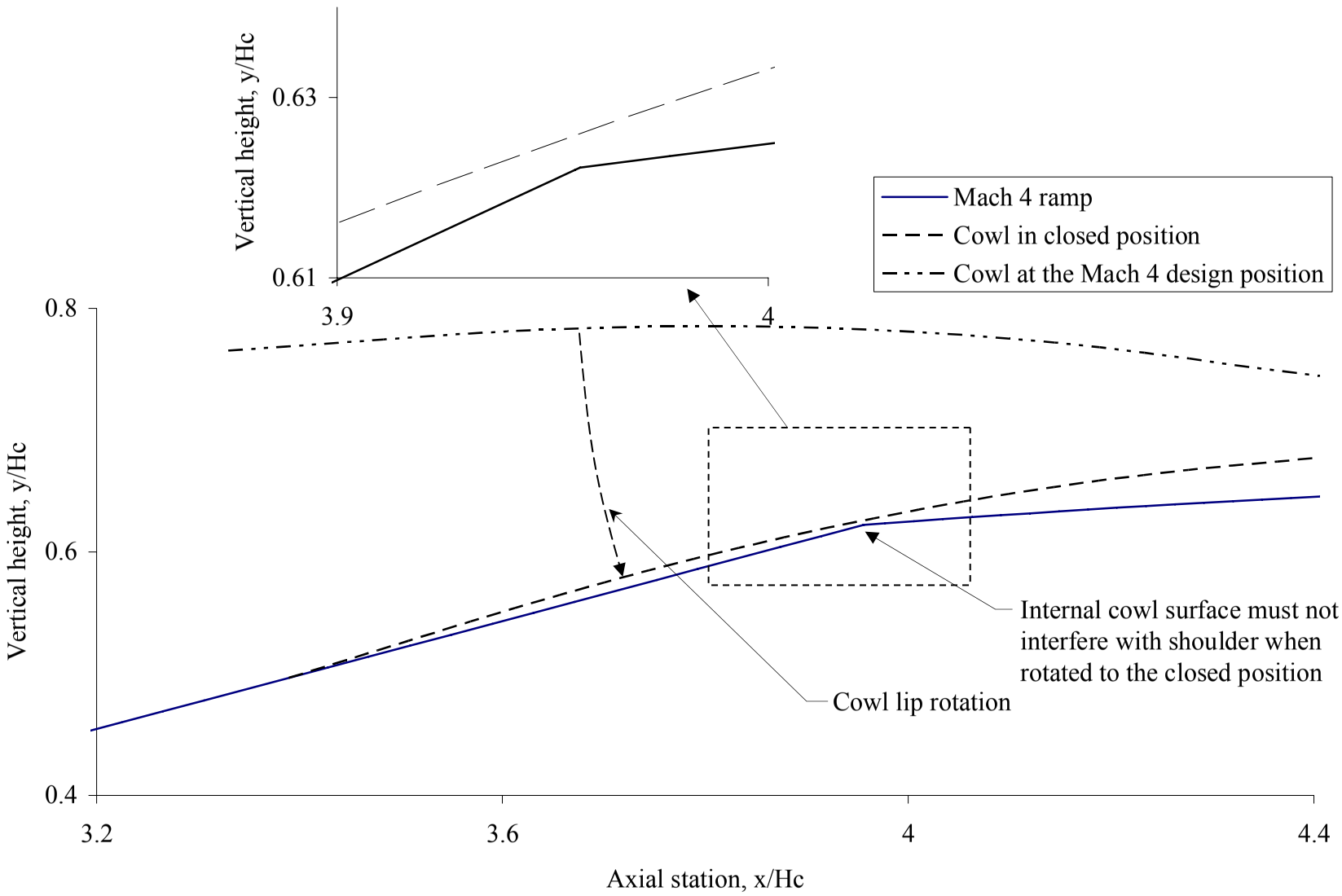

Figure 21. – Closed cowl position relative to low speed inlet ramp when the second ramp is in the Mach 4 to 7 position.

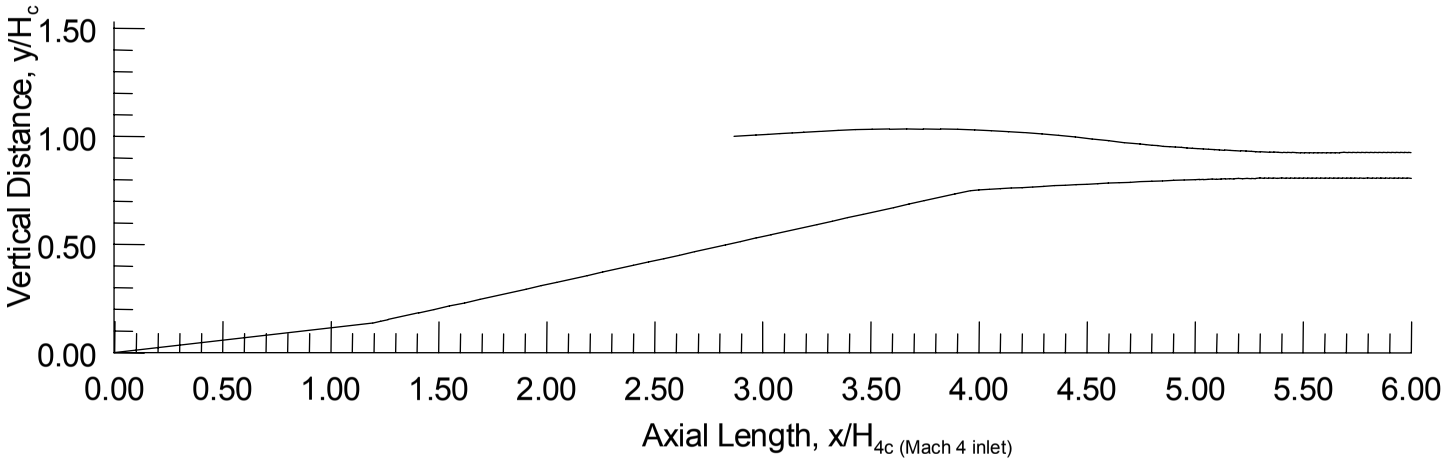

(a). Inlet surface contours and shock system.

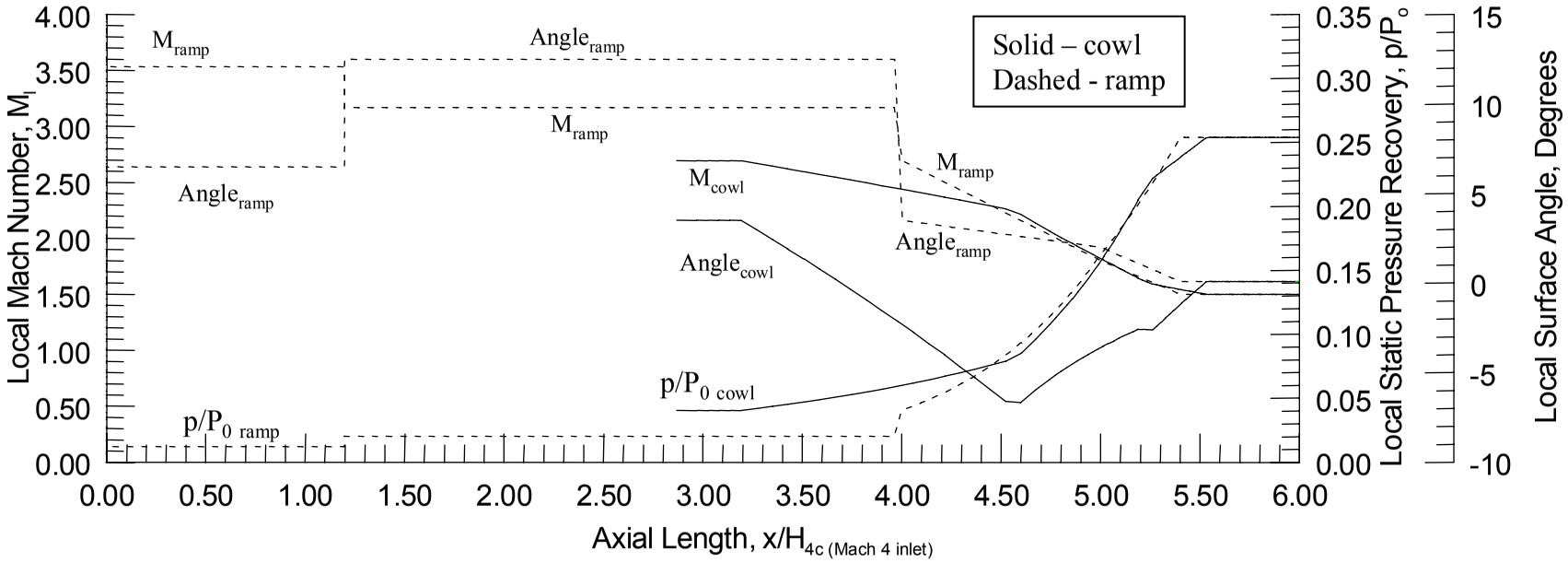

(b). Inlet aerodynamics at design (Mach 4).

Figure 22. – Aerodynamics of Mach 4 inlet (throat Mach number of 1.5).

Two-Dimensional Mach 4 Inlet			
	Ramp 1	Ramp 2	Cowl
Incoming Mach number	4	3.53271743	3.16790122
Surface deflection angle (degrees)	6.5	6	8.99930106
Surface angle (degrees)	6.5	12.500001	3.50069994
Leading edge x/H_c	0	2.3651394	3.32990445
Leading edge y/H_c	0	0.26947361	0.76524881
Local shock angle (degrees)	19.21692256	20.8105477	25.3589133
Local Mach, M_l	3.532717482	3.16790122	2.69343763
Shock recovery, P_1/P_2	0.976392956	0.9863627	0.9682838
Local recovery, P_l/P_0	0.976392956	0.96307759	0.93253243
Static recovery, p_l/H_0	0.012221277	0.02042367	0.04045863
Static pressure rise, p_l/p_0	1.855620237	3.10103258	6.14304513
Capture streamtrace, m_i/m_0	0.57191674	0.69198539	0.7634416

Figure 23. – Theoretical aerodynamics of low-speed Mach 4 inlet.

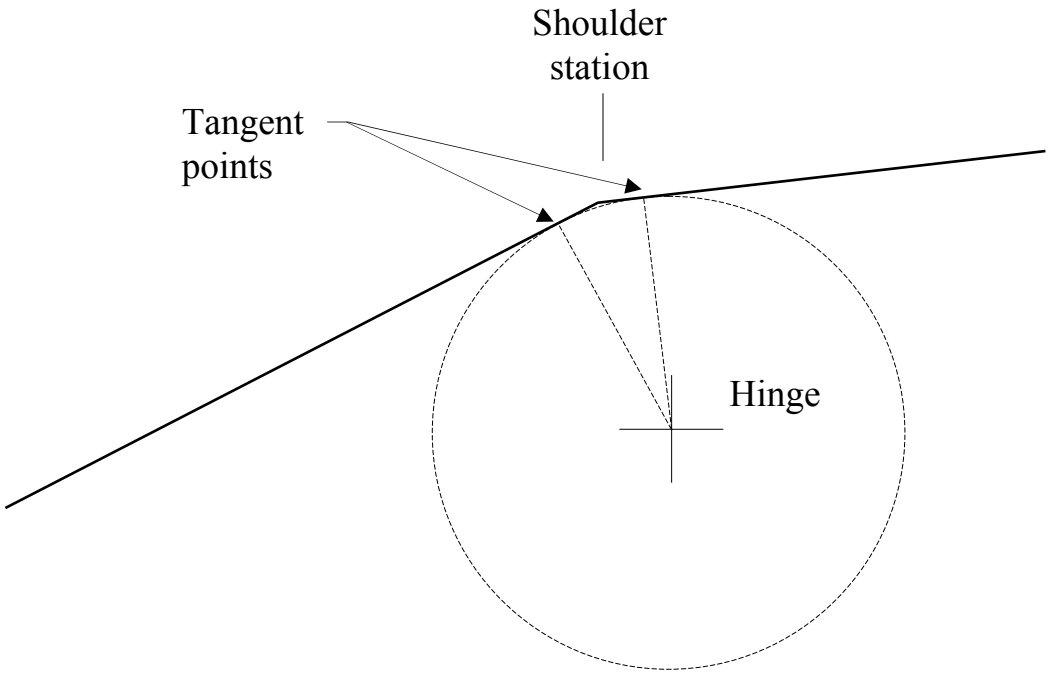

Figure 24. – Shoulder hinge.

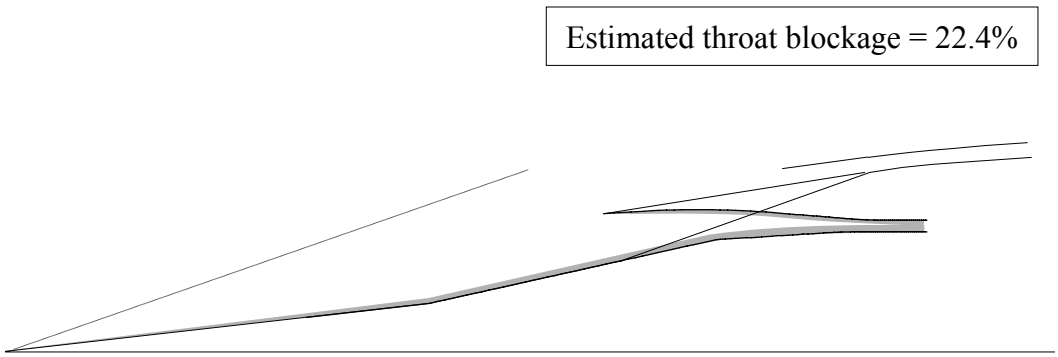

Figure 25. – Boundary layer dominates the throat of the Mach 4 inlet.

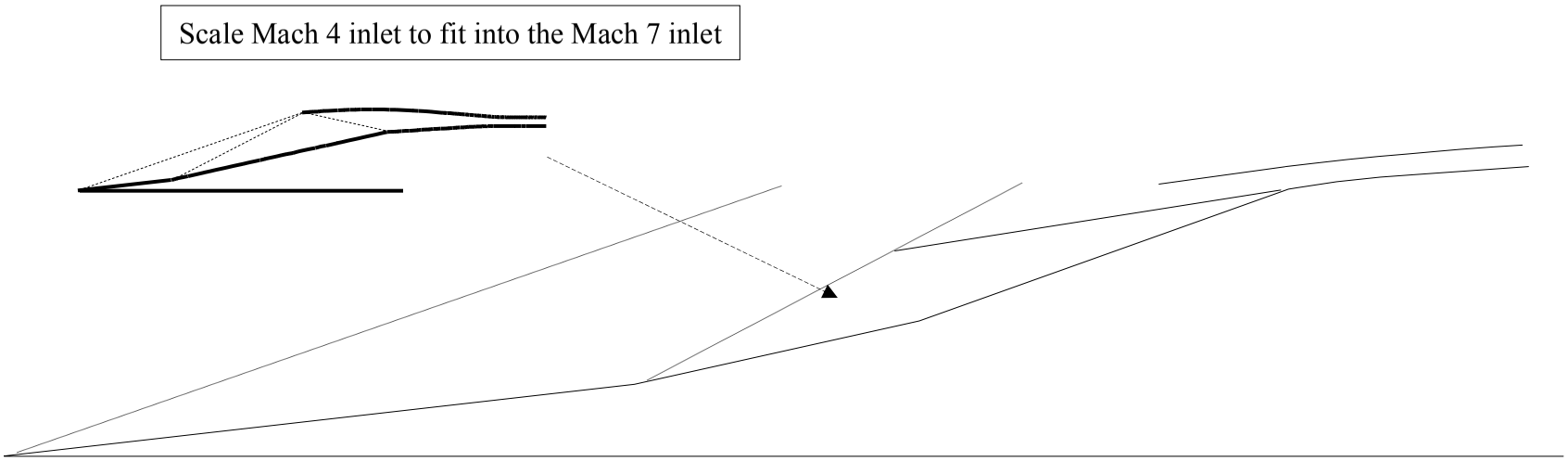

(a) Scale Mach 4 inlet until it fits into Mach 7 inlet.

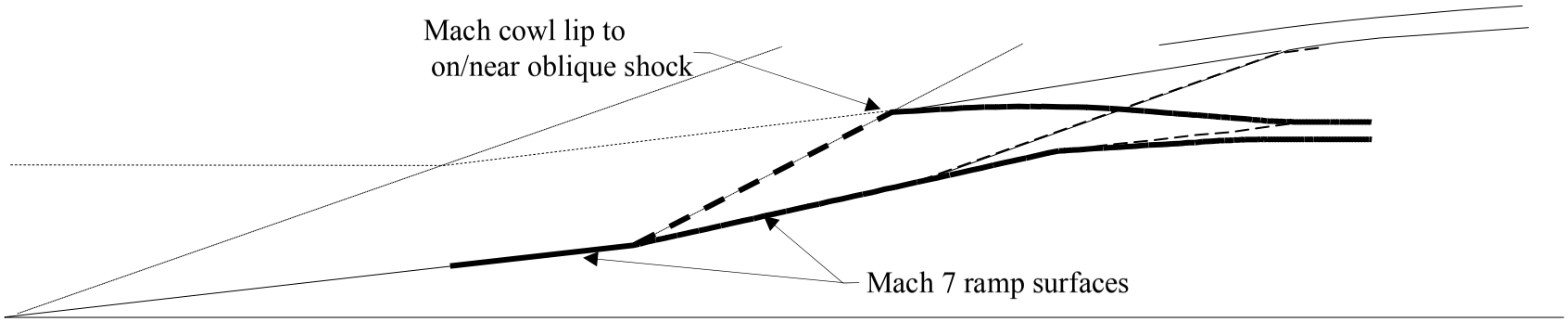

(b) Mach 4 inlet integrated into Mach 7 inlet..

Figure 26. – Mach 4 integrated into Mach 7 inlet to obtain a dual-flow Hypersonic inlet sytem.

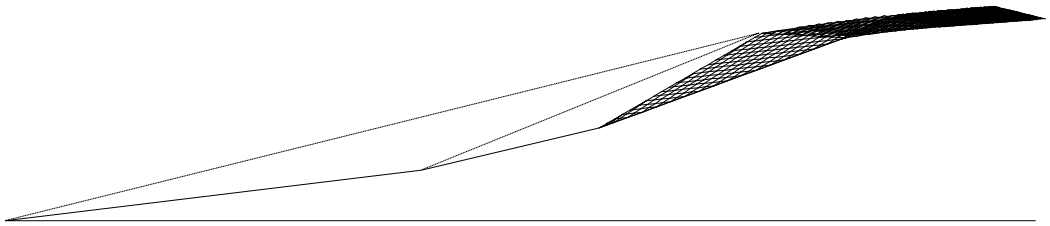

(a). Aerodynamic design of Mach 7 inlet

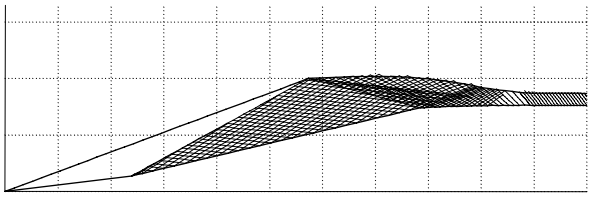

(b). Aerodynamic design of Mach 4 inlet

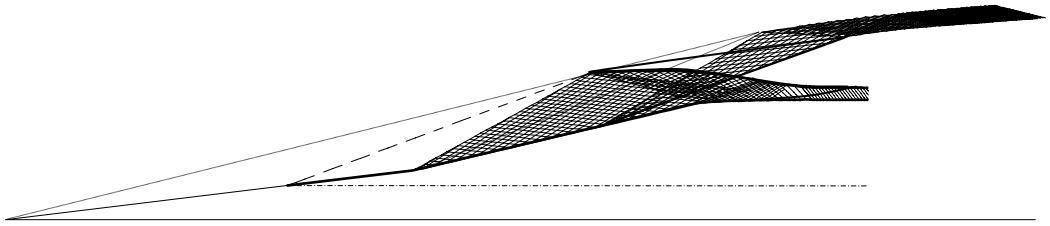

(c). Dual-mode hypersonic inlet system. Mach 4 inlet integrated into the Mach 7 inlet.

Figure 27. – Integration of high and low speed inlet designs.

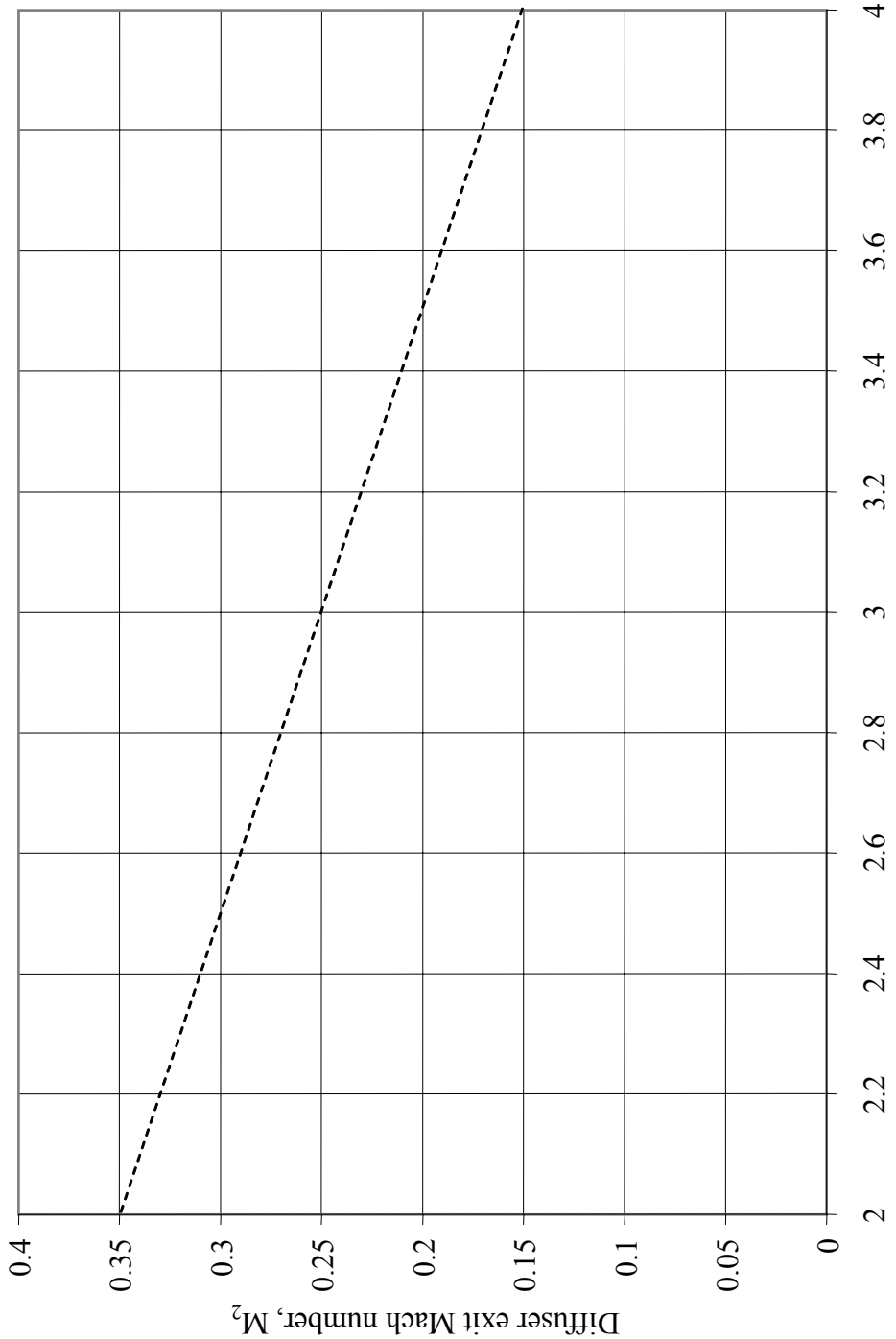

Figure 28. – Generic engine airflow schedule

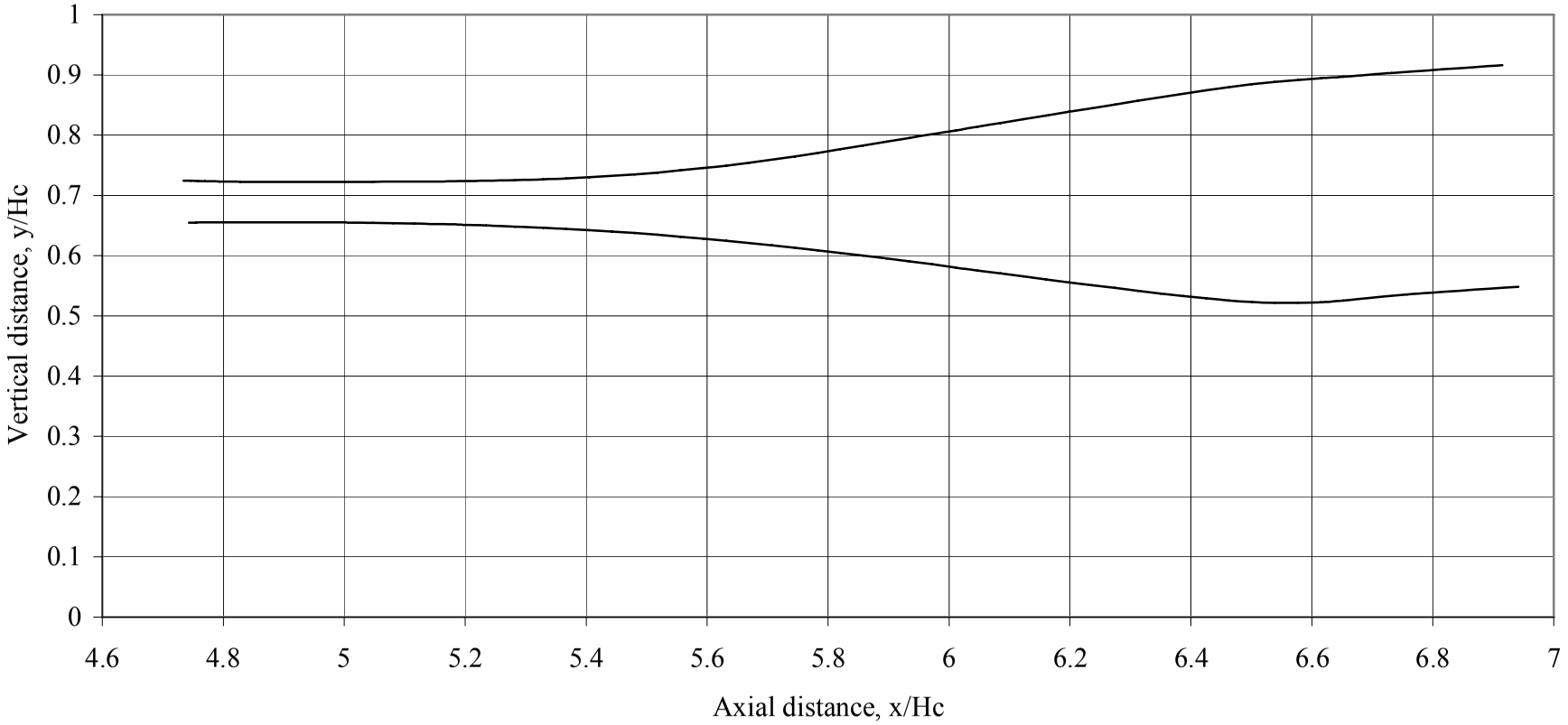

Figure 29. – Subsonic diffuser for low-speed Mach 4 inlet.

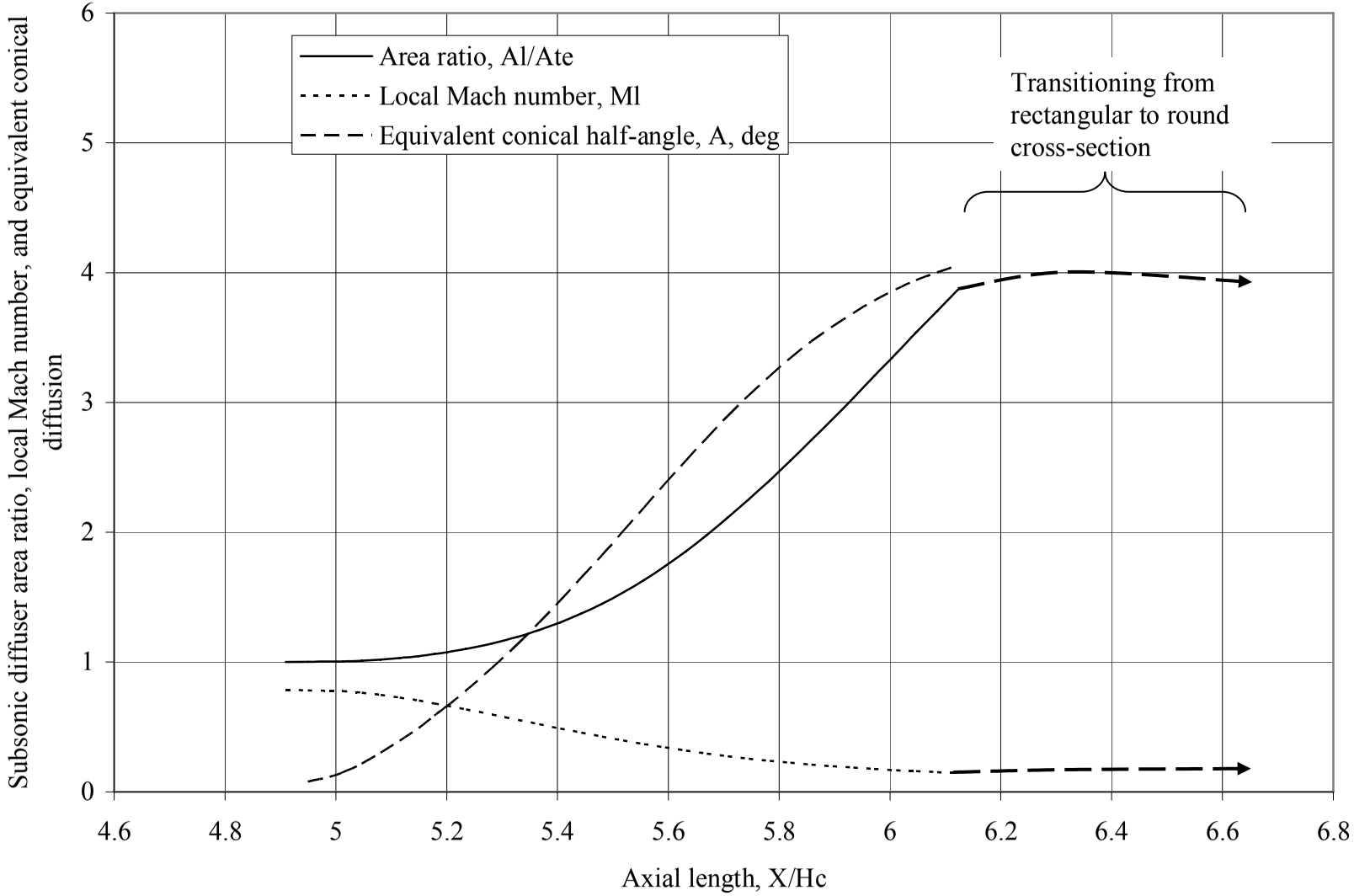

Figure 30. – Aerodynamic design characteristics for the subsonic diffuser.

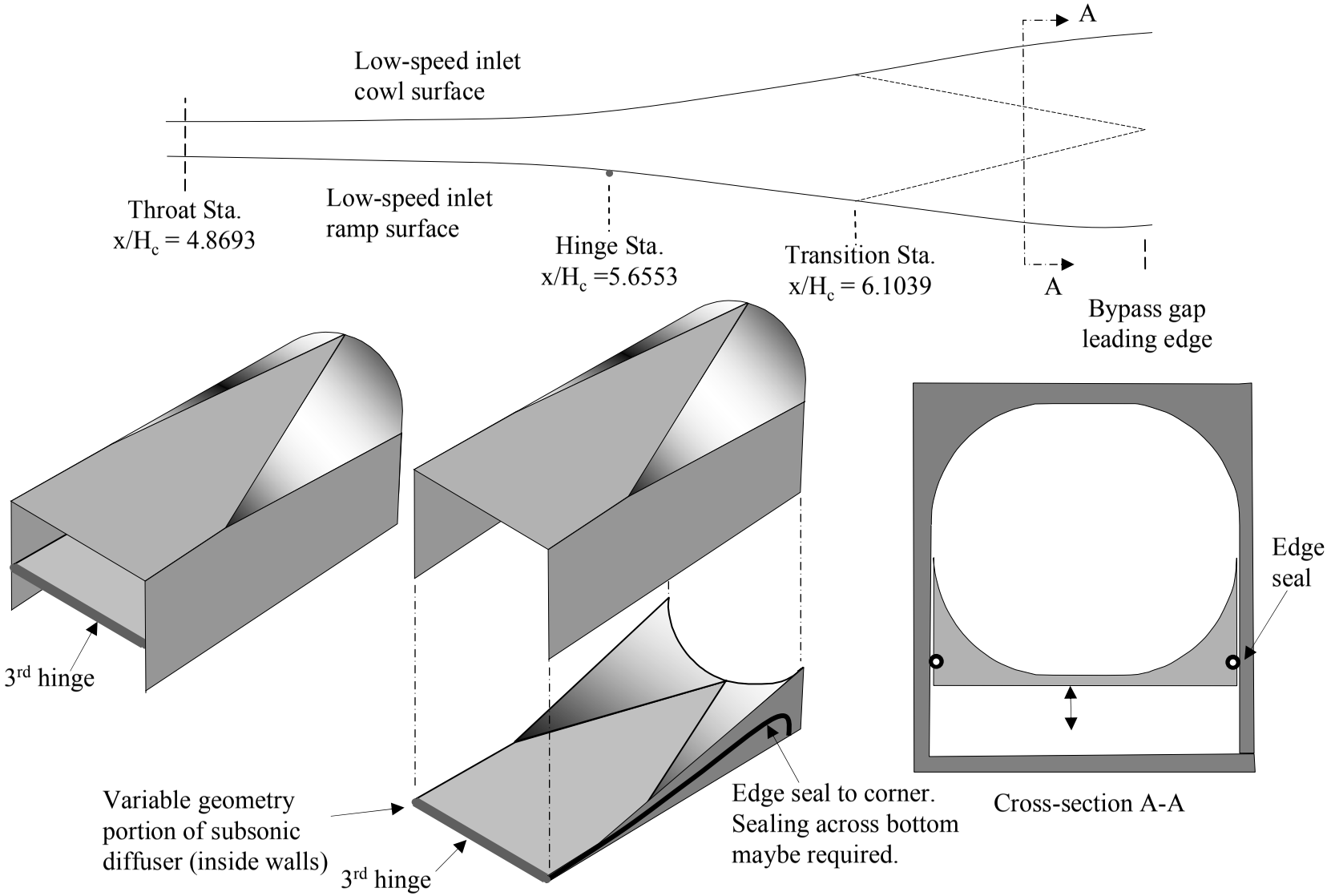

Figure 31. – Transitioning of the ramp variable geometry part of subsonic diffuser.

Ramp Coordinates for Mach 4 Inlet

x/Hc	y/Hc	x/Hc	y/Hc	x/Hc	y/Hc	x/Hc	y/Hc
0	0	4.572173	0.651756	4.869586	0.655353	5.78321	0.608747
2.365363	0.2695	4.583612	0.65211	4.910051	0.655353	5.821006	0.604405
2.365363	0.2695	4.595051	0.652442	4.949831	0.655282	5.858802	0.600077
3.956575	0.622273	4.60649	0.652757	4.989198	0.65513	5.896919	0.595424
3.977346	0.623519	4.617928	0.653054	5.013199	0.654972	5.934395	0.590628
4.005944	0.625252	4.629367	0.653329	5.04729	0.654604	5.972191	0.585651
4.034541	0.626945	4.640806	0.653586	5.081156	0.654057	6.011688	0.580226
4.063138	0.628598	4.652245	0.653821	5.11564	0.65341	6.047783	0.575471
4.091736	0.630216	4.663684	0.654044	5.150124	0.652641	6.085579	0.570558
4.120333	0.631795	4.675123	0.654244	5.178471	0.651893	6.123375	0.565702
4.148931	0.633339	4.686562	0.654427	5.20017	0.651245	6.161172	0.560664
4.177528	0.634843	4.698001	0.654587	5.235165	0.650132	6.198968	0.555766
4.206126	0.636313	4.70944	0.65473	5.28241	0.64831	6.236764	0.550994
4.234723	0.637743	4.720879	0.654856	5.329079	0.646248	6.27456	0.546384
4.26332	0.639133	4.732318	0.654959	5.367452	0.644254	6.312356	0.541787
4.291918	0.640488	4.743757	0.655045	5.405248	0.642174	6.350152	0.537134
4.320515	0.64181	4.755196	0.655113	5.443044	0.639832	6.387949	0.533213
4.349113	0.643085	4.766635	0.655159	5.48084	0.637386	6.425745	0.529665
4.37771	0.644332	4.778074	0.655193	5.518637	0.634574	6.463541	0.526653
4.406308	0.645533	4.789513	0.65521	5.556433	0.631525	6.501337	0.524428
4.434905	0.6467	4.800952	0.655233	5.594229	0.628129	6.539133	0.523506
4.463502	0.647832	4.812391	0.65525	5.632025	0.624598	6.576929	0.523926
4.4921	0.648925	4.82383	0.655273	5.655603	0.622273	6.614726	0.525593
4.520697	0.649977	4.835269	0.655291	5.669821	0.620854	6.66547	0.529142
4.549295	0.650995	4.846708	0.655313	5.707617	0.61693	6.757355	0.535558
4.560734	0.651384	4.858147	0.655331	5.745414	0.612945	6.941094	0.548415

Cowl Coordinates for Mach 4 Inlet

x/Hc	y/Hc	x/Hc	y/Hc	x/Hc	y/Hc	x/Hc	y/Hc
3.330089	0.765291	4.451629	0.74076	4.828571	0.722704	5.745414	0.764752
3.388645	0.768872	4.46714	0.739508	4.84009	0.722658	5.78321	0.770435
3.420143	0.770799	4.482491	0.738313	4.851558	0.722653	5.821006	0.77645
3.45164	0.772727	4.497699	0.73718	4.863003	0.722656	5.858802	0.782797
3.483137	0.774654	4.512793	0.736105	4.910051	0.722668	5.896919	0.789069
3.514629	0.776576	4.527715	0.735081	4.949831	0.72268	5.934395	0.795179
3.559881	0.779138	4.542511	0.734109	4.989198	0.722688	5.972191	0.801549
3.605128	0.781272	4.557188	0.733188	5.013199	0.722693	6.011688	0.807885
3.650363	0.782987	4.571772	0.732307	5.04729	0.722705	6.047783	0.813959
3.695593	0.784263	4.586214	0.731472	5.081156	0.722742	6.085579	0.820227
3.7408	0.785104	4.600553	0.730677	5.11564	0.722868	6.123375	0.826499
3.785972	0.785498	4.614817	0.729928	5.150124	0.723118	6.161172	0.832772
3.831093	0.785441	4.628944	0.729207	5.178471	0.723435	6.198968	0.838841
3.876163	0.784926	4.642991	0.728526	5.20017	0.723701	6.236764	0.844911
3.921152	0.783948	4.656958	0.727886	5.235165	0.724316	6.27456	0.851153
3.966062	0.782501	4.670828	0.727257	5.28241	0.725351	6.312356	0.857051
4.010874	0.78058	4.684663	0.726628	5.329079	0.726808	6.350152	0.862829
4.055572	0.778183	4.698453	0.725998	5.367452	0.728291	6.387949	0.868669
4.100144	0.775306	4.71055	0.725472	5.405248	0.730178	6.425745	0.874225
4.144578	0.771949	4.722589	0.724992	5.443044	0.732414	6.463541	0.879711
4.188859	0.7681	4.734577	0.724557	5.48084	0.735033	6.501337	0.884567
4.232979	0.763759	4.746508	0.724168	5.518637	0.738054	6.539133	0.888501
4.276921	0.758931	4.758388	0.723831	5.556433	0.741465	6.576929	0.89181
4.320567	0.753721	4.770216	0.723533	5.594229	0.745286	6.614726	0.894929
4.362954	0.749037	4.781986	0.723282	5.632025	0.74948	6.639572	0.896666
4.404088	0.744959	4.793711	0.723076	5.655603	0.752286	6.731457	0.903082
4.420114	0.743483	4.805379	0.72291	5.669821	0.754075	6.915197	0.915945
4.435957	0.742087	4.817001	0.722784	5.707617	0.759242		

Figure 32. – Coordinates for the Mach 4 low-speed inlet.

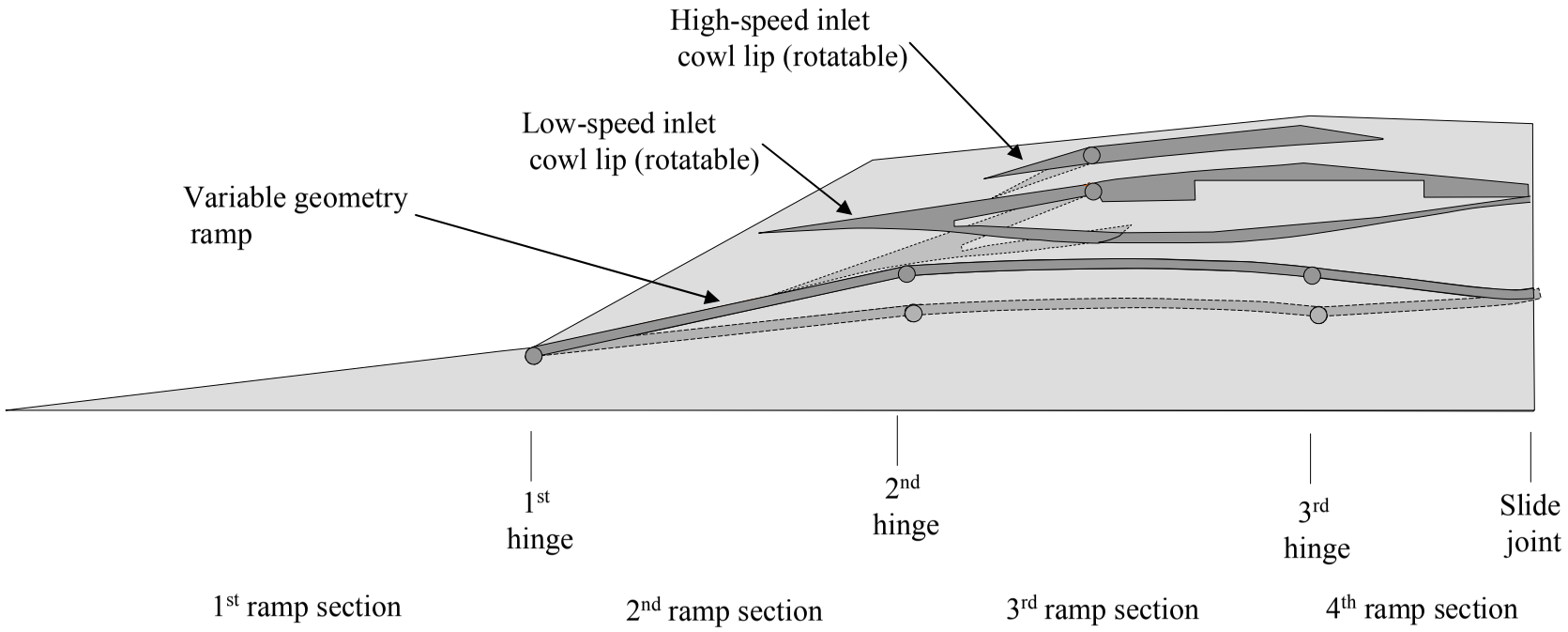

Figure 33. – Hypersonic dual mode propulsion inlet variable geometry.

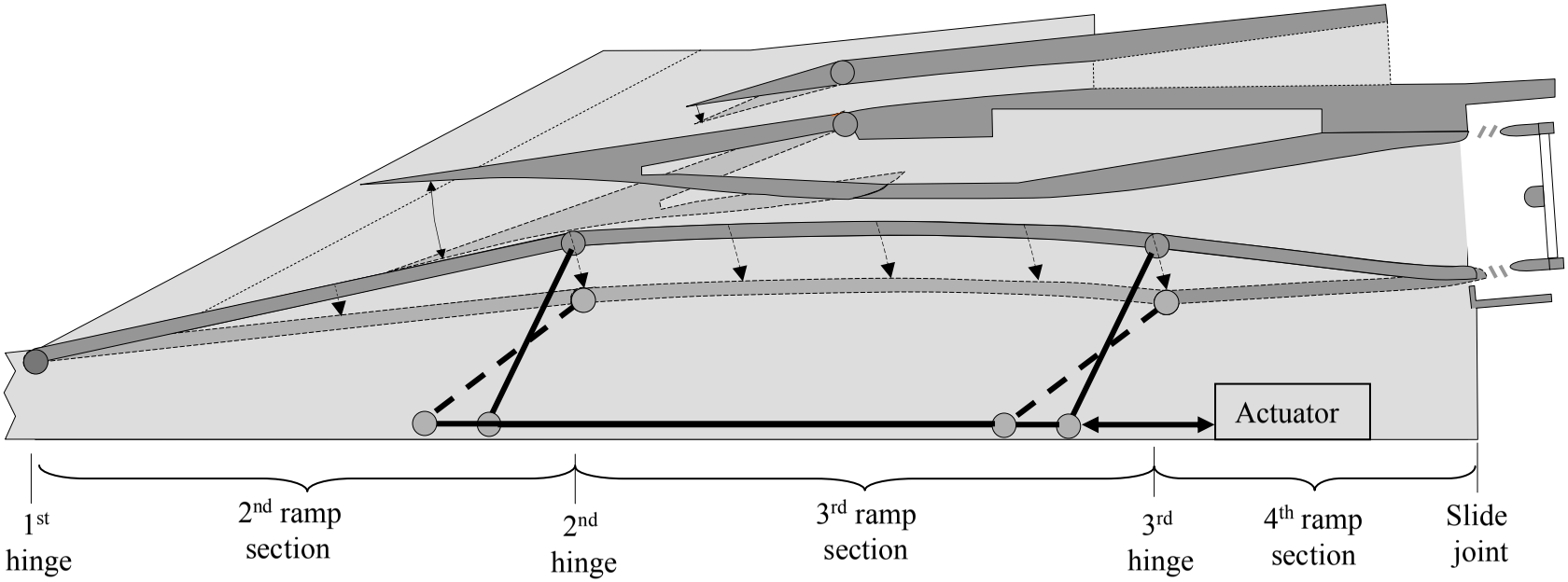

Ramp variable geometry operation

- 2nd ramp section rotates about 1st hinge
- 3rd ramp section rotates about 2nd hinge such that the 3rd ramp section contour remains parallel to the original design contour
- 4th ramp section rotates about 3rd hinge such that the contour at the aft end of the section provides a smooth duct to the engine face. This generally requires that the section be directed into the overboard bypass cavity because the ramp motion (flattening) results in an increased overall axial length. Control of the aft end of the segment can be provided by a roller in a guide slot.
- Variable geometry can be accomplished by a single actuator and selected hinged sections

Cowl lip variable geometry

- Low-speed inlet cowl lip rotates about a hinge located at the ramp shoulder of the Mach 7 inlet, rotates from the Mach 4 position to closed.
- High-speed inlet cowl lip rotates about a hinge located in the high speed cowl at the same axial station as the hinge for the low speed inlet.

Figure 34. – Inlet variable geometry

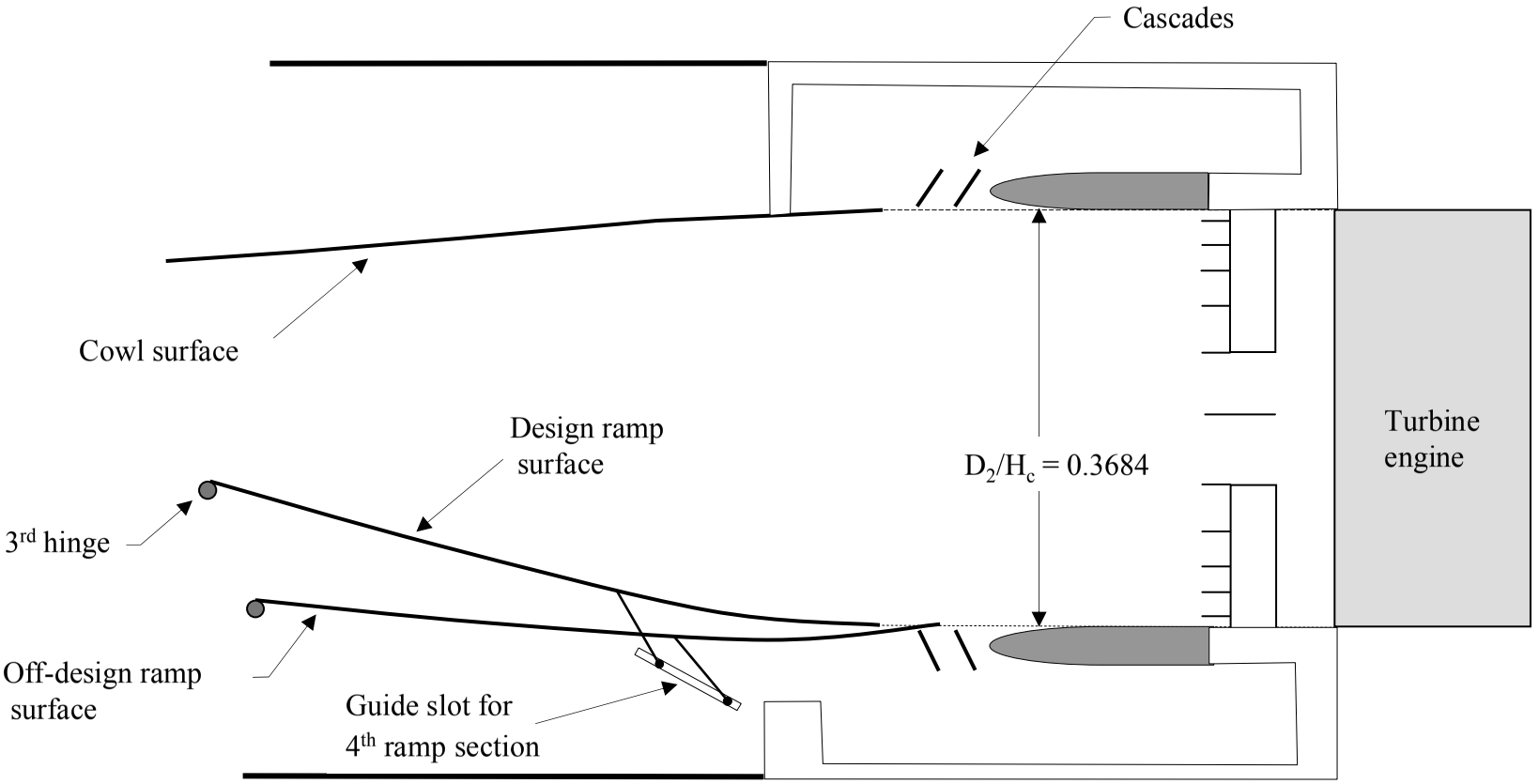

Figure 35. – Overboard bypass system and variable geometry of 4th ramp section.

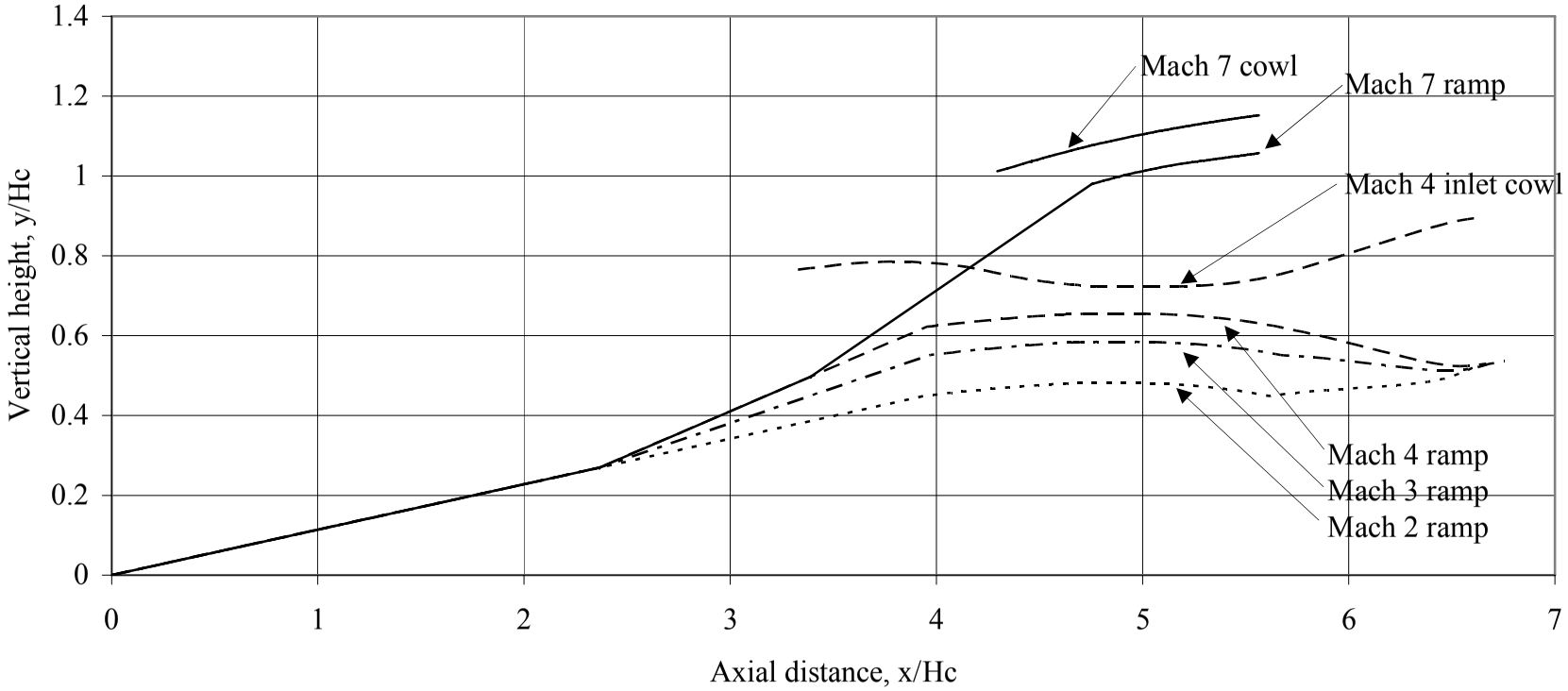

Figure 36. – Surface contours for Mach 7, Mach 4, Mach 3, and Mach 2 inlet configurations.

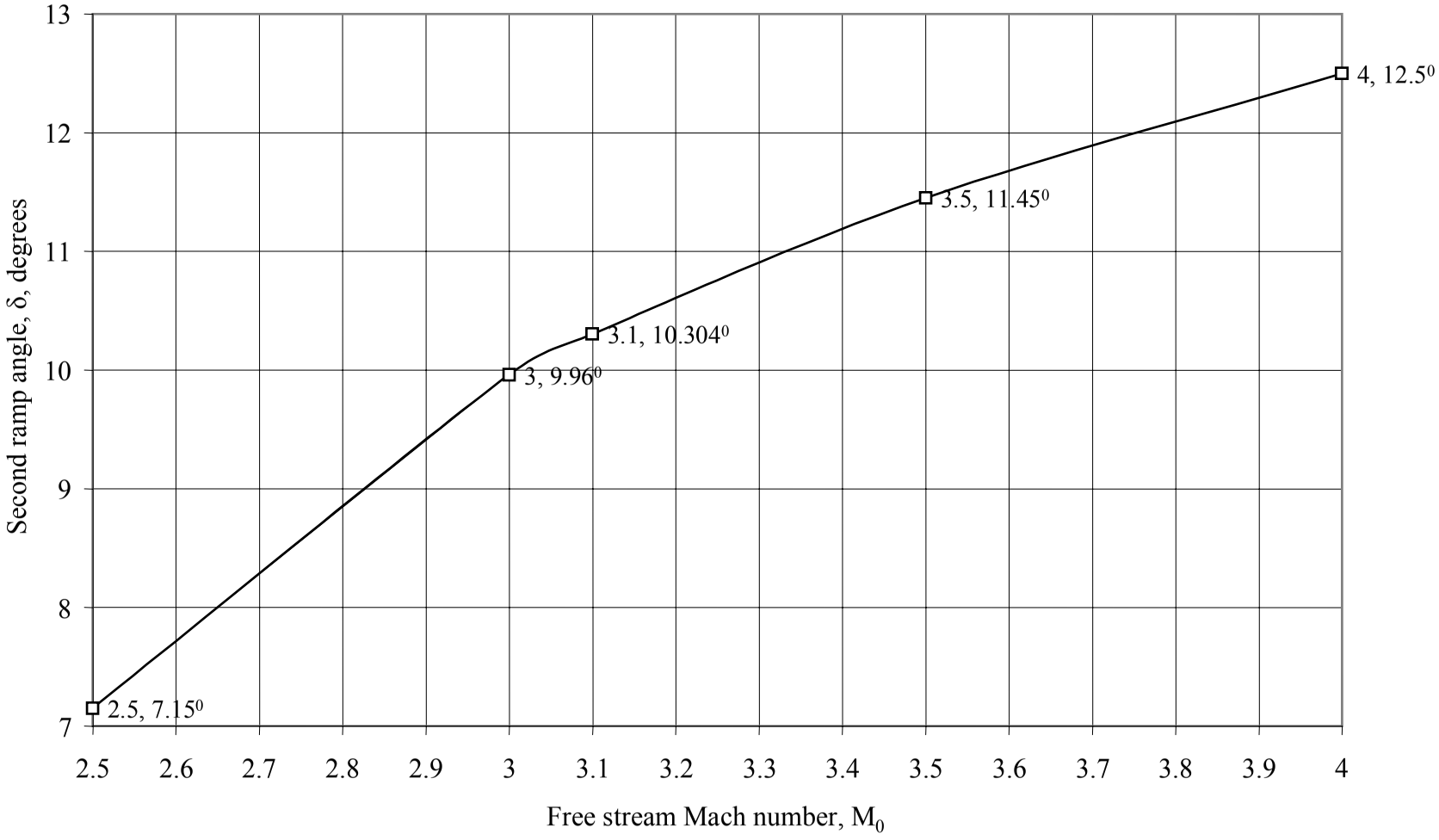

Figure 37. – Schedule of second ramp angle with free stream Mach number.

Ramp Coordinates for Mach 3 Operation (Second ramp collapsed to 9.96 degrees)

x/Hc	y/Hc	x/Hc	y/Hc	x/Hc	y/Hc	x/Hc	y/Hc
0	0	4.586245	0.580882	4.883658	0.58448	5.797915	0.546833
2.365363	0.2695	4.597684	0.581237	4.924123	0.58448	5.835923	0.545146
2.365363	0.2695	4.609122	0.581569	4.963903	0.584408	5.873929	0.543473
3.970647	0.551399	4.620561	0.581883	5.00327	0.584256	5.912278	0.541497
3.991418	0.552645	4.632	0.582181	5.027271	0.584098	5.949997	0.539335
4.020016	0.554378	4.643439	0.582455	5.061362	0.58373	5.988049	0.537014
4.048613	0.556071	4.654878	0.582712	5.095228	0.583184	6.027829	0.534366
4.07721	0.557724	4.666317	0.582947	5.129712	0.582536	6.064168	0.532147
4.105808	0.559343	4.677756	0.58317	5.164196	0.581767	6.102215	0.52989
4.134405	0.560921	4.689195	0.58337	5.192543	0.581019	6.140259	0.52769
4.163003	0.562465	4.700634	0.583553	5.214242	0.580371	6.178315	0.525309
4.1916	0.56397	4.712073	0.583713	5.249237	0.579259	6.216361	0.523067
4.220198	0.56544	4.723512	0.583856	5.296482	0.577437	6.254398	0.52095
4.248795	0.566869	4.734951	0.583982	5.343151	0.575374	6.292424	0.518996
4.277392	0.568259	4.74639	0.584085	5.381524	0.57338	6.33045	0.517054
4.30599	0.569615	4.757829	0.584171	5.41932	0.5713	6.368479	0.515056
4.334587	0.570936	4.769268	0.58424	5.457116	0.568958	6.406457	0.513789
4.363185	0.572211	4.780707	0.584285	5.494912	0.566512	6.444408	0.512893
4.391782	0.573458	4.792146	0.58432	5.532709	0.5637	6.482323	0.512533
4.420379	0.574659	4.803585	0.584337	5.570505	0.560651	6.520182	0.512957
4.448977	0.575826	4.815024	0.58436	5.608301	0.557255	6.55795	0.514682
4.477574	0.576959	4.826463	0.584377	5.646097	0.553724	6.595624	0.517745
4.506172	0.578051	4.837902	0.5844	5.669675	0.551399	6.633211	0.522052
4.534769	0.579103	4.849341	0.584417	5.683958	0.550979	6.683583	0.529142
4.563367	0.580121	4.86078	0.58444	5.721936	0.549708	6.757355	0.535558
4.574806	0.58051	4.872219	0.584457	5.759918	0.548377	6.915197	0.915945

Cowl Coordinates for Mach 3 Operation (Cowl at Mach 4 position)

x/Hc	y/Hc	x/Hc	y/Hc	x/Hc	y/Hc	x/Hc	y/Hc
3.330089	0.765291	4.451629	0.74076	4.828571	0.722704	5.745414	0.764752
3.388645	0.768872	4.46714	0.739508	4.84009	0.722658	5.78321	0.770435
3.420143	0.770799	4.482491	0.738313	4.851558	0.722653	5.821006	0.77645
3.45164	0.772727	4.497699	0.73718	4.863003	0.722656	5.858802	0.782797
3.483137	0.774654	4.512793	0.736105	4.910051	0.722668	5.896919	0.789069
3.514629	0.776576	4.527715	0.735081	4.949831	0.72268	5.934395	0.795179
3.559881	0.779138	4.542511	0.734109	4.989198	0.722688	5.972191	0.801549
3.605128	0.781272	4.557188	0.733188	5.013199	0.722693	6.011688	0.807885
3.650363	0.782987	4.571772	0.732307	5.04729	0.722705	6.047783	0.813959
3.695593	0.784263	4.586214	0.731472	5.081156	0.722742	6.085579	0.820227
3.7408	0.785104	4.600553	0.730677	5.11564	0.722868	6.123375	0.826499
3.785972	0.785498	4.614817	0.729928	5.150124	0.723118	6.161172	0.832772
3.831093	0.785441	4.628944	0.729207	5.178471	0.723435	6.198968	0.838841
3.876163	0.784926	4.642991	0.728526	5.20017	0.723701	6.236764	0.844911
3.921152	0.783948	4.656958	0.727886	5.235165	0.724316	6.27456	0.851153
3.966062	0.782501	4.670828	0.727257	5.28241	0.725351	6.312356	0.857051
4.010874	0.78058	4.684663	0.726628	5.329079	0.726808	6.350152	0.862829
4.055572	0.778183	4.698453	0.725998	5.367452	0.728291	6.387949	0.868669
4.100144	0.775306	4.71055	0.725472	5.405248	0.730178	6.425745	0.874225
4.144578	0.771949	4.722589	0.724992	5.443044	0.732414	6.463541	0.879711
4.188859	0.7681	4.734577	0.724557	5.48084	0.735033	6.501337	0.884567
4.232979	0.763759	4.746508	0.724168	5.518637	0.738054	6.539133	0.888501
4.276921	0.758931	4.758388	0.723831	5.556433	0.741465	6.576929	0.89181
4.320567	0.753721	4.770216	0.723533	5.594229	0.745286	6.614726	0.894929
4.362954	0.749037	4.781986	0.723282	5.632025	0.74948	6.639572	0.896666
4.404088	0.744959	4.793711	0.723076	5.655603	0.752286	6.731457	0.903082
4.420114	0.743483	4.805379	0.72291	5.669821	0.754075	6.915197	0.915945
4.435957	0.742087	4.817001	0.722784	5.707617	0.759242		

Figure 38. – Coordinates for the low-speed inlet at a Mach 3 condition.

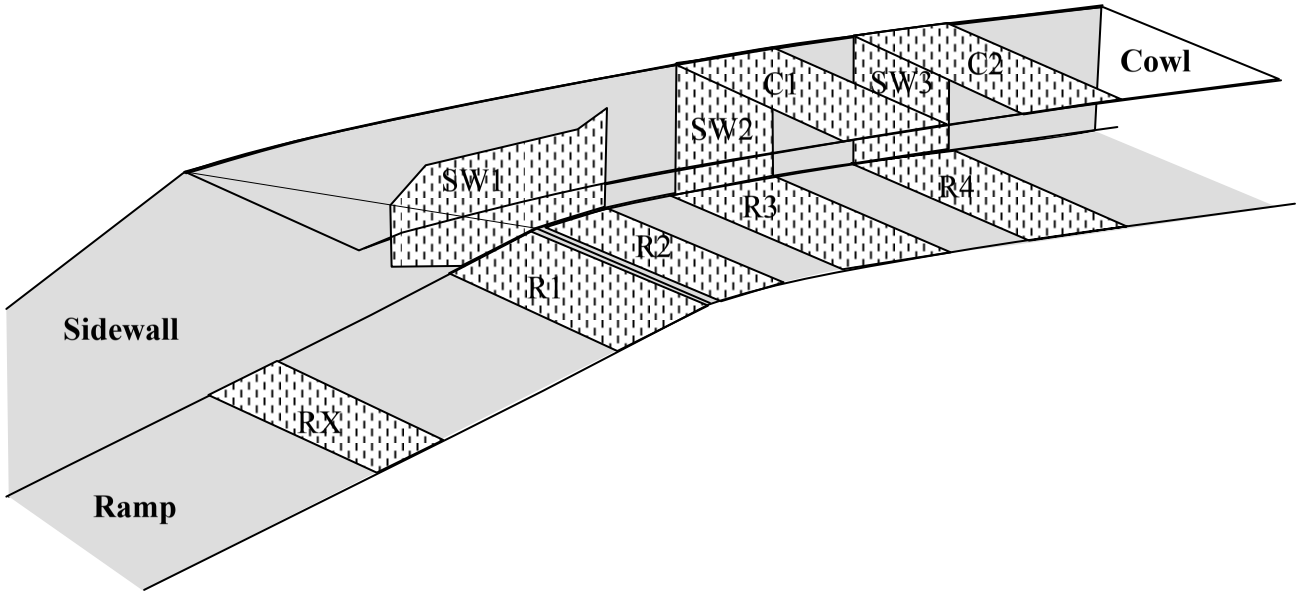

Figure 39. – Low-speed inlet bleed regions (Mach 4 coordinates).

Bulkhead between	Station, x/H_c
RX - R1	3.5917
R1 - R2	Ramp shoulder
R2 - R3	4.1443
R3 - R4	4.6047
R4 - aft cavity	5.2187
C1 - C2	4.7582
SW1 - SW2	4.1443
SW2 - SW3	4.6047

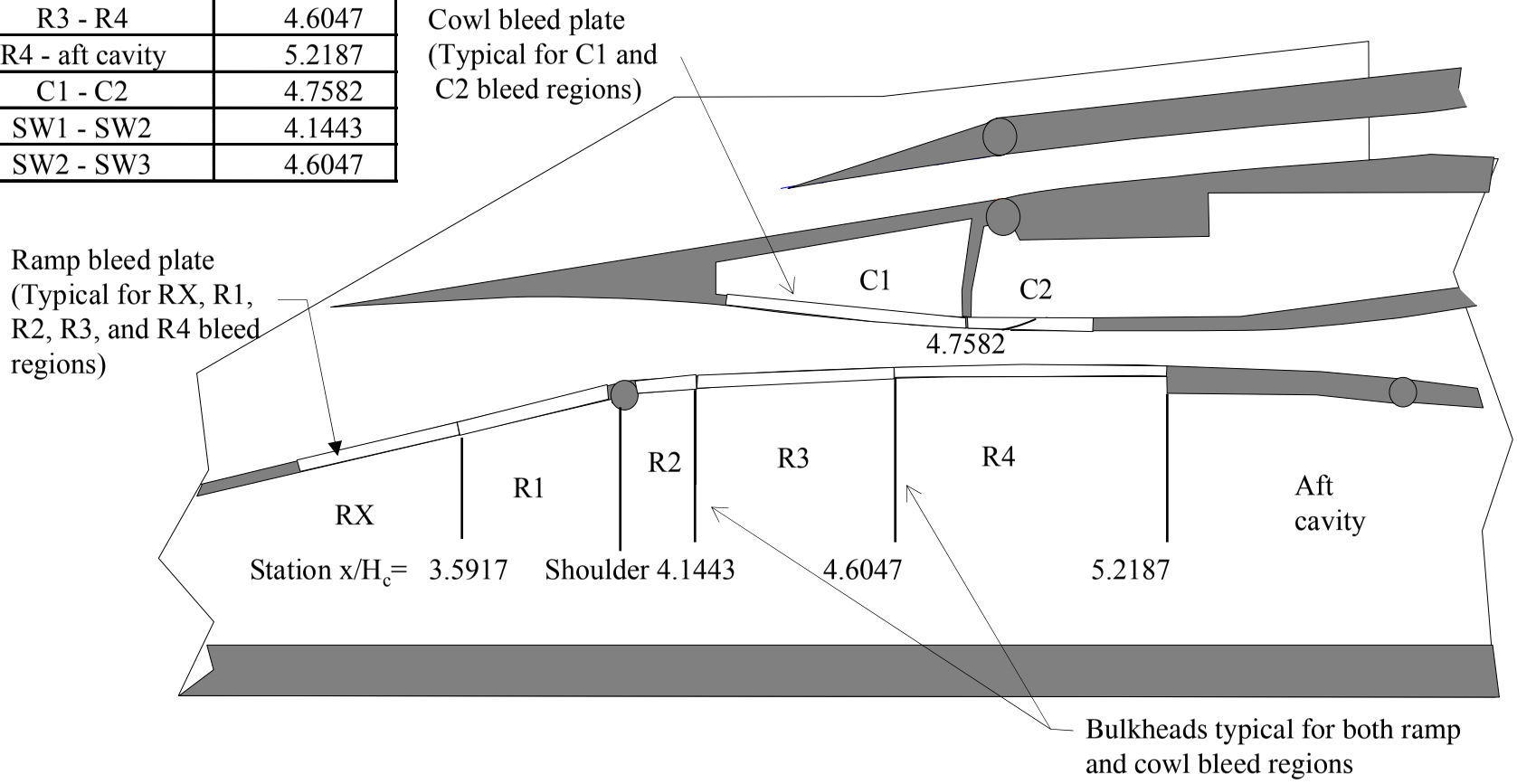

Figure 40. – Bulkhead stations between bleed regions on the inlet ramp and cowl.

Figure 41. –Ramp bleed and bleed bulkheads.

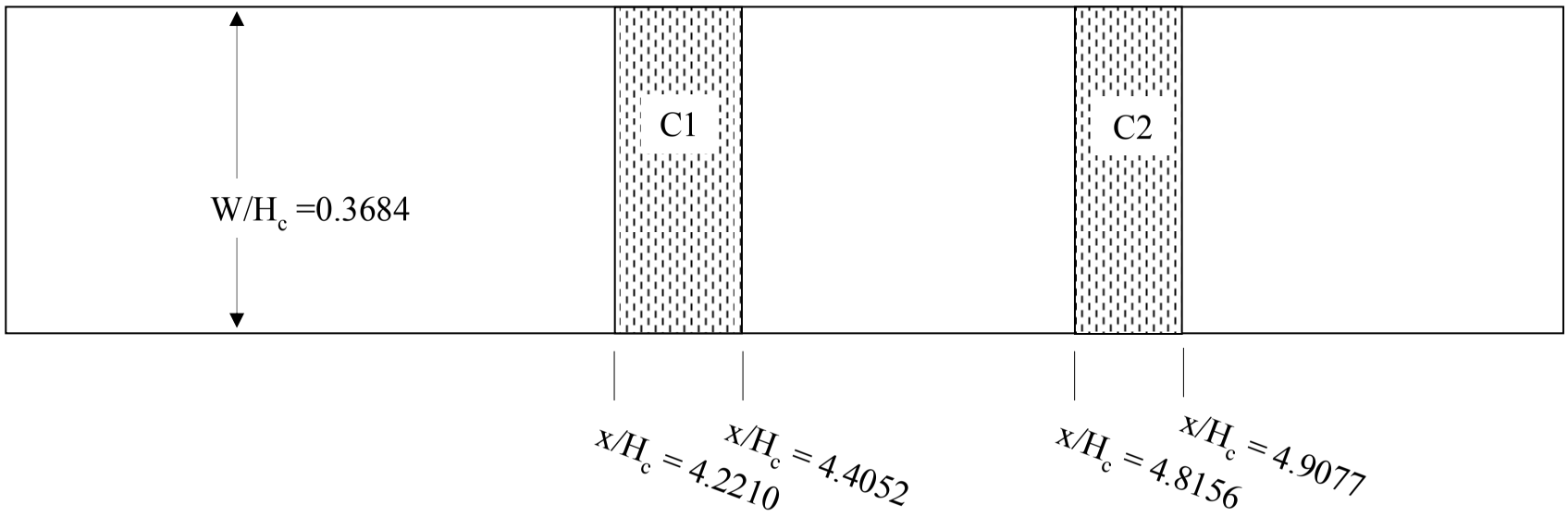

Figure 42. – Mach 4 inlet cowl bleed regions (C1 AND C2)

SW1 bleed pattern		
Point	x/H_c	y/H_c
A	3.6838	0.5526
B	3.8373	0.5526
C	3.8373	Min ramp
D	4.0460	Min ramp
E	4.0460	0.5526
F	4.1136	0.5526
G	4.1136	0.7521
H	3.9908	0.7214
I	3.7452	0.7214
J	3.6838	0.6754

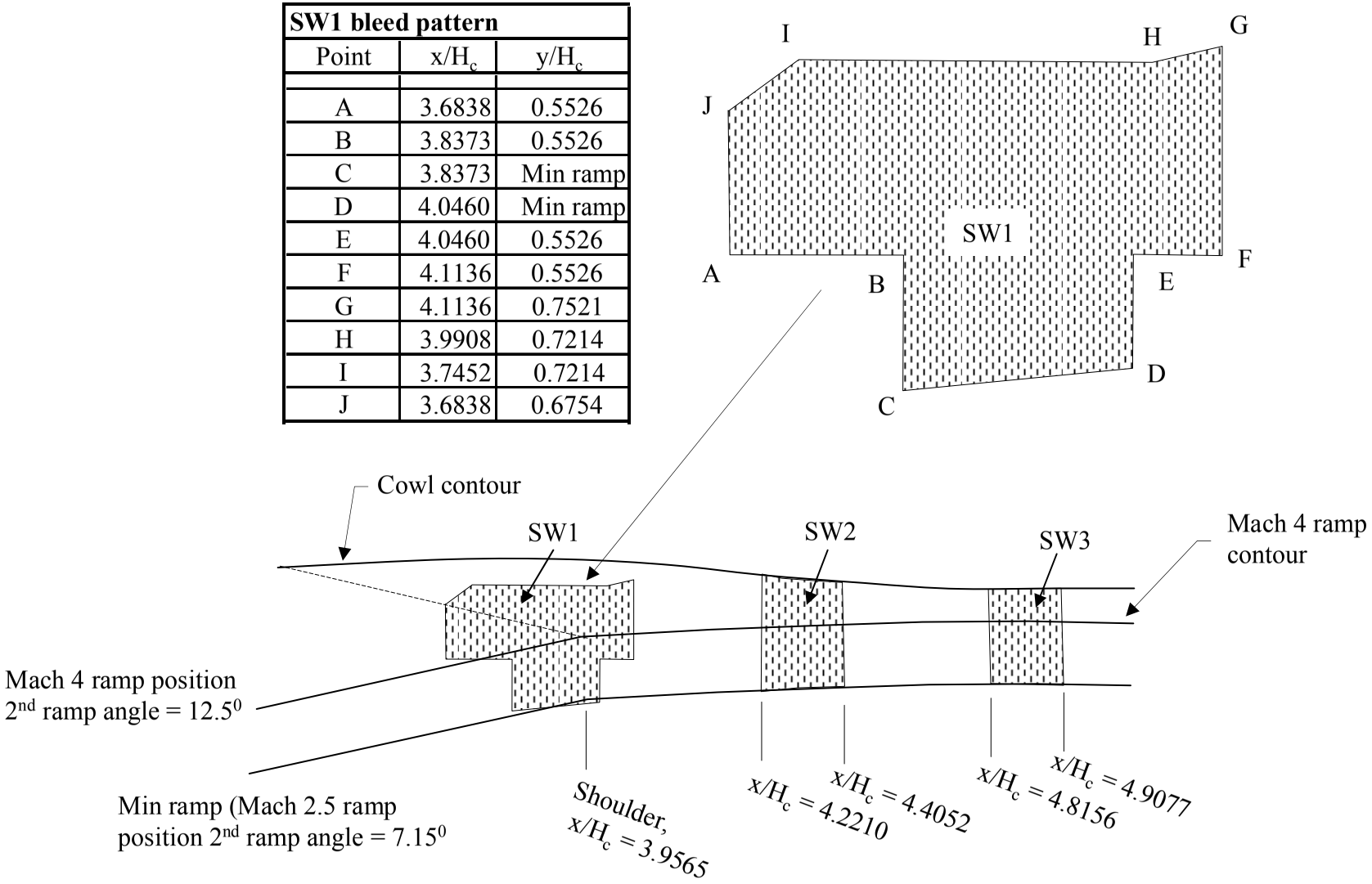

Figure 43. – Mach 4 inlet sidewall bleed (SW1, SW2, and SW3)

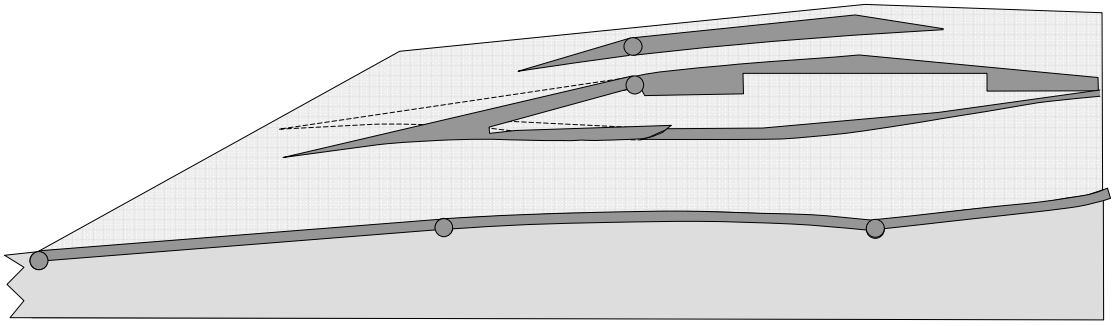

(a). Takeoff inlet configuration.

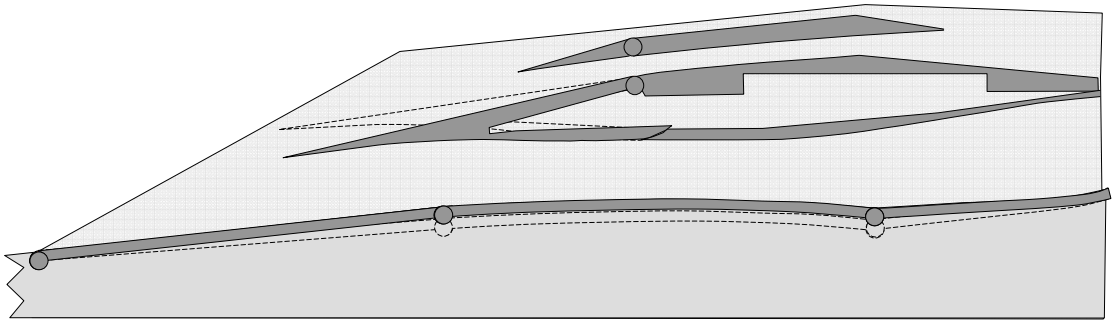

(b). Mach 2 inlet operation.

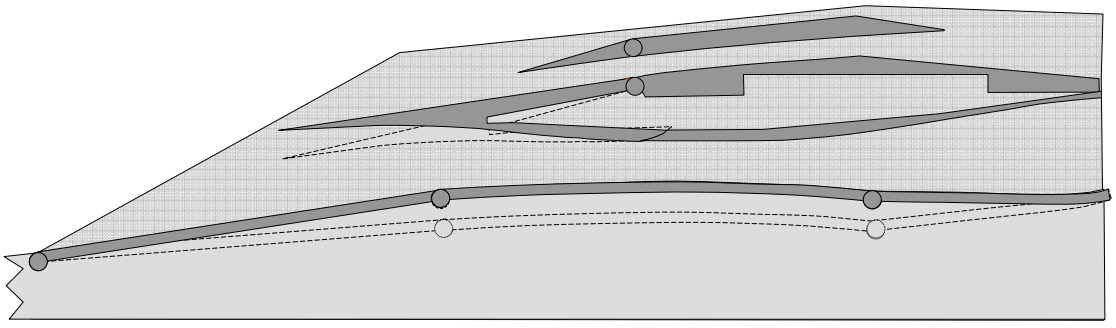

(c). Mach 3 inlet operation.

Figure 44. – Inlet configurations for Mach numbers from takeoff to Mach 3.

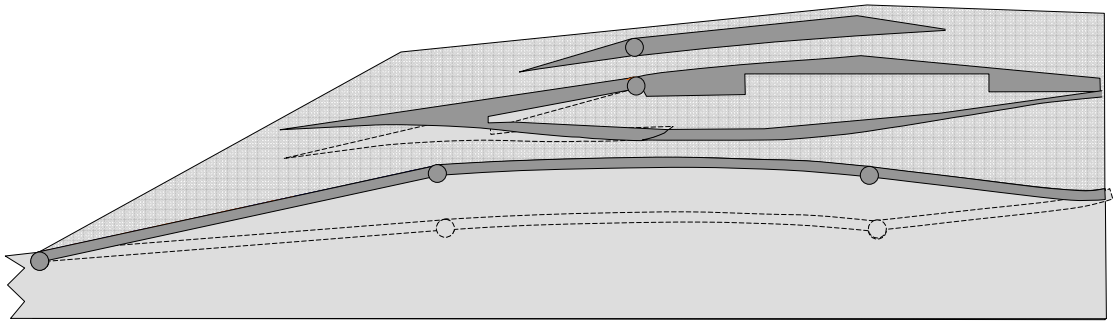

(a). Mach 4 operation.

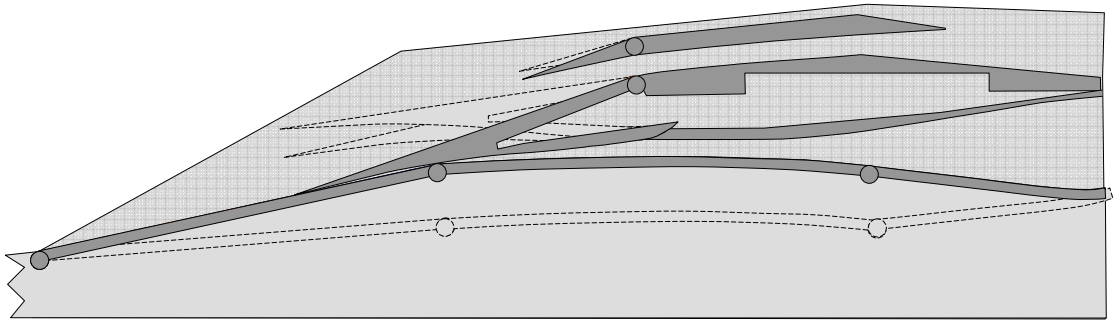

(b). Mach 4 operation with low-speed inlet closed (end of mode transition).

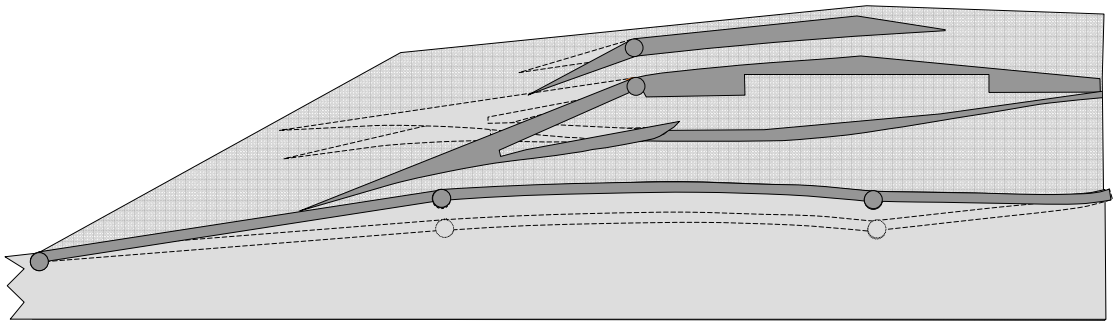

(c). Mach 3 operation with low-speed inlet closed (alternate mode transition Mach number).

Figure 45. – Inlet configurations for operation near mode transition: Mach 4 before mode transition, Mach 4 with low-speed inlet closed after mode transition, and Mach 3 with cowl lip closed after mode transition.

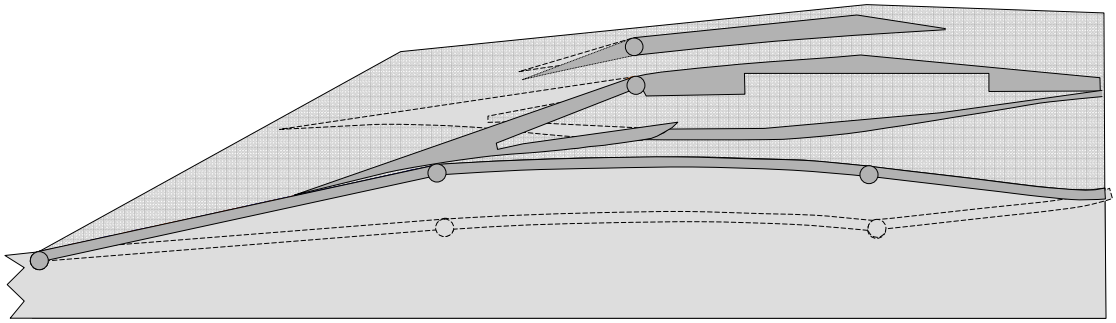

(a). Mach 4 to 7, low-speed inlet closed.

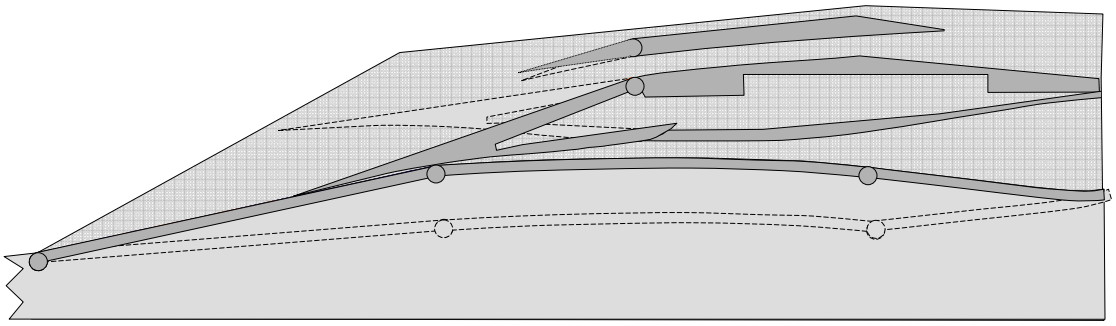

(b). Mach 7, low-speed inlet closed.

Figure 46. – Inlet configurations for Mach operation from Mach 4 to 7.

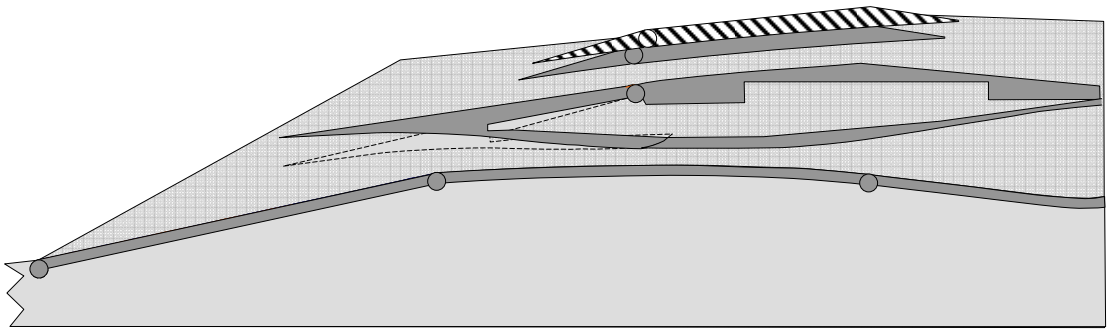

(a). High-speed cowl translation.

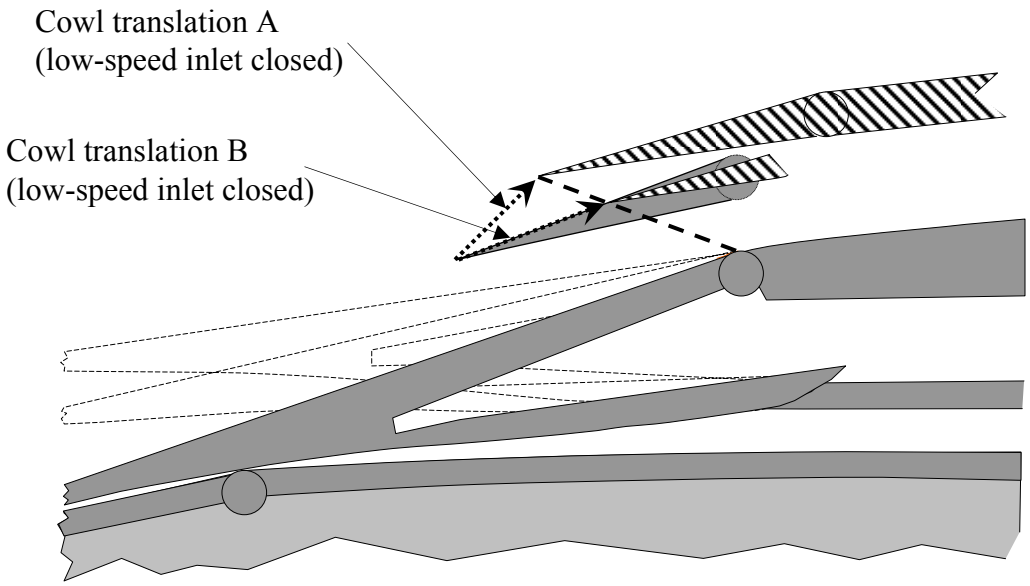

(b). Possible high-speed cowl translation schedules.

Figure 47. – Versatility of IMX design with cowl translation for aerodynamics: put shock on shoulder, adjust for increased capture at off-design conditions, or for additional adjustment of boundary layer blockage.

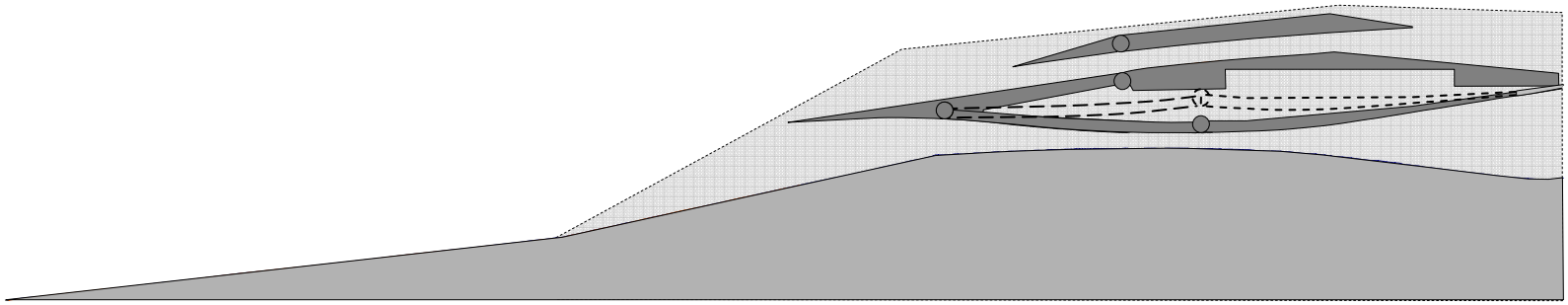

(a) Configuration VGC, variable geometry cowl and cowl lip at design Mach number of 4.

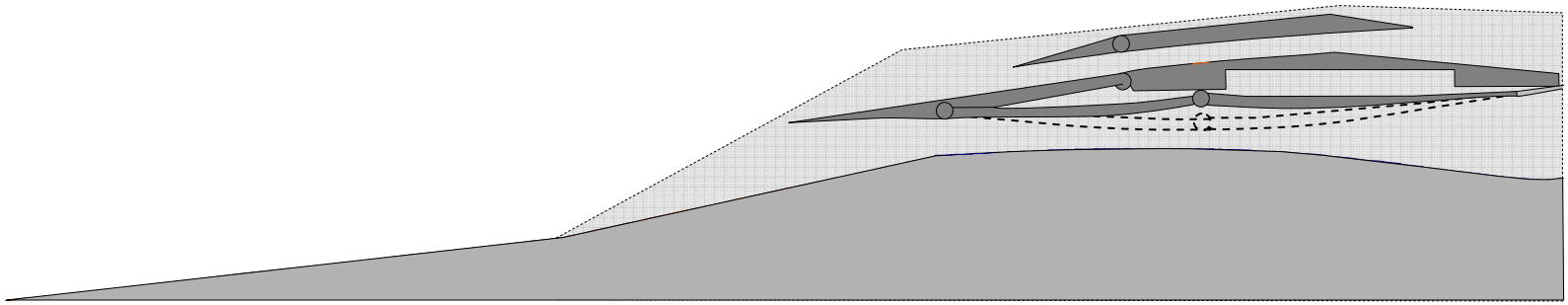

(b) Variable geometry cowl (VGC) collapsed for Mach 3 operation.

Figure 48. – Variable cowl inlet configuration (VGC)

Variable geometry cowl coordinates for Mach 3 operation									
x/Hc	y/Hc		x/Hc	y/Hc		x/Hc	y/Hc		x/Hc	y/Hc
3.330089	0.765291		4.453333	0.771256		4.830550	0.782171		5.747804	0.811908
3.388645	0.768872		4.468894	0.771197		4.842038	0.783009		5.785902	0.814974
3.420143	0.770799		4.484292	0.771183		4.853472	0.783883		5.824022	0.818372
3.451640	0.772727		4.499542	0.771220		4.864883	0.784765		5.862166	0.822100
3.483137	0.774654		4.514674	0.771306		4.911792	0.788387		5.900624	0.825731
3.514629	0.776576		4.529630	0.771430		4.951454	0.791450		5.938432	0.829246
3.559881	0.779138		4.544458	0.771596		4.990704	0.794478		5.976577	0.832996
3.605128	0.781272		4.559161	0.771804		5.014633	0.796325		6.016417	0.836597
3.650363	0.782987		4.573770	0.772045		5.048624	0.798953		6.052845	0.840170
3.695593	0.784263		4.588234	0.772320		5.082386	0.801587		6.090983	0.843820
3.740800	0.785104		4.602591	0.772627		5.116759	0.804359		6.129121	0.847473
3.785972	0.785498		4.616871	0.772975		5.151123	0.807253		6.167260	0.851127
3.831093	0.785441		4.631012	0.773340		5.179362	0.809744		6.205384	0.854578
3.876163	0.784926		4.645070	0.773739		5.201028	0.808515		6.243509	0.858030
3.921152	0.783948		4.659045	0.774172		5.235982	0.806717		6.281645	0.861654
3.966062	0.782501		4.672922	0.774609		5.283186	0.804496		6.319758	0.864934
4.010874	0.780580		4.686765	0.775043		5.329845	0.802734		6.357862	0.868094
4.055572	0.778183		4.700562	0.775473		5.368228	0.801570		6.395971	0.871317
4.100233	0.778734		4.712663	0.775877		5.406065	0.800849		6.425745	0.874225
4.144794	0.778796		4.724704	0.776322		5.443925	0.800476		6.463541	0.879711
4.189239	0.778355		4.736690	0.776808		5.481812	0.800486		6.501337	0.884567
4.233562	0.777411		4.748616	0.777335		5.519726	0.800896		6.539133	0.888501
4.277746	0.775970		4.760486	0.777910		5.557668	0.801695		6.576929	0.891810
4.321663	0.774123		4.772302	0.778521		5.595637	0.802903		6.614726	0.894929
4.364284	0.772705		4.784057	0.779173		5.633633	0.804484		6.639572	0.896666
4.405610	0.771794		4.795763	0.779868		5.657348	0.805659		6.731457	0.903082
4.421702	0.771553		4.807410	0.780597		5.671656	0.806464		6.915197	0.915945
4.437606	0.771377		4.819007	0.781363		5.709718	0.809015			

Figure 49. – Variable geometry cowl coordinates for Mach 3 operation.

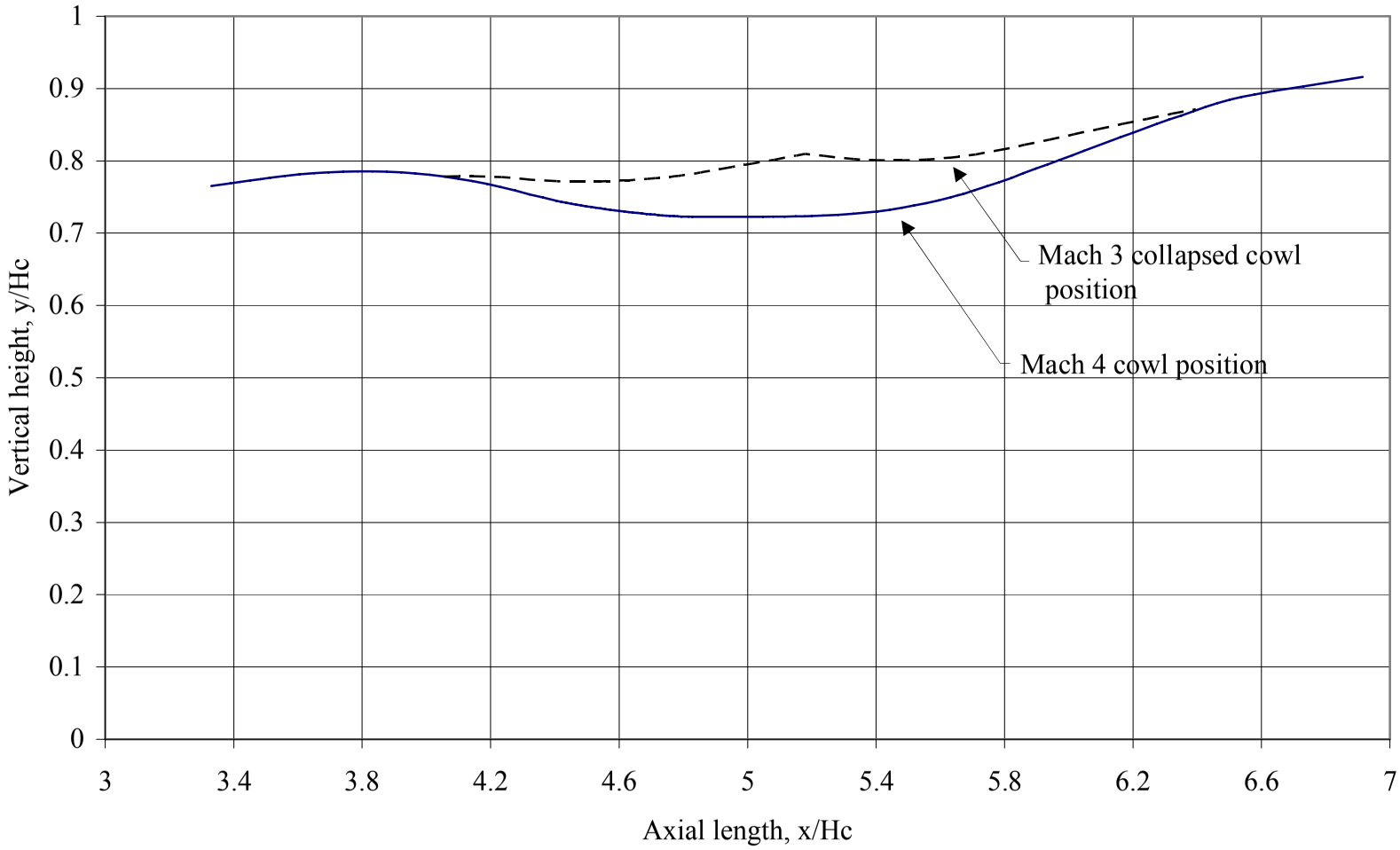

Figure 50. – Variable cowl inlet surface, for Mach 4 operation and for Mach 3 operation..

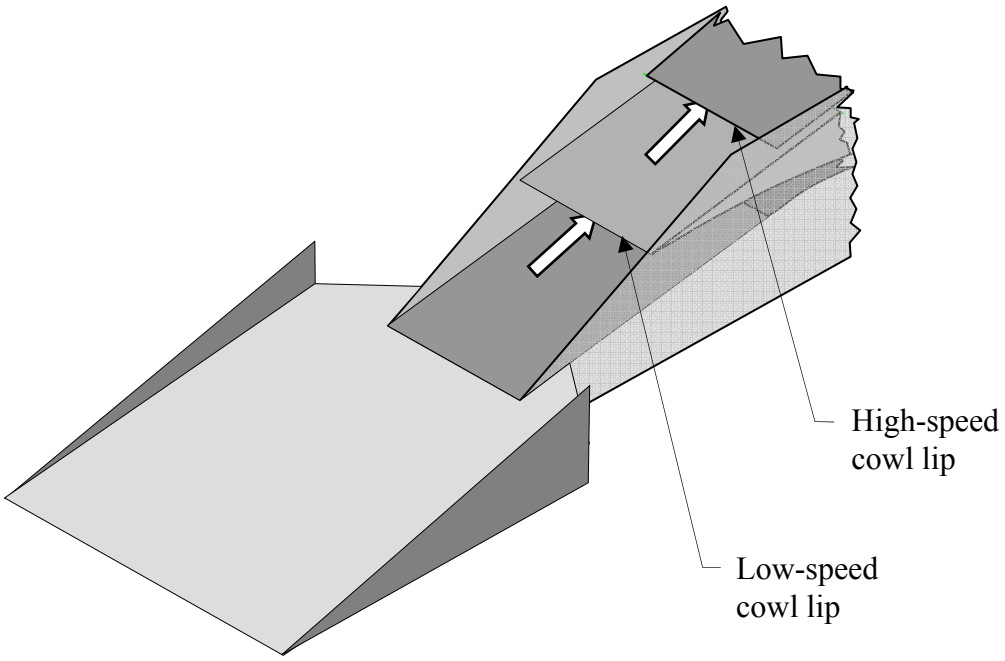

(a). Isometric view of small-scale inlet model.

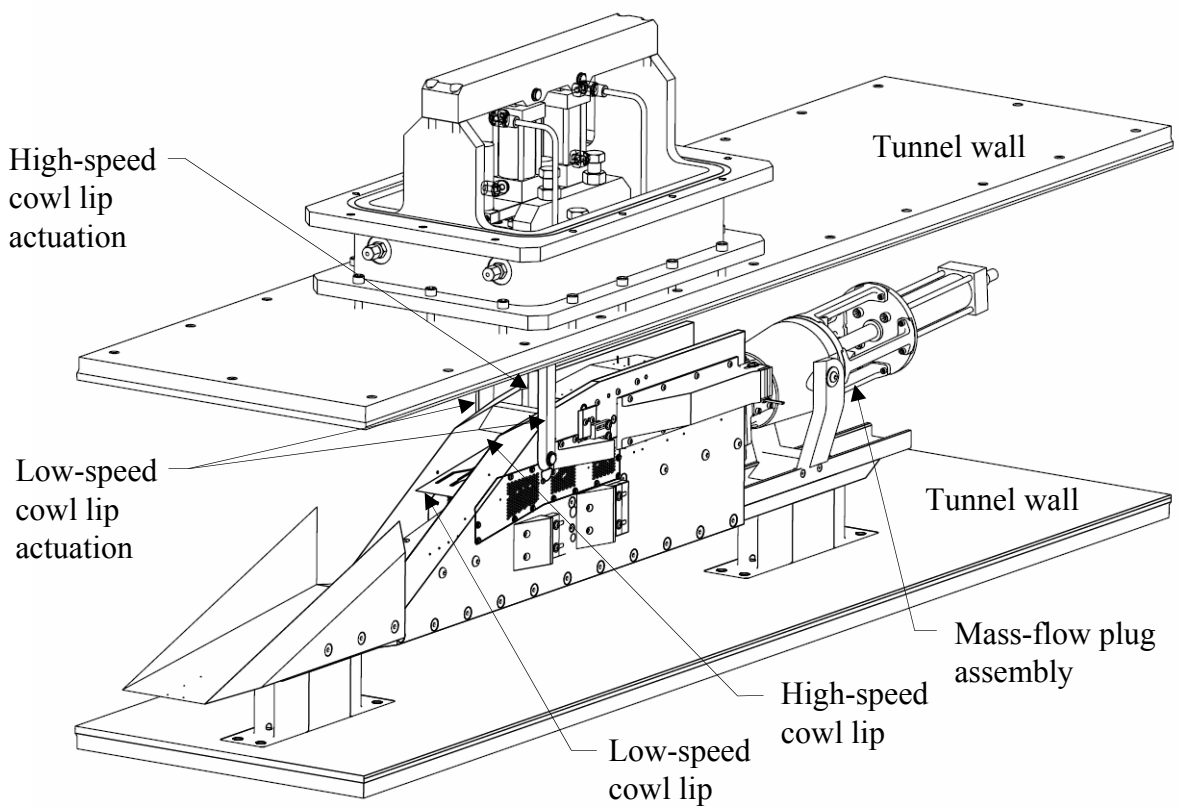

(b). Sketch of small-scale inlet model as mounted in the NASA Glenn 1X1 Supersonic Wing Tunnel.

Figure 51. – Small-scale IMX inlet model.

Figure 52. - Small-scale dual-mode hypersonic inlet installed in the NASA Glenn 1X1 SWT. Low-speed inlet cowl lip is in the Mach 4 (design) position.

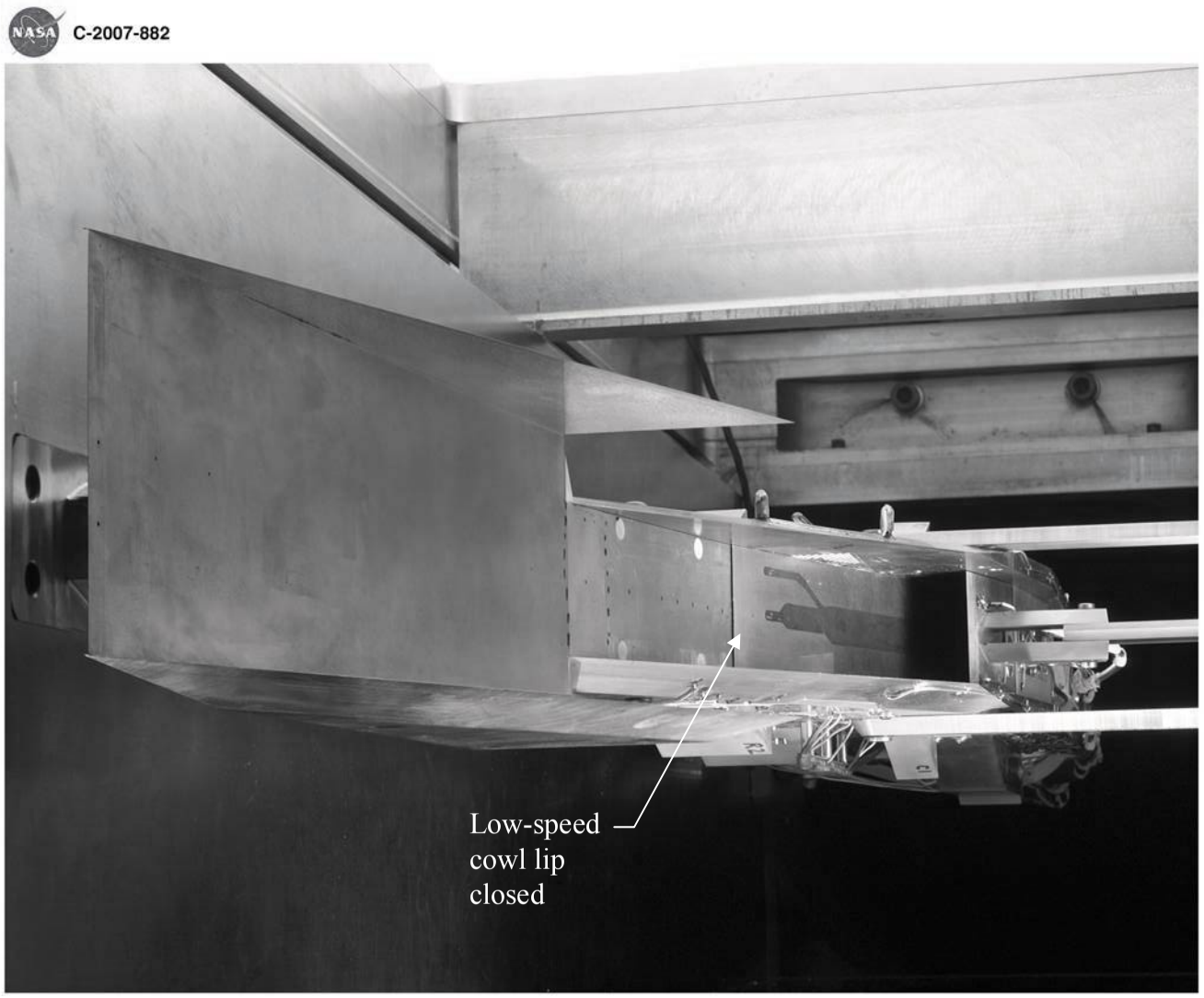

Figure 53. - Small-scale Dual-mode hypersonic inlet installed in the NASA Glenn 1X1 SWT. Low-speed inlet cowl lip is in the closed position.

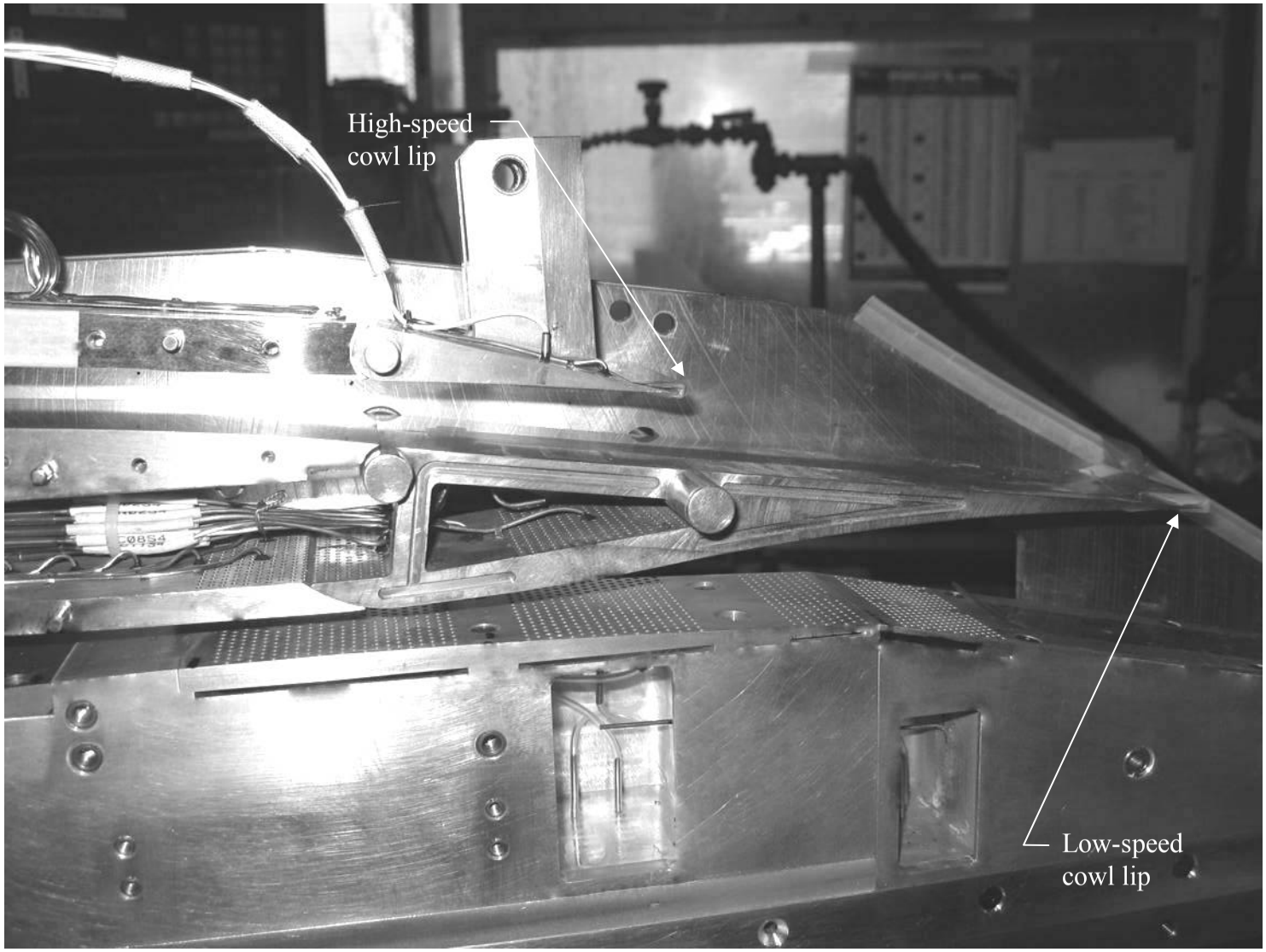

Figure 54. - Picture of the low-speed inlet with sidewall removed.

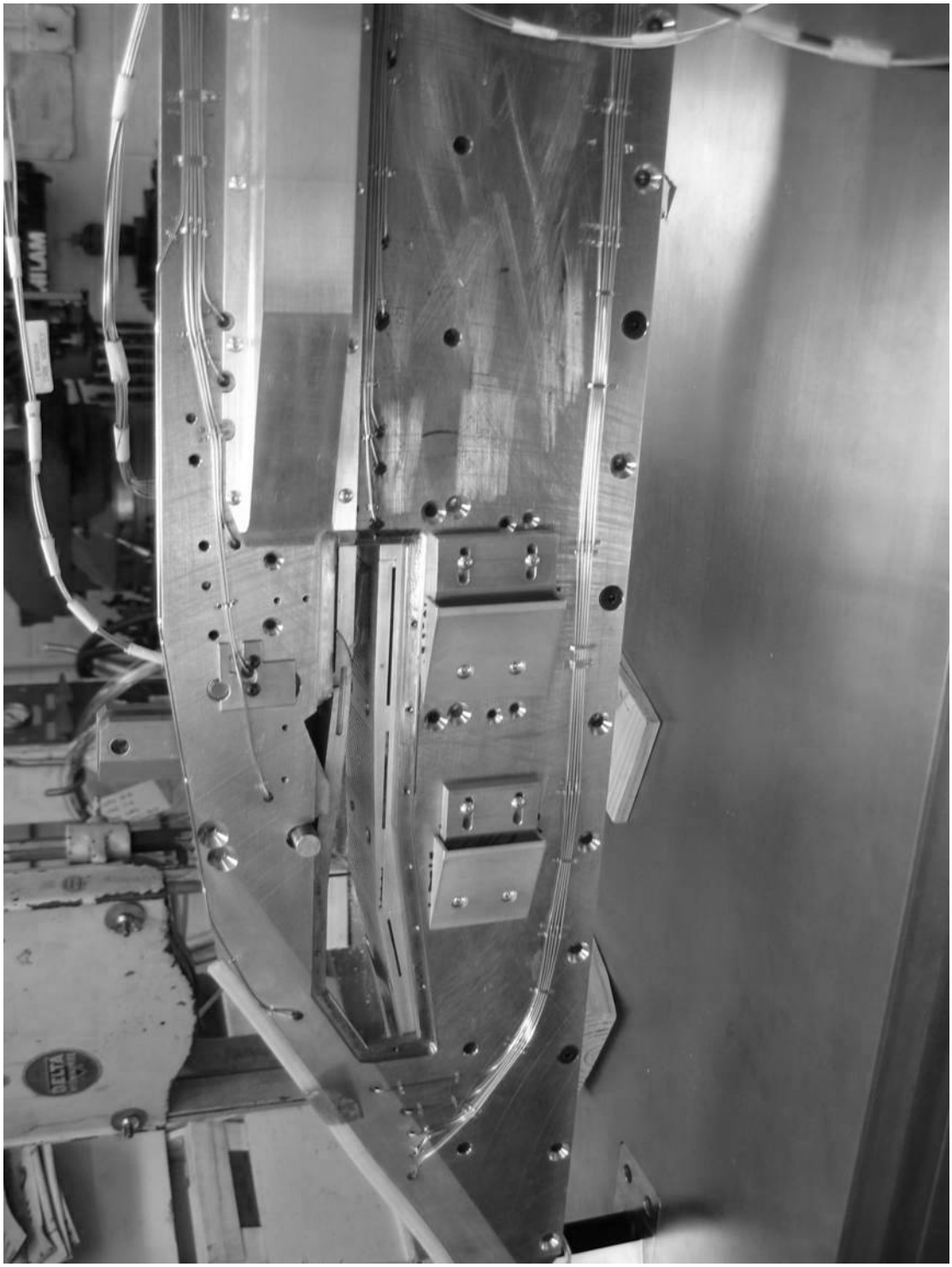

Figure 55. - Picture of low-speed inlet with sidewall bleed plate removed.

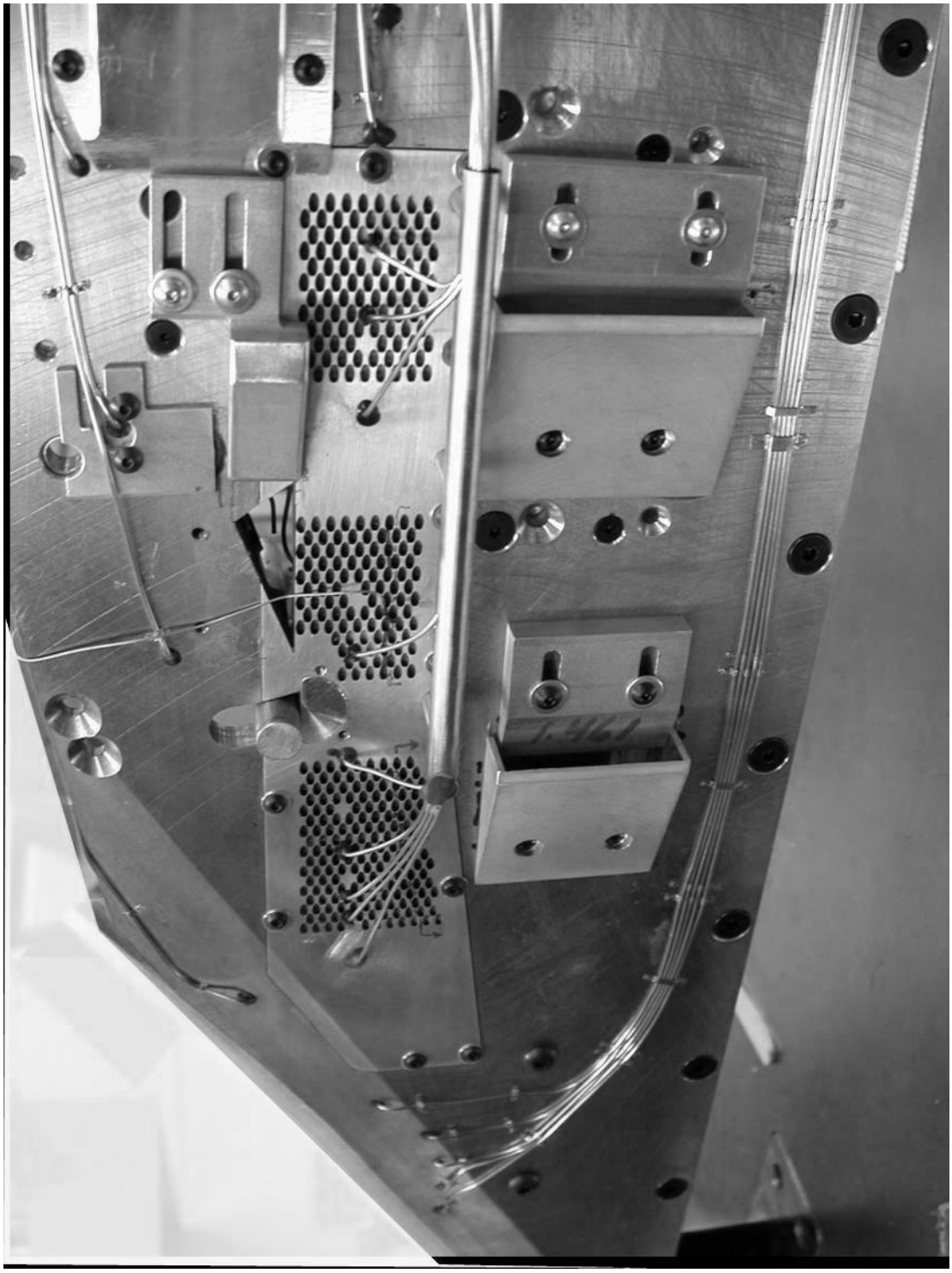

Figure 56. – Side view of low-speed inlet.

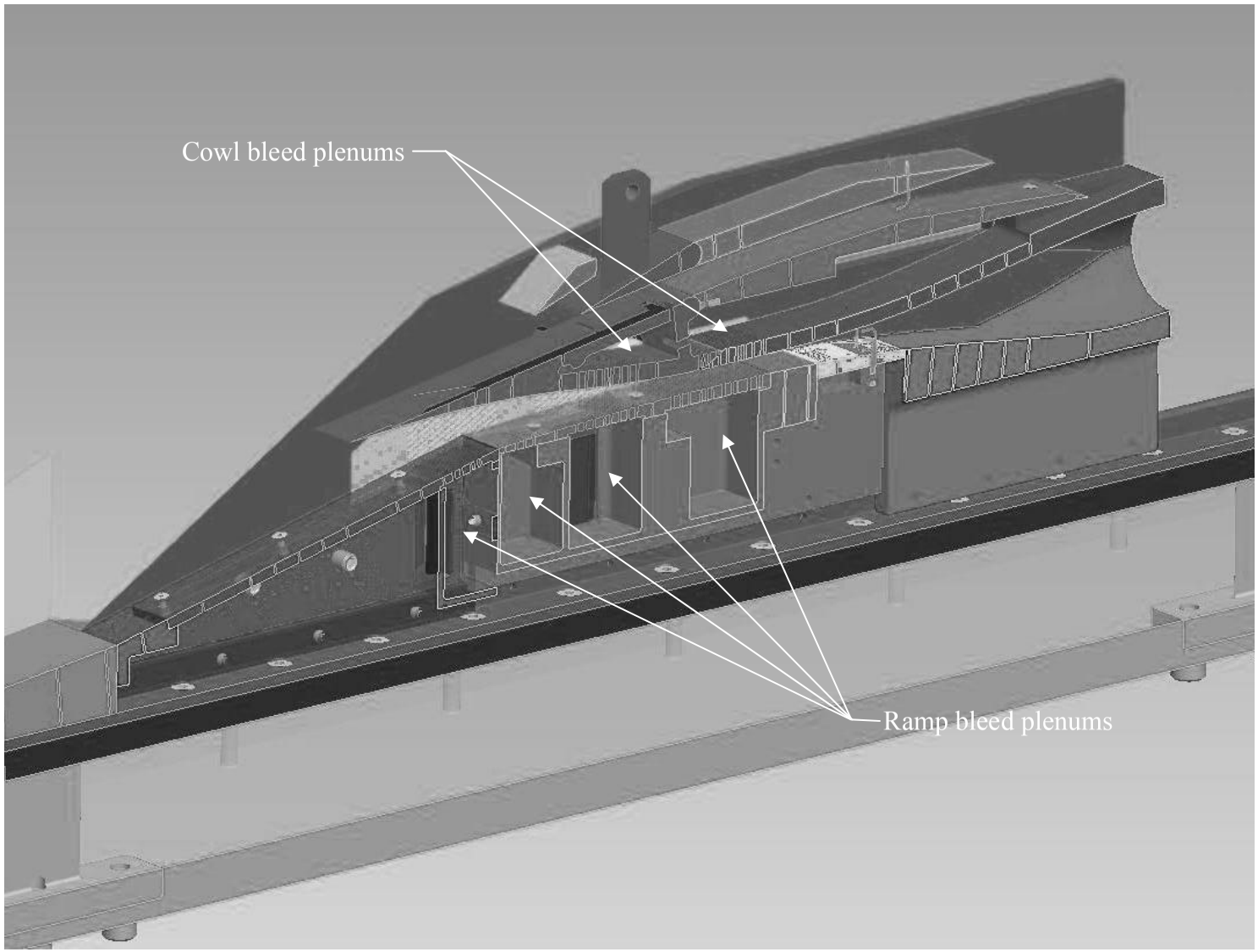

Figure 57. – Cut-away view of small-scale inlet model showing inlet bleeds.

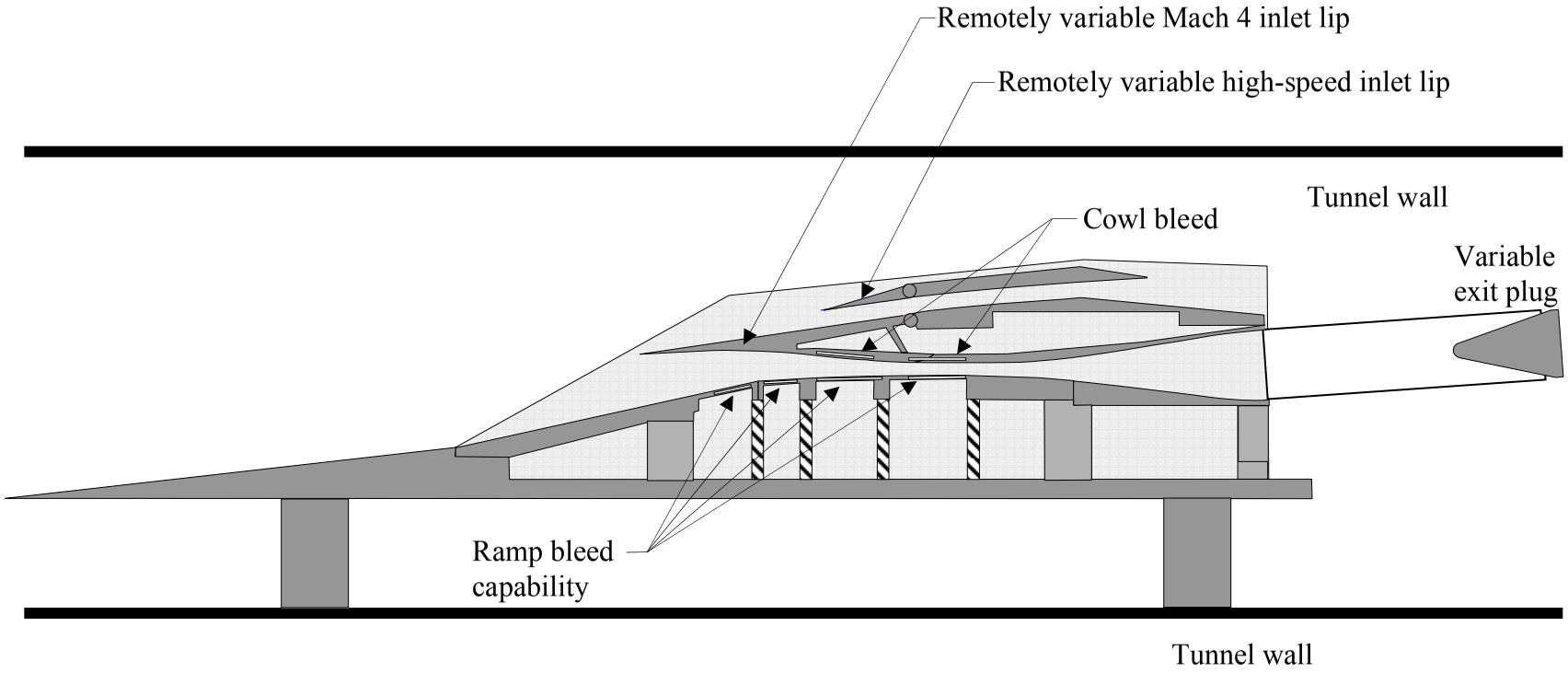

Figure 58. – Axial cross-section of small-scale model.

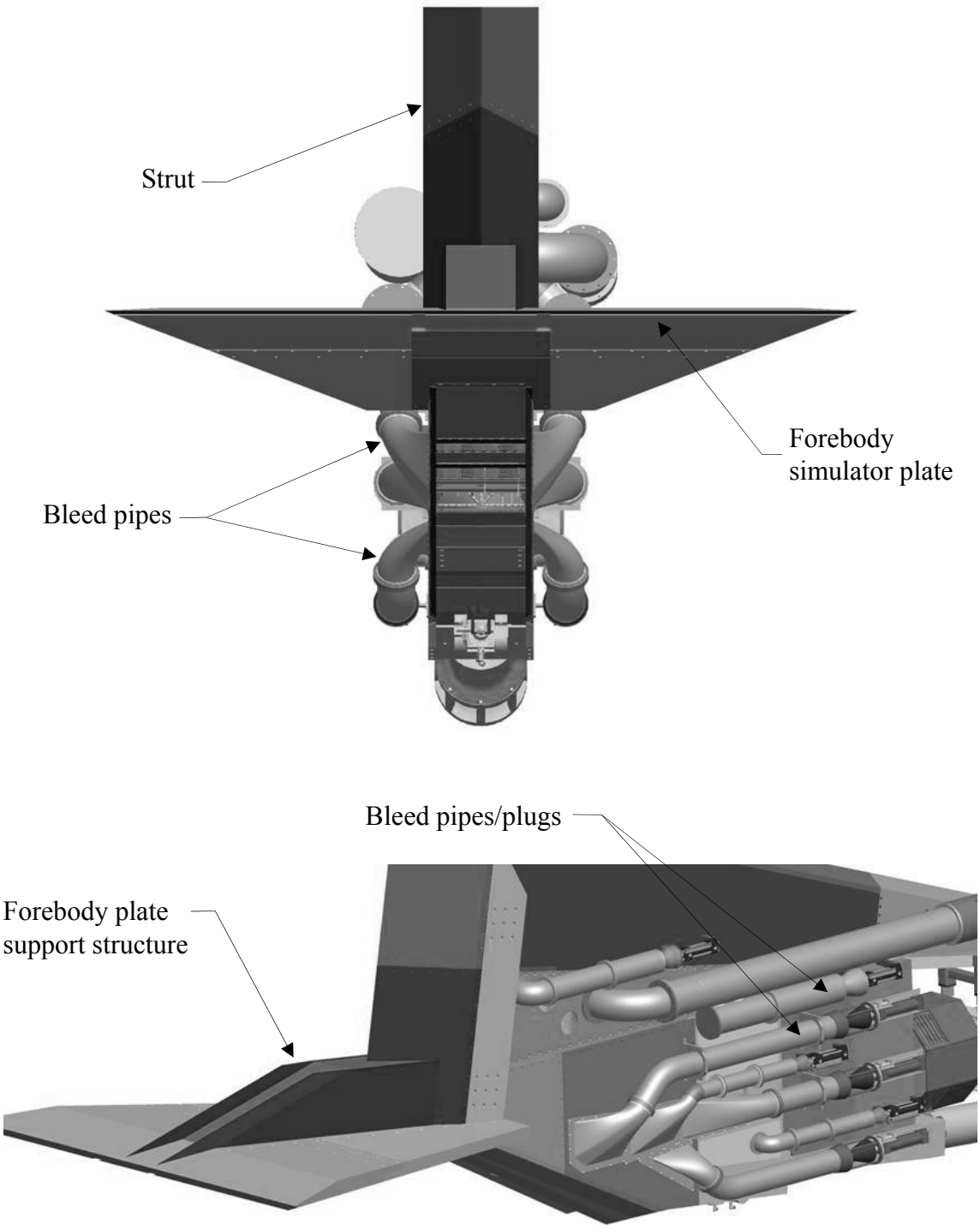

Figure 59. – Large-scale inlet designed by ATK for testing in the NASA Glenn 10X10 Foot Supersonic Wind Tunnel.

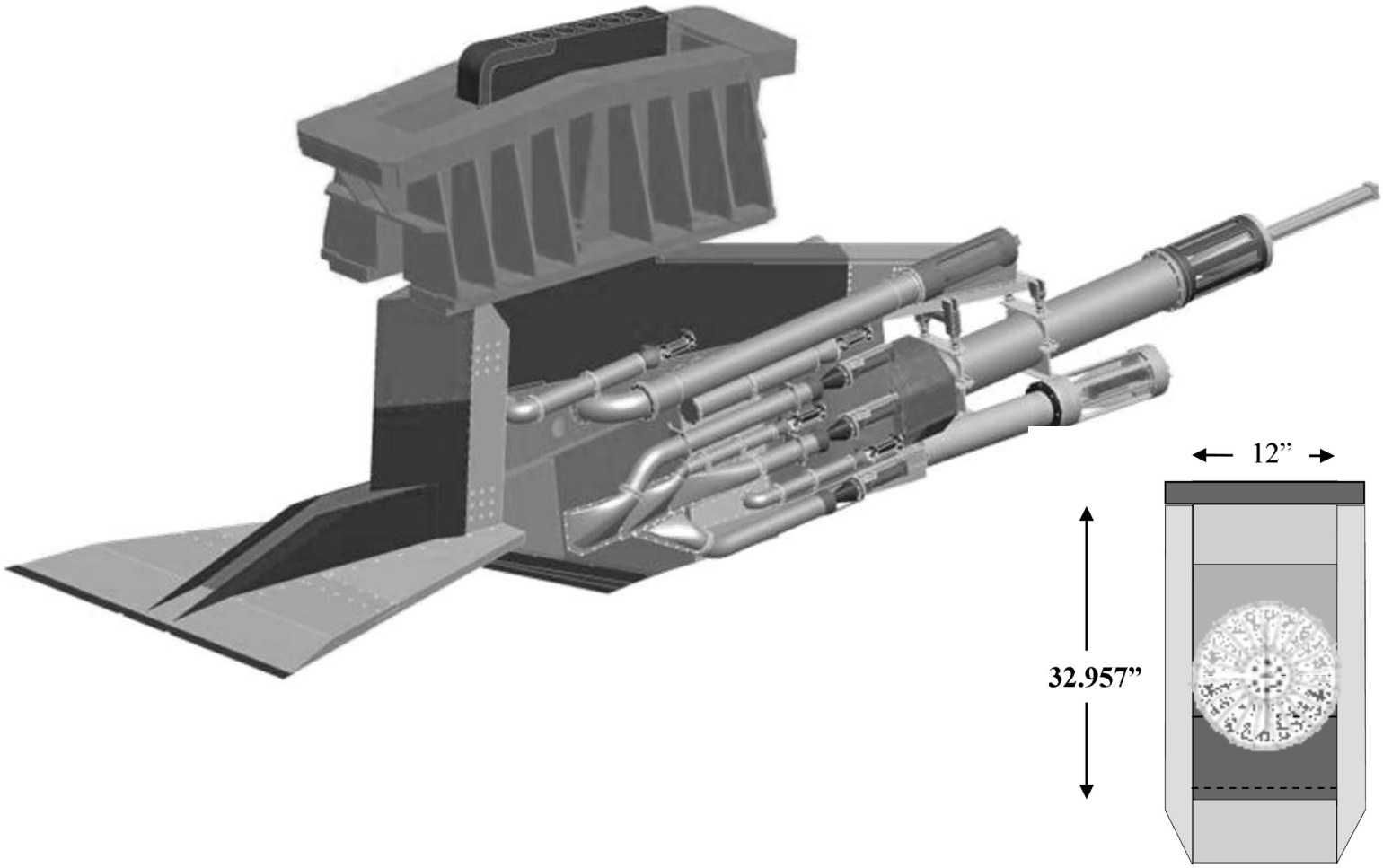

Figure 60. – Large-scale inlet designed by ATK. Inlet shown attached to the strut box for the NASA Glenn 10X10 Foot Supersonic Wind Tunnel.

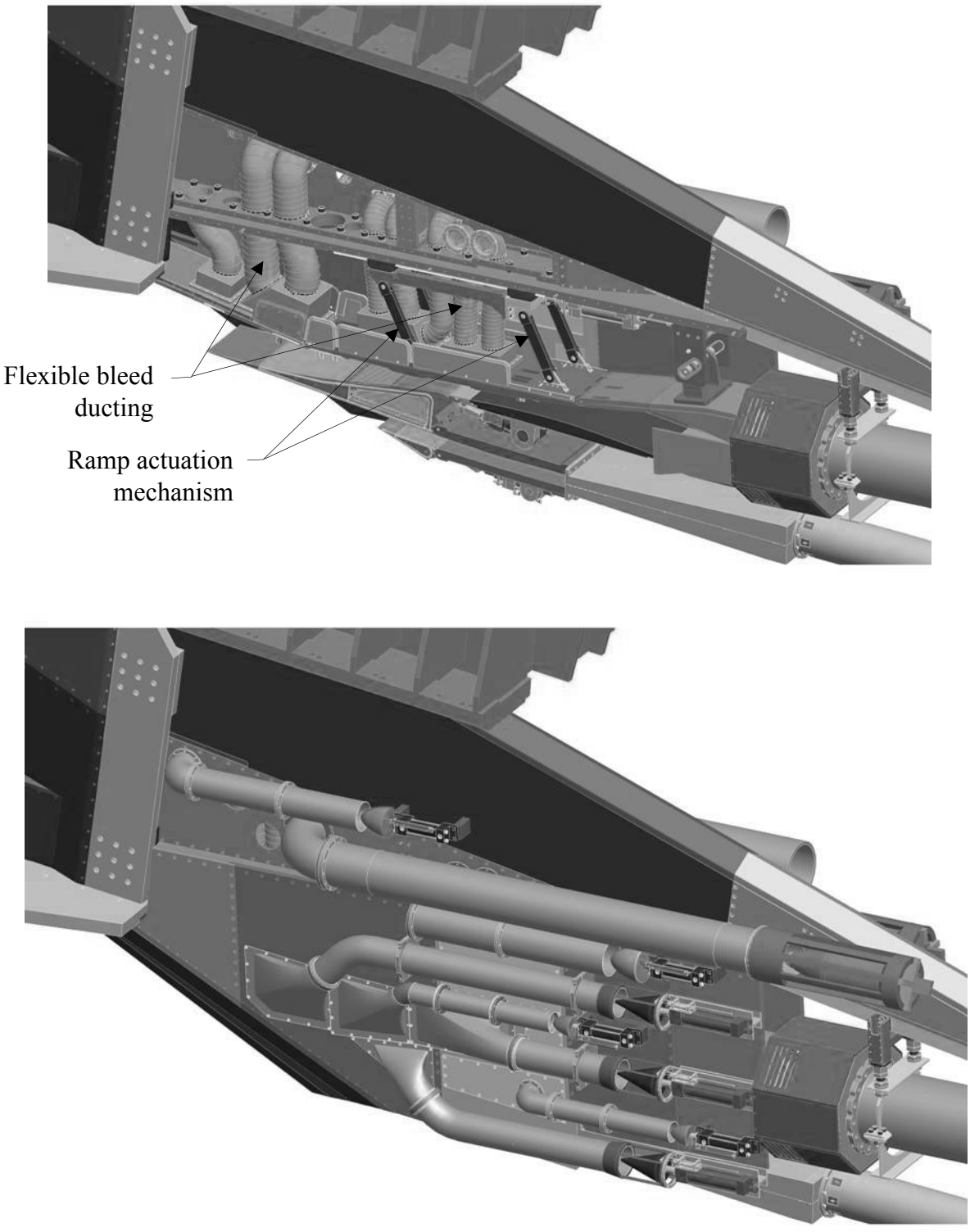

Figure 61. – Solid modeling of the large-scale inlet showing bleed ducting to coldpipe/plug measuring/control systems.

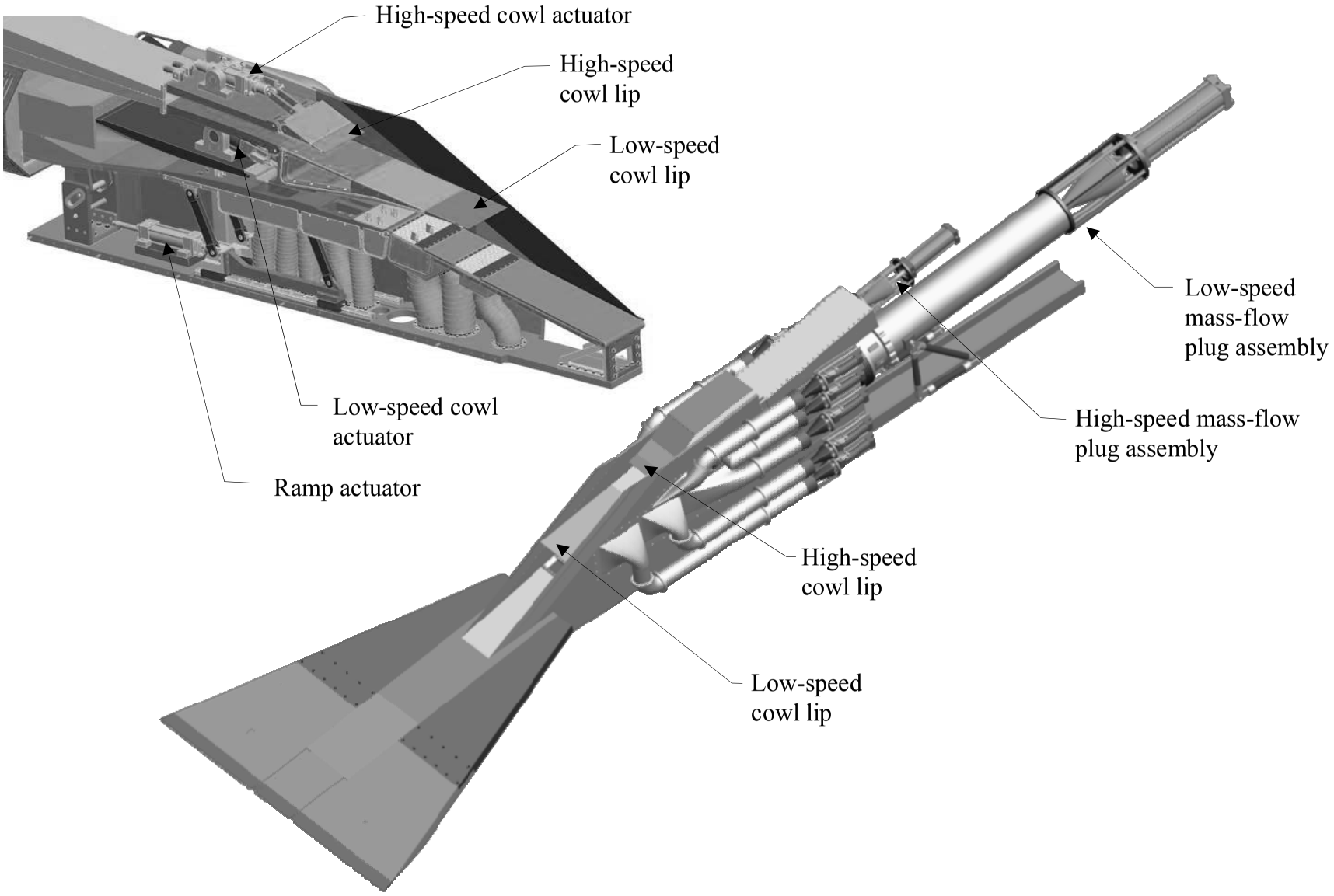

Figure 62. – Bottom view of large-scale inlet model

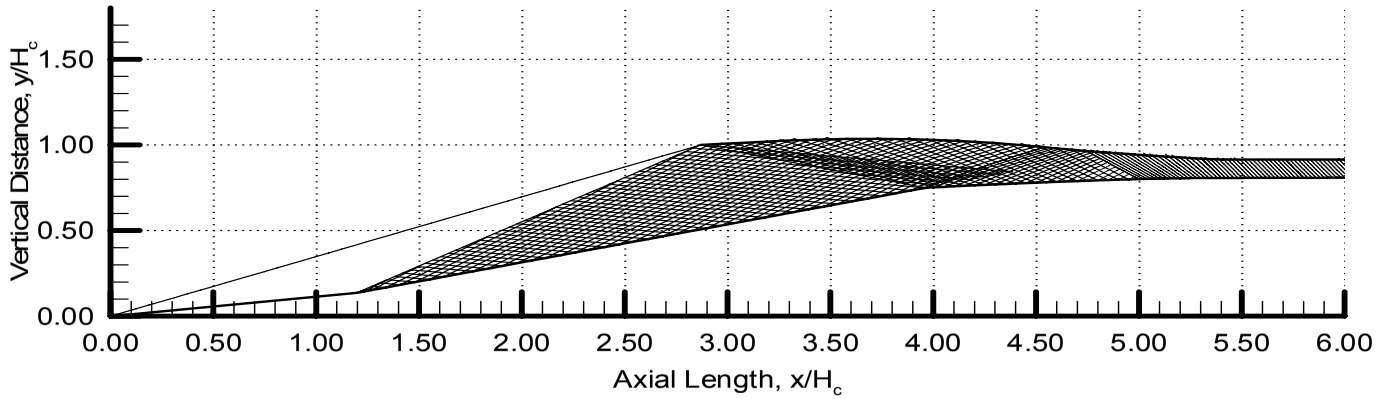

(a). Inlet surface contours. shock system, and method-of-characteristics net.

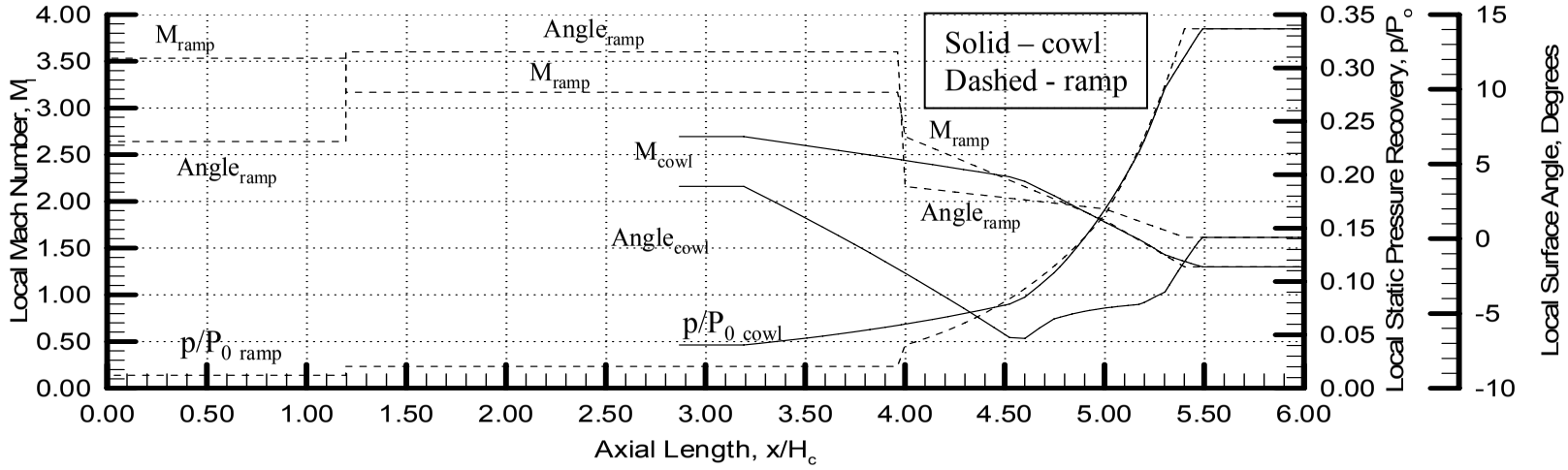

(b). Inlet aerodynamics.

Figure 63. – Aerodynamics of alternate Mach 4 inlet (throat Mach number of 1.3).

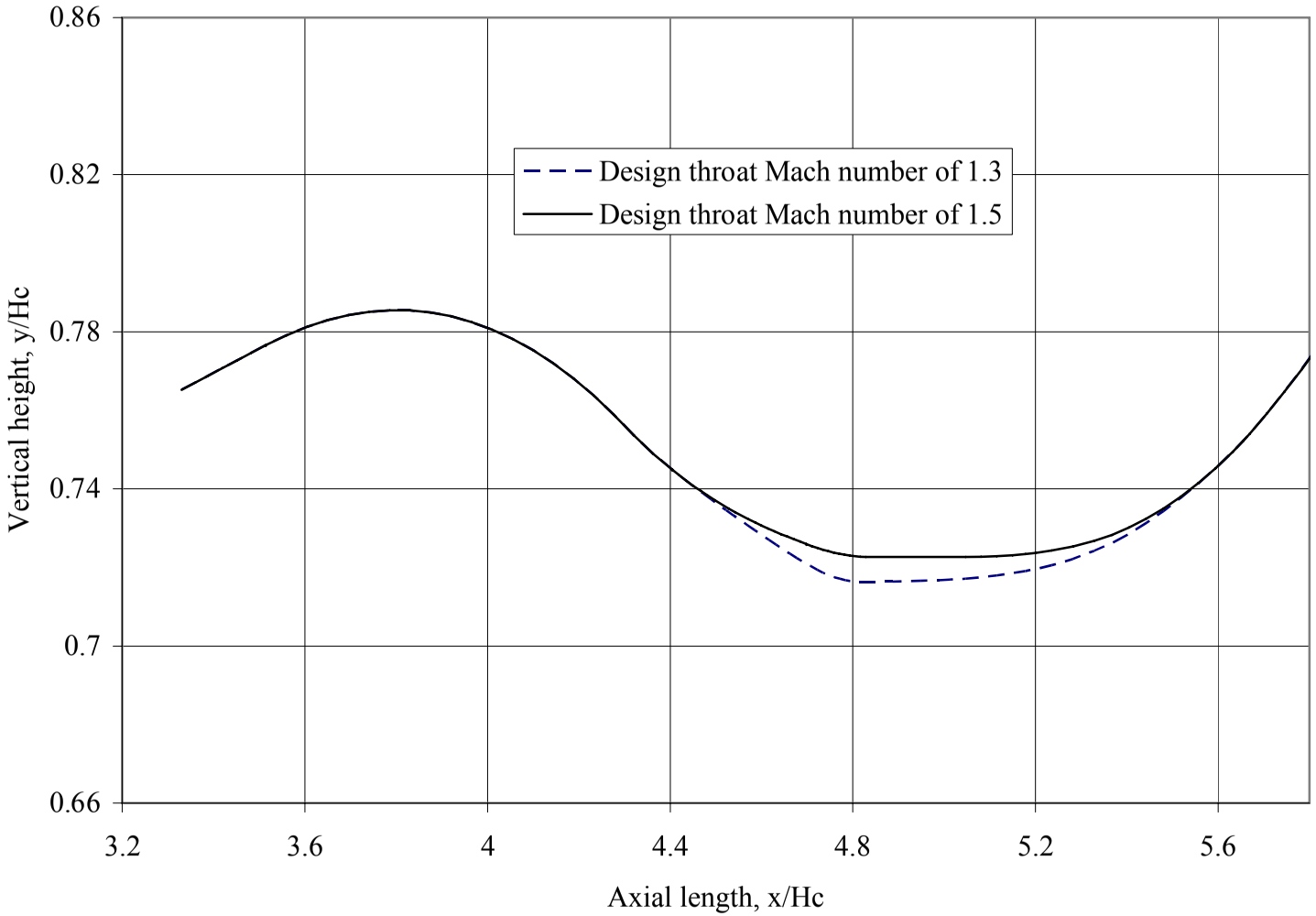

Figure 64. – Comparison of cowl geometries for Mach 4 inlets designed for throat Mach numbers of 1.5 and 1.3.

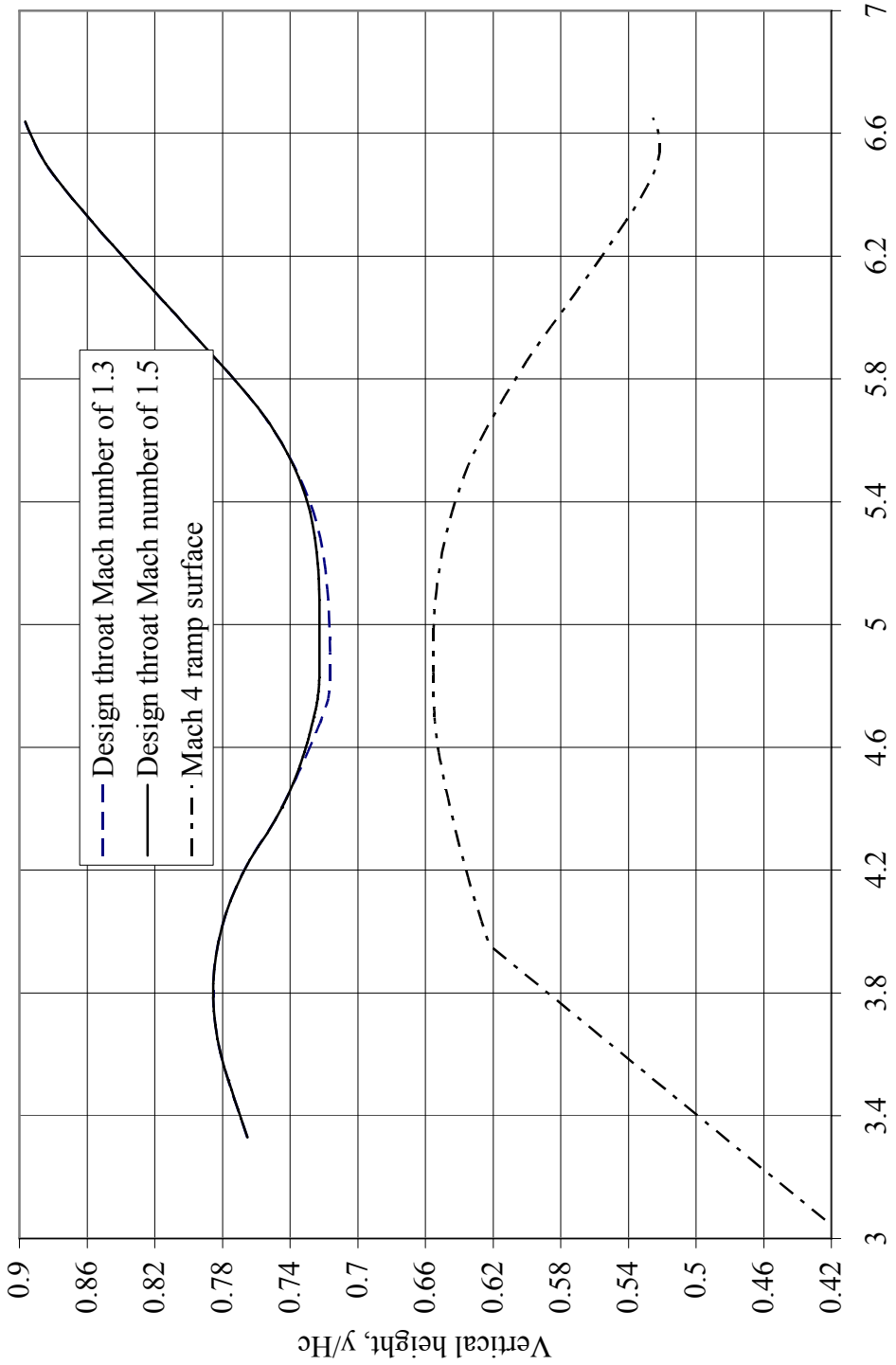

Figure 65. – Comparison of cowl geometries with ramp geometry for Mach 4 inlets designed for throat Mach numbers of 1.5 and 1.3.

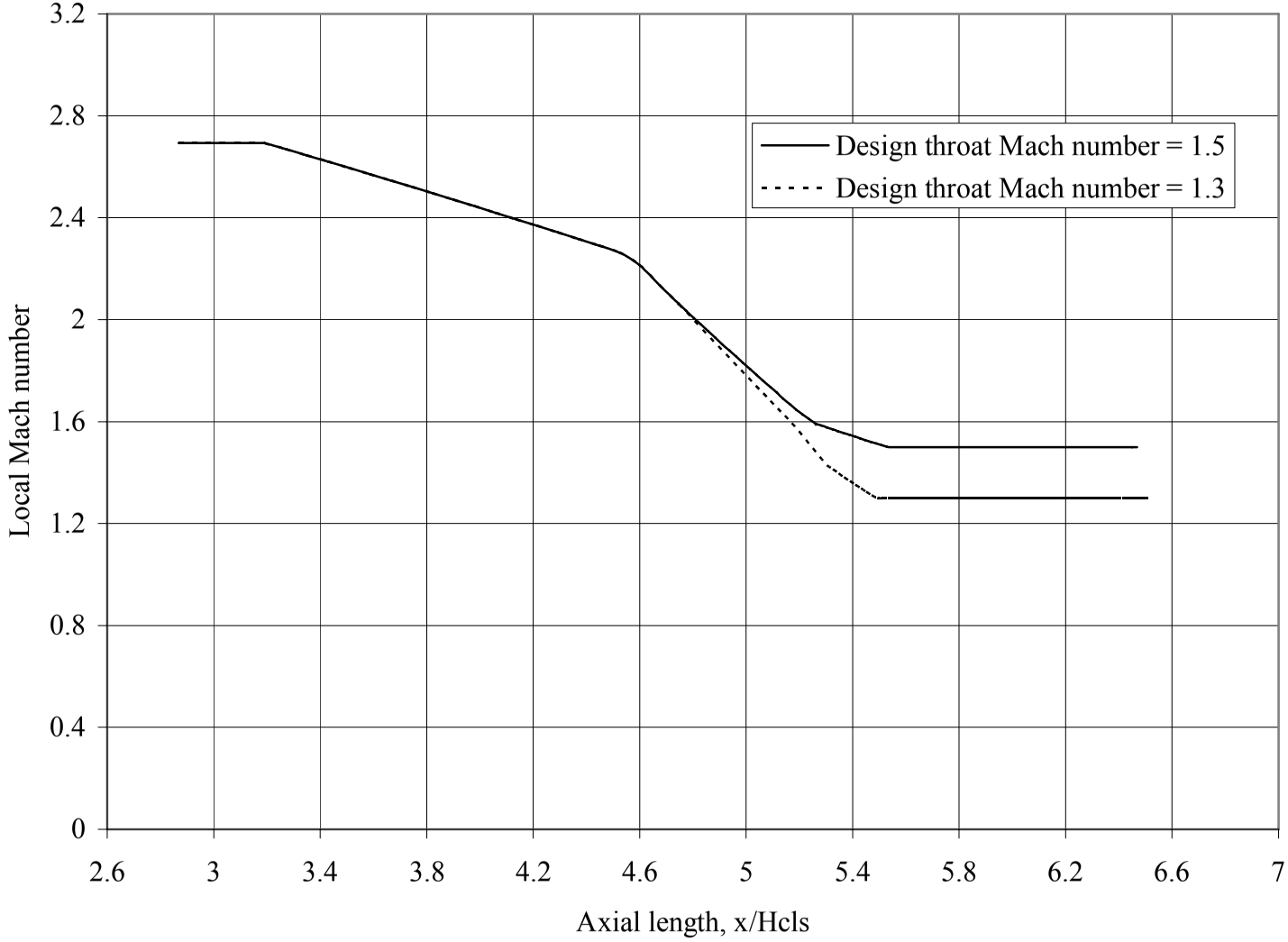

Figure 66. – Local cowl surface inviscid Mach numbers for Mach 4 inlets designed for throat Mach numbers of 1.5 and 1.3.

Cowl coordinates for the throat Mach 1.3 inlet design

x/Hc	y/Hc		x/Hc	y/Hc		x/Hc	y/Hc
3.329904	0.765249		4.58553	0.729418		5.328783	0.724182
3.388457	0.768829		4.601109	0.728183		5.367153	0.726159
3.419953	0.770756		4.61658	0.726976		5.404948	0.728541
3.451448	0.772684		4.631958	0.725781		5.442742	0.731268
3.482944	0.774611		4.647229	0.724603		5.480536	0.734348
3.514433	0.776533		4.662419	0.723447		5.51833	0.737712
3.514433	0.776533		4.677494	0.722349		5.556124	0.741319
3.559683	0.779095		4.692456	0.721303		5.593918	0.745211
3.604928	0.781228		4.707337	0.720313		5.631712	0.749433
3.650161	0.782944		4.722138	0.71937		5.655289	0.752245
3.695388	0.784219		4.722138	0.71937		5.669506	0.754033
3.740592	0.78506		4.734657	0.718643		5.7073	0.759199
3.785762	0.785455		4.747057	0.718026		5.745094	0.764709
3.83088	0.785397		4.759307	0.717511		5.782888	0.770392
3.875948	0.784883		4.77142	0.717093		5.820682	0.776407
3.920934	0.783905		4.783425	0.716767		5.858476	0.782754
3.965841	0.782458		4.795281	0.716527		5.896591	0.789025
4.010651	0.780536		4.807011	0.716373		5.934065	0.795135
4.055346	0.77814		4.818626	0.716293		5.971859	0.801504
4.099916	0.775263		4.83011	0.716287		6.011353	0.807841
4.144348	0.771906		4.841549	0.71631		6.047447	0.813914
4.188626	0.768057		4.852987	0.716327		6.085241	0.820182
4.232743	0.763716		4.864425	0.71635		6.123035	0.826453
4.276684	0.758889		4.875864	0.716367		6.160829	0.832725
4.320327	0.753679		4.887302	0.71639		6.198623	0.838795
4.362711	0.748995		4.909778	0.716441		6.236417	0.844864
4.403844	0.744917		4.949556	0.716563		6.274211	0.851106
4.403844	0.744917		4.988921	0.716737		6.312005	0.857003
4.421344	0.743293		5.01292	0.716887		6.349799	0.862781
4.438616	0.741726		5.04701	0.71714		6.387593	0.86862
4.455659	0.74021		5.080873	0.717459		6.425388	0.874176
4.472491	0.73874		5.115355	0.717925		6.463182	0.879662
4.489134	0.737311		5.149838	0.718502		6.500976	0.884518
4.505588	0.735921		5.178183	0.719066		6.53877	0.888452
4.521876	0.734565		5.199881	0.719578		6.576564	0.89176
4.538004	0.733239		5.234874	0.720539		6.614358	0.894879
4.553978	0.73194		5.282117	0.722127		6.639203	0.896616
4.569831	0.730665						

Figure 67. - Cowl coordinates for throat Mach 1.3 design.

REPORT DOCUMENTATION PAGE	Form Approved OMB No. 0704-0188

1. REPORT DATE *(DD-MM-YYYY)*	2. REPORT TYPE	3. DATES COVERED *(From - To)*
01-06-2008	Final Contractor Report	

4. TITLE AND SUBTITLE
Aerodynamic Design of a Dual-Flow Mach 7 Hypersonic Inlet System for a Turbine-Based Combined-Cycle Hypersonic Propulsion System

5a. CONTRACT NUMBER
NAS3-03110

5b. GRANT NUMBER

5c. PROGRAM ELEMENT NUMBER

6. AUTHOR(S)
Sanders, Bobby, W.; Weir, Lois, J.

5d. PROJECT NUMBER

5e. TASK NUMBER

5f. WORK UNIT NUMBER
WBS 599489.02.07.03.07.02.02

7. PERFORMING ORGANIZATION NAME(S) AND ADDRESS(ES)
TechLand Research, Inc.
28895 Lorain Road, Suite 201
North Olmsted, Ohio 44070

8. PERFORMING ORGANIZATION REPORT NUMBER
E-16505

9. SPONSORING/MONITORING AGENCY NAME(S) AND ADDRESS(ES)
National Aeronautics and Space Administration
Washington, DC 20546-0001

10. SPONSORING/MONITORS ACRONYM(S)
NASA

11. SPONSORING/MONITORING REPORT NUMBER
NASA/CR-2008-215214

12. DISTRIBUTION/AVAILABILITY STATEMENT
Unclassified-Unlimited
Subject Category: 07
Available electronically at http://gltrs.grc.nasa.gov
This publication is available from the NASA Center for AeroSpace Information, 301-621-0390

13. SUPPLEMENTARY NOTES
Project manager, John D. Saunders, Aeropropulsion Division, NASA Glenn Research Center, organization code RTE, 216-433-6278.

14. ABSTRACT
A new hypersonic inlet for a turbine-based combined-cycle (TBCC) engine has been designed. This split-flow inlet is designed to provide flow to an over-under propulsion system with turbofan and dual-mode scramjet engines for flight from takeoff to Mach 7. It utilizes a variable-geometry ramp, high-speed cowl lip rotation, and a rotating low-speed cowl that serves as a splitter to divide the flow between the low-speed turbofan and the high-speed scramjet and to isolate the turbofan at high Mach numbers. The low-speed inlet was designed for Mach 4, the maximum mode transition Mach number. Integration of the Mach 4 inlet into the Mach 7 inlet imposed significant constraints on the low-speed inlet design, including a large amount of internal compression. The inlet design was used to develop mechanical designs for two inlet mode transition test models: small-scale (IMX) and large-scale (LIMX) research models. The large-scale model is designed to facilitate multi-phase testing including inlet mode transition and inlet performance assessment, controls development, and integrated systems testing with turbofan and scramjet engines.

15. SUBJECT TERMS
Inlet; Supersonic inlet, Hypersonic inlet, Mix-compression inlet; Turbine-base combined-cycle engine; Inlet design

16. SECURITY CLASSIFICATION OF:			17. LIMITATION OF ABSTRACT	18. NUMBER OF PAGES	19a. NAME OF RESPONSIBLE PERSON
a. REPORT	b. ABSTRACT	c. THIS PAGE			STI Help Desk (email:help@sti.nasa.gov)
U	U	U	UU	89	19b. TELEPHONE NUMBER *(include area code)* 301-621-0390